University of Stavanger

Faculty of Science and Technology

MASTER'S THESIS

Study program/ Specialization: Offshore Technology - Industrial Technology and Asset Management	Spring semester, 2016 Open / ~~Restricted~~ access
Writer: Anders Aasen	…… (Writer's signature)
Faculty supervisor: Professor Ove Tobias Gudmestad, University of Stavanger External supervisor(s): Dag Abel Sveen, DeepOcean Group	
Thesis title: Analysis of an offshore lifting operation according to DNV -How to find the characteristic load by repeated dynamic simulations in the time domain	
Credits (ECTS): 30	
Key words: - Offshore lifting operations - Short term sea state - Splash zone loads - Characteristic load - Statistics - Probability papers - Confidence- levels and intervals	Pages: 98 +Appendix: 13 pages Stavanger, 08.06.2016

Abstract

In order to analyze a lift offshore performed from a vessel, focus is often put on preparing a good model of the main lifted object, the vessel motions (RAOs), the crane characteristics plus the sea state characteristics. However, something that is not so often put into focus is how to find the correct characteristic load that is affecting the object based on statistical data.

Usually, an irregular sea state is used when analyzing lifts at sea. In this thesis, a consideration of an object launch through the splash zone in a defined sea state has been analyzed. The resulting hydrodynamic forces in such a case are highly dependent on the timing with the incoming wave and the vessel motions. Therefore, several simulations of the same situation need to be performed in order to see the resulting characteristic load based on statistics.

In the industry today, there has not been established a standardized way of finding such a characteristic load. Neither has it been accurately determined what an acceptable probability of non-exceedance should be, or how statistical confidence is to be determined, meaning how many simulations that is sufficient to reproduce a result within a given accuracy.

DNV RP-H103 (2014) shows how the characteristic load can be determined from repeated time-domain simulations if the loads are Rayleigh distributed. In this thesis; the main case of a ROV lift performed by a LARS (Launch and Recovery System) arrangement are considered to cover a typical light lift scenario offshore. The simulation software Orcaflex has been used for the dynamic lifting analyses, while Excel has been used to analyze the statistical results using probability distributions. The non-linear effects such as slamming and drag forces and the short duration of the simulations are governing keys to explain the resulting extreme value load distributions.

The calculated results reveal that given repeated dynamic simulations for lifting operations offshore in a short term sea state does:

1. The most extreme loads experienced not always follow a Gumbel distribution and that the tail region given the use of probability papers should be considered;
2. The given characteristic loads may have a large statistical scatter depending on the simulation size, and;
3. Given the DNV standard regulations where a probability of structural failure should be less than 1 per 10000 lifting operations (DNV-OS-H101, 2011, Section 1, A201), large sample/simulation sizes are required in order to get a high level of confidence. A second criterion has therefore been proposed for implementation.

Preface and Acknowledgement

This thesis is written as a final closure of my master degree in "*Offshore technology – Industrial Technology and Assets Management at the University of Stavanger*". The work has been performed in cooperation with DeepOcean AS between January and June 2016. The main dynamic analysis carried out in this thesis has been performed in Orcaflex, while analyzes of Orcaflex values is performed using Excel spreadsheets.

First of all, I would like to thank my academic and internal supervisor at UiS, Professor Ove Tobias Gudmestad for his regular feedback on topics and setup of the thesis, English grammar, and other valuable support. In addition, associate Professor Sverre K. Haver has been hugely helpful in guiding me through statistical issues and worries. Furthermore, I would like to thank DeepOcean Group for giving me the opportunity to write this thesis, and especially my external supervisor at DeepOcean, Dag Abel Sveen who came up with the main topic of the thesis. He has also given me support, information, and other help through this semester. In addition, I would also thank Roger Jensen, lead engineer at DeepOcean, for his opinions and guiding.

Finally, I appreciate the support and interest in my master thesis writing from my mom and dad.

Anders Aasen

Table of Contents

List of Figures

List of Tables

Abbreviations

ALARP	As Low As Reasonable Practical
ALS/ULS/SLS/FLS	Accidental-/Ultimate-/Serviceability-/Fatigue Limit State
CDF	Cumulative Distribution Function
CFD	Computational Fluid Dynamics
COB	Centre Of Buoyancy
COG	Centre Of Gravity
DAF	Dynamic Amplification Factor
DOF	Degrees Of Freedom
DNV	Det Norske Veritas
IMR	Inspection, Maintenance, Repair
JONSWAP	Joint North Sea Wave Observation Project
LARS	Launch and Recovery System
LRFD	Load- and Resistance Factor Design
MBL	Minimum breaking load
OROV	Observation Remotely Operated Vehicles
PDF	Probability Density Function
RAO	Response Amplitude Operator
ROV	Remotely Operated Vehicle
SE	Standard Error
SWL	Safe Working Load
Te	Ton equivalent
TMS	Tether Management System
WROV	Working Remotely Operated Vehicles

Terminology

The terms described in cursive below is a direct copy of the terminology as described in DNV-OS-H101 (2011, p.9):

Airy/linear wave theory: A theory of surface waves on the water where the nonlinear boundary conditions have been linearized.

"Characteristic condition: A condition which has a defined probability of being exceeded within a defined time period".

"Characteristic load: The reference value of a load to be used in the determination of load effects. The characteristic load is normally based upon a defined fractile in the upper end of the distribution function for the load".

"Design load: A load or load condition which forms basis for design and design verification".

"Displacement: The mass of the vessel/object including permanent equipment".

Ergodic process: Attribute to a stochastic process where the expected value is time and place independent.

"Marine operation: Non-routine operation of a limited defined duration related to handling of object(s) and/or vessel(s) in the marine environment during temporary phases. In this context the marine environment is defined as construction sites, quay areas, inshore/offshore waters or sub-sea".

"Object: The structure handled during the marine operation, typically a module, deck structure, jacket, GBS, sub-sea structures, risers, pipes, etc."

"Operation: Used as a short form for marine operation in this standard."

"Short term: A period of time wherein statistical environmental parameters may be assumed stationary. This period is normally taken as 3 hours."

"Significant wave height: Four times the standard deviation of the surface elevation in a short term wave condition (close to the average of the one third highest waves)."

Stochastic Process: The process $x(t)$ is stochastic if $x(t)$ for any value of t in the interval (a, b) is a random variable. A stochastic process can be seen as all possible realizations in terms of sequences of data from an experiment that involves a certain degree of randomness.

Turbulence: The opposite of a laminar flow. The following characteristics are common:

- Irregular and random flow
- Diffusive and gives a quick mix and increased transport of heat motions and mass across the mainstream
- High Reynolds numbers

- Three-dimensional fluctuating eddies of varying size.
- Dissipative: Kinetic energy is dissipated in the inner fluid.
- Continuously and exists in the entire flow stream (not in the main fluid).

"Unrestricted operations: Operations with characteristic environmental conditions estimated according to long term statistics."

"Vessel: Barge, ship, tug, mobile offshore unit, crane vessel or other vessel involved in the marine operation."

"VMO (Veritas Marine Operations): The unit(s) within Det Norske Veritas providing marine warranty survey and marine advisory services."

"Weather restricted operations: Operations with defined restrictions to the characteristic environmental conditions, planned performed within the period for reliable weather forecasts."

Nomenclature

Latin symbols

A	Areal
a_r	Fluid particle acceleration relative to the earth and body
a_w	Water particle accelerations
A_{33}	Added mass
A_{33}^0	Sectional added mass
A_{33}^∞	High-frequency limit added mass
A_p	Projected area
A_w	Slamming area
B	Minimum breaking load (MBL), (DNV Standard No.2.22)
b_1/b_2	Non-dimensional damping coefficients
B_1	Linear drag constant in an oscillatory flow
B_2	Quadratic drag constant in an oscillatory flow
c	Damping constant
C	Damping ratio
C_a	Added mass
c_{crit}	Critical damping
C_d	Drag coefficient in oscillatory flow
C_{ds}	Drag coefficient in steady state flow
C_e	Water exit coefficient
C_s	Slamming coefficient
C_1	Constant for the Gumbel distribution
C_2	Constant for the Gumbel distribution
d	Water depth $(-z)$
D	Characteristic dimension of the structural member
$D(\theta)$	Direction spreading of wave system
$d-hour\ (dh)$	d amount of hours
E	Cross-sectional Young`s modulus
F	Force or load
F_B	Buoyancy force
F_D	Drag force
F_H	Hydrodynamic force
F_{HD}	Hydrodynamic drag
$\mathrm{F_L}$	Lift line force
$\mathrm{F_{Max}}$	Maximum force
F_R	Reaction force
F_s	Slamming force
F_W	Wave/fluid force
f	Frequency
$f(x)$	Probability density function
$F(x)$	Cumulative distribution function
g	Gravitational force (9.81 m/s^2)

h	Time interval
$h_{\Xi X}$	Transfer function
H_s	Significant wave height
$H_{s,lim}$	Limiting significant design wave height
$H_{s,OP}$	Maximum significant operational wave height
$H_{s,Design}$	Significant design wave height
H_{max}	Maximum wave height
$H_{\max\_WF}$	Forecasted maximum wave height
i	Individual number
i_0	Imaginary number
m	Slope of line
M	Mass
M_s	Structural mass
M_0	Zero moment of load spectrum
M_2	Second moment of load spectrum
$\bar{n}$	Global Maxima
N	Total number
N_{K-C}	Keulegan-Carpenter number
N_{Lim}	Limiting number
K	Stiffness
k	Shape parameter
$\hat{k}$	Shape parameter estimator
k_i	Wave number i
K_p	Frequency factor
L	Length
OP_{lim}	Operational environmental limiting criteria
OP_{WF}	Forecasted (monitored) operation criteria
p	Probability/Percentage
p_{exceed}	Probability of exceeding a value
$p_{non-exceed}$	Probability of not exceeding a value
$p_{non-exceed,actual}$	The actual probability of not exceeding a value
$p_{pressure}$	Pressure at surface
p_0	Atmospheric pressure
R	Random variable
R_C	Characteristic resistance
R_D	Design Resistance
R^2	Squared error
r_1	Random number generated
$Rand()$	Random number ranging from 0 to 1
$\tilde{r}_{max}$	Largest maximum load
S	Maximum load in the wire rope
S_D	Design load

S_F	Safety factor
S_J	JONSWAP spectrum
S_k	Characteristic load component
S_{PM}	Pierson-Moskowitz spectrum
S_{Swell}	Wave spectrum for pure swell sea
$S_{wind\ sea}$	Wave spectrum for pure wind sea
$S(f)$	Frequency domain of the load spectrum
$S(\omega)$	Angular frequency domain of the load spectrum
$S(\theta, \omega)$	Directional wave spectrum
$S_{\Xi\Xi}$	Wave spectrum
t	Time in seconds
T	Period
T_C	Contingency time
T_P	Peak Period
T_{PF}	Spectral Peak Period
T_R	Return Period
T_{REF}	Reference Period
T_{POP}	Planned Operational Period
T_z	Average Zero-up-crossing period
r	Number of parameters
u	Threshold value
v	Degrees of freedom
v_e	Water exit velocity
v_r	Velocity between the object and the water particles
v_w	Water particle velocities
V	Volume
VA	Variance in letter terms
V_o	Volume of object
$\vec{V}$	Vector
W	Weight of an object submerged
W_0	Weight of object in air
y	Number
x	Value or motion vector
$\dot{x}$	Velocity vector
$\ddot{x}$	Acceleration vector
$\bar{x}$	Mean/average value
x_{MPL}	Most probable largest value
x_p	x given a probability of occurrence p
$x_{p,L}$	Upper end of the confidence level given p
$x_{p,H}$	Lower end of the confidence level given p
x_s	Significant response
z	Water depth

$z_{1-\propto/2} = -z\propto/2$	Standard normal variable

Greek symbols

α	Alfa factor
β	Beta
β_0	Frequency ratio
β_1	Skewness
β_2	Kurtosis
$\hat{\beta}$	Beta estimator parameter
Δ	Delta
Δ_{Lim}	Motion amplitude limit
Δ_x	Pendulum motion
Δ_y	Motion amplitude
∇	Laplace operator
ε	Random phase angle
ϵ	Wire strain
δ	Deflection
γ	Gamma or Euler number (0.57722)
γ_1	Shape parameter – Weibull distribution
γ_2	Peak enhancement factor
γ_c	Consequence factor
γ_d	Design factor
γ_f	Load factor
γ_m	Material factor
γ_r	Reduction factor
γ_{sf}	Safety factor
γ_{tw}	Twist reduction factor
γ_w	Wear and application factor
Γ	Gamma function
φ	Velocity Potential
φ_n	Phase angle
η	Vertical Motion
η_n	Vessel displacement
η_{tz}	Crane tip motion
μ	Mean value
$\hat{\mu}$	Mean estimator value
λ	Wave length
θ	Angle/Wave direction
θ_p	Main direction
ρ	Density
σ	Standard Deviation
σ_p	Standard deviation for a given level of probability

σ_r	Standard deviation of the dynamic load
σ_w	Standard deviation of water particle velocity
ω	Angular wave frequency
ω_p	Angular spectral peak frequency
ω'	Non-dimensional frequency of oscillations
χ	Chi
ξ	Free surface elevation
ξ_0	Wave amplitude
$\dot{\varsigma}$	Vertical velocity of the real sea surface

1. Introduction

1.1 Background and motivation

Today, DeepOcean is a service company providing subsea operations as inspection, maintenance and repair (IMR), survey, de-commissioning work, installations, pipeline repairs, and "*Subsea, Umbilical, Riser and Flowline*" (SURF) work. In order to keep a vessel fully operative during weather restricted operations, downtime caused by the environment (i.e. sea state, wind, current, and water depth issues) must be kept to a minimum.

In general, operations offshore performed from an offshore construction- or survey vessel involve using either one or two remotely operated vehicles (ROVs) at a time. When launching and recovering an object through the upper water columns, critical drag- and slamming forces may occur due to large incoming waves and resulting water particle kinematics. The water columns where critical forces may occur is therefore in the literature often referred to as the splash zone. During a lifting phase, hydrodynamic forces on the object from an incoming wave may cause uplift with a corresponding slack wire. A wire undergoing slack is resulting in large forces, and limiting criteria will most often be related to the forces experienced after a snap load has occurred in the wire.

As design loads are of major importance when lowering objects through the wave zone, accurate prediction of these loads may increase the number of suitable offshore vessels, increase the safety level of operations, and reduce the total cost of an operation.

A way of finding a characteristic load is described in many regulations and standards all over the world. However, as the DNV standards are known to be very detailed and are the main source of information and regulations for especially Norwegian based offshore vessel companies, the DNV standards will often be used as a direct source when evaluating the procedure of finding a characteristic load.

A characteristic load as defined in DNV-OS-H102 (2012, Section 1, C200) is *"the reference value of load to be used in the determination of load effects. The characteristic load is normally based upon a defined fractile in the upper end of the distribution function for the load"*.

The characteristic load is in the DNV RP-H103 (2014) determined from a time domain simulation using a Rayleigh statistical distribution. This procedure is often lacking when considering lifting phases of less than 1 minute due to maximum loads not being Rayleigh distributed, and uncertainties in both the statistical confidence and the probability of exceeding a given characteristic load. Therefore, another method will be suggested in this thesis in order to establish a method for finding a characteristic load for lifting operations from a vessel through the splash zone offshore.

1.2 Objective

The main objective of this thesis is to establish a procedure for finding characteristic load when lifting of light objects from a vessel through the splash zone. In DNV-RP-H103 (2014, chapter 9.1.1.6), a lifting operation may be divided into either a heavy- or a light lift operation. In a light lift, the lifted object weight is less that 1-2% of the vessel displacement, and the lifted object does not affect vessel motions. A heavy lift would then mean an object weight of more than 1-2% of the vessel displacement, typically more than 1000 tons. Often, heave compensation would not be possible for such cases, although other methods may be used to minimize dynamic loads.

The purpose is thereby to establish a way of finding a sufficiently accurate and reliable characteristic load for light lifts in a short term wave condition performed by an offshore vessel. The analysis will be based on requirements described in the DNV standards, and statistical methods.

Today, repeated simulations in the time domain are time consuming, and limitations on the simulation size have to be done. The DNV standards propose a Gumbel distribution for use when analyzing extreme value data (DNV-RP-C205, 2010, 10.7.3), which is a practice offshore vessel companies has taken as a standardized distribution for use. The alternative is to use a Rayleigh distribution in a long term stationary analysis ($t > 30$ minutes) of the wave process (DNV RP-H103, 2014, 3.4.3.5) and corresponding forces as the object is fixed in a selected position in the splash zone. These distributions will be scrutinized throughout the thesis and compared with some other well-known distributions that may prove better for simulations that have to be repeated in the time domain in order to find a suitable characteristic load where a given level of non-exceedance is maintained.

A characteristic load is important for the design consideration of the lifted equipment and its rigging arrangement. It is also important in order to establish a correct value for the consideration of possible snap loads caused by a slack in the wire. Orcaflex analyses in the time domain are to be performed, where the results will be evaluated by use of a proposed/recommended statistical method in Excel.

1.3 Structure of the Report

The thesis is divided into 11 chapters. In chapter 2, investigations on what the DNV standards says about analysis of weather restricted operations in a short term wave condition is conducted.

Chapter 3 and 4 provide a discussion on relevant wave spectrums and different relevant statistical distributions, including how they are used in different scenarios, and how they relate to what the DNV standards recommend when finding a characteristic load through the use of simulation software.

In chapter 5, the loads acting on an object in the splash zone is discussed.

In chapter 6, the software programs used in this thesis are presented and explained. Also, the vessel and the ROV launch and recovery system (LARS) used are described. This is the basis for the input used in the time domain simulations in Orcaflex.

Chapter 7 presents the analysis methodology relevant for this thesis, while chapter 8 presents the results obtained from the dynamic time domain calculations in Orcaflex. Further analyses of these results in order to find a characteristic load are here carried out using Excel spreadsheets.

Chapter 9 addresses a discussion on the results obtained, while the conclusions of this thesis and recommendations for further work are given in chapters 10 and 11.

2. Offshore Lifting Operations in accordance with DNV

2.1 DNV Standards

DNV GL is an international certification society created in 2013 as a result of an amalgamation between Det Norske Veritas, DNV (Norway) and Germanischer Lloyd, GL (Germany). Although DNV GL is a recently merged company, its history goes all the way back to 1864 when DNV was established in Norway to lead the technical inspection and evaluation of Norwegian merchant vessels. DNV has developed rules and standards for ships and vessels for over a century (The Maritime Executive, 2016).

On the other hand, Germanischer Lloyd was founded in 1867 by a group of 600 ship owners, ship builders and insurers. The classification society was created in order to ensure the safety of life and properties at sea, as well as prevent any pollution of the marine environment (Edumaritime, 2016).

Today, DNV and Germanischer Lloyd form DNV GL which is divided into 5 divisions, respectively (1) Maritime; (2) Oil & Gas; (3) Energy; (4) Business Assurance, and (5) Software. As this thesis is directed towards (1) maritime, focus will be directed towards the current offshore standards (OS) and recommended practices (RP) for marine operations. The offshore standards provide acceptance criteria and technical provisions for general use by the offshore industry, while the recommended practices provide proven technology and engineering practice. Some of these (RP-/OS-) standards give marine service companies as DeepOcean AS guidelines on how to engineer their operations and equipment. Especially the VMO standards (DNV-OS-H101, DNV-OS-H102 and DNV-OS-H201 through DNV-OS-H206) are important as they cover marine operations.

In the following sections, a literature study of relevant DNV standards will be carried out, focusing on what DNV recommends when finding a characteristic load, and how this load shall be taken towards limiting factors of the lifting system used. Also, relevant statistics and sea state specifics will be scrutinized.

2.1.1 Limit State design for lifting systems

Generally, a limit state can be defined as a state in which the structure is unable to fulfill its purpose and satisfy the conditions for which it was meant to. As mentioned in chapter 1, a characteristic load is important for the design consideration of the lifted equipment and its rigging arrangement. When looking at a LARS/crane lift performed in an irregular sea state, some limiting safety criteria must be applied to the crane/LARS fundament.

The ultimate limit state (ULS) criteria are related to the maximum load carrying capacity. ULS is one of the four criteria a structure has to cope with to ensure a safety level is as high as reasonable practical. The other criteria that is important for lifting at sea is the accidental limit state (ALS) criterion that copes with accidental loads, and ensures a 10^{-4} probability of

failure to be maintained. The other 2 criteria are the serviceability limit state (SLS), and the fatigue limit state (FLS).

After finding the characteristic load from wave impacts, a consideration has to be assessed for whether the lifting arrangement and the object can handle the load impacts. To ensure that safety concerns are maintained, DNV-OS-H102 (2012, sec.5, A100) recommends using the LRFD (load- and resistance factor design) method. This method is a design code where partial load- and material factors reflects uncertainties in the structural design. By using this method, load components may be considered individually.

Generally, one has to fulfill (DNV-OS-H102, 2012, sec.5, A400):

$$S_D \leq R_D \tag{1}$$

Where S_D represents the design load, and R_D represents the design resistance.

As described, A *characteristic load* is in DNV-OS-H102 (2012, Section 1, C200) referred to as the value of loads to be used in the determination of load effects. A *characteristic resistance* (R_c) refers to the reference value of the maximum (structural) resistance to be used in determination of the *design resistance*. *"R_c may be calculated based on the characteristic values of the relevant parameters or determined by testing. Characteristic values should be based on the 5th or the 95th percentile of the test results, whichever is the most conservative"* (DNV-OS-H102, sec.5, A500).

One thereby gets:

$$\sum_i (\gamma_{f,i}) * S < \frac{R_C}{\gamma_m}, \quad i = G, Q, D, E, A \tag{2}$$

γ_f : Load factor
γ_m: Material factor
S : Characteristic load component
R_C : Characteristic resistance
i : Load Categories (See Table 1)

With reference to the load factors, they shall comply with (1) ULS-A which takes into consideration extreme permanent and variable loads in regular environmental conditions, and (2) ULS-B where permanent loads with more extreme environmental conditions are present.

Table 1: Load factors (DNV-OS-H102, 2012, sec.5, B200)

Load Conditions	*Load Categories*				
	G (permanent loads)	*Q (Variable functional loads)*	*D (Deformation loads)*	*E (Environmental loads)*	*A (Accidental loads)*
A	1.3	1.3	1.0	0.7	NA
B	1.0	1.0	1.0	1.3	NA

The material factor (γ_m) is to be taken as minimum 1.15 for steel structures (DNV-OS-H102, Section 5, B401).

It should however be noted that the main lifting system fundament most often not are of concern when evaluating lifts offshore.

2.1.2 Limit State design for lifting wire and slings

In order to check the capacity of the wire/rigging on a LARS or a crane, DNV proposes different methods for establishing a safety reduction factor (γ_{sf}).

Method 1

The first method stated by DNV-OS-H205 (chapter 4.1.5.2) says that the maximum characteristic sling load ($F_{sling} = SWL$) should be less than:

$$F_{sling} < \frac{MBL_{sling}}{\gamma_{sf}} \tag{3}$$

Where MBL_{sling} gives the minimum breaking load of the sling(s) used. The nominal safety factor (γ_{sf}) for slings and grommets are taken as the greatest of the following two products of partial factors (DNV-OS-H205, chapter 4.1.5.):

$$\gamma_{sf} = \gamma_f \gamma_c \gamma_r \gamma_w \gamma_m \gamma_{tw}$$
$$\gamma_{sf} = 2.3 \gamma_r \gamma_w \gamma_{tw}$$

Where: $\gamma_f = load\ factor, \gamma_c = Consequence\ factor, \gamma_r = Reduction\ factor, \gamma_w = Wear\ and\ application\ factor, \gamma_m = Material\ factor\ and\ \gamma_{tw} = Twist\ reduction\ factor$

The different factors are found in DNV-OS-H205, chapter 4.1.5.3 through 4.1.5.13.

Method 2

The second method given in the DNV Standard for certification No.2.22 (2011, ch.2, section 3, B505) says that the "*Minimum breaking load B of steel wire ropes shall not be less than:*

$$B = S_F * S \tag{4}$$

Where S is the maximum load in the wire rope". The launch and recovery system (LARS) of an ROV consists of a tether (lifting wire) on top of either the TMS (Tether Management System), or directly onto the ROV (if no TMS). The minimum breaking load for a tether or a crane wire can be found by the certification certificate where the minimum breaking load (MBL) has been tested and verified in accordance to DNV-OS-H102 (2012) to obtain a 95% upper safety percentile. A load test is normally to be performed ones a year.

DNV Standard for certification No.2.22 (2011, ch.2, section 3, B505) says that the *"steel wire rope safety factor* (S_F) *for running applications or forming part of sling and for mast stays, pendants and similar standing applications shall be the greater of:*

not less than 3 and:

$$S_F = \frac{10^4}{0.885 * SWL[kN] + 1910} \tag{5}$$

But not exceed 5.

Or, $S_F = 2.3 * DAF$

SWL is in this thesis the "*Safe Working Load*" of the lifting equipment.

Conclusion:

As shown, two methods may prove reliable when finding a safety factor for use on a crane/LARS wire or typical rigging equipment. Anyway, some distinctions must be drawn. The first method is mostly directed towards rigging equipment (i.e. slings, chains, shackles, etc.) and not for stationary lifting equipment on fixed installations (i.e. cranes/LARS/Module handling systems). Therefore, method 1 may be applicable for finding a safety factor for rigging equipment used for instance during a crane lift operation (i.e. Figure 1), while method 2 should be used for the main crane/LARS lifting wire.

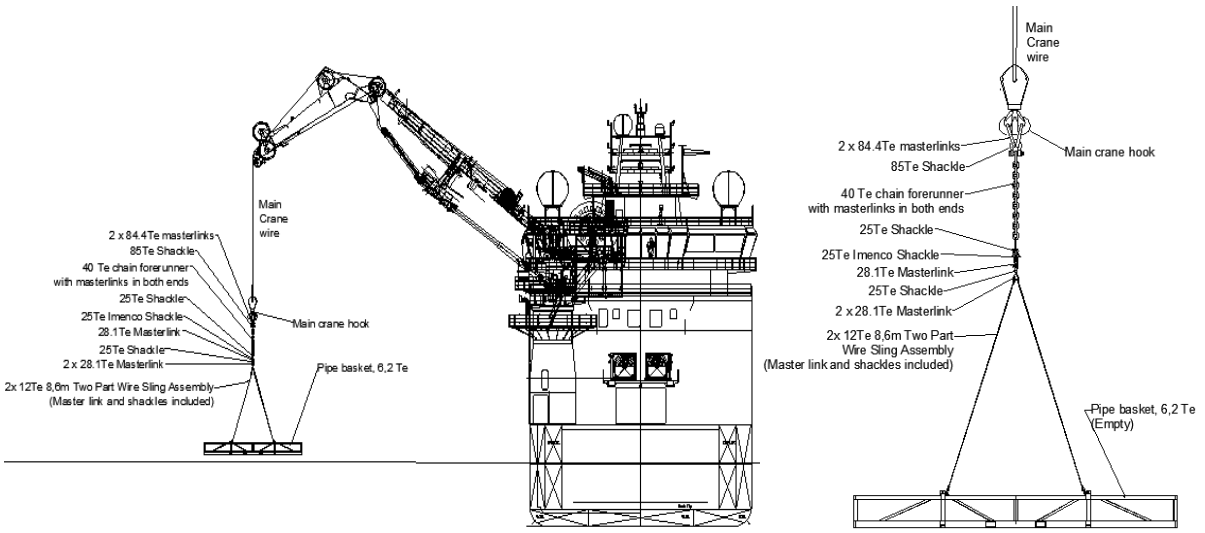

Figure 1: Illustration of a typical lifting arrangement using a vessel crane

The second method proposed is more directed towards wire ropes for lifting appliances. Also, in the DNV Standard for certification No.2.22 (2011, section 11) it is stated that *"the requirements given in Sec.6 for offshore cranes are valid for launch and recovery arrangement for ROV"* as well.

DNV Standard for certification No.2.22 (2011, section 3, B200) finds the dynamic amplification factor as 1.3 for jib cranes, in this thesis representative to the lifting arrangements used. Anyway, *"for offshore lifting operations it is advisable to ascertain that the load stipulations include necessary reserves for dynamic amplifications that follow from lifting in waves"* (DNV Standard for certification No.2.22, 2011, appendix E, A307). Therefore, certified de-rating tables are required for use during offshore lifting operations.

2.2 Limiting Criteria's

According to the DNV standards, only one absolute limiting criterion has to be applied for lifting of structures offshore. This first criterion has to be fulfilled if a sea state is to be taken as acceptable. The second criterion stated in the summary below is a proposal based on research performed in chapter 8. This is a criterion that would make it more predictable to see if a lift is safe or not as the first criterion may have a very large statistical scatter. The third criterion is applicable in particular if no time domain software is being used, meaning simplified hand calculations (i.e. according to DNV-RP-H103, chapter 4). It should however be noted that a slack sling that is undergoing slack may result in large forces of high unpredictability. Therefore, this criterion should be applied to large and/or heavy lifting operations with high consequences if a failure occurs.

It should also be noted that light objects (i.e. ROVs, light baskets, etc.) have a higher degree of slack in the wire during splash zone lifts. But as it is the resulting peak load that imposes a limitation, this criterion might be omitted by having a reliable method for handling dynamic

loads after a slack sling has occurred. This can be done by time domain calculation in a software program as Orcaflex.

In addition, some other criteria (number 4-6) proposed by Sandvik and Kopsov (1995) may be applicable for some specific cases:

1. The ultimate analysis states that the total structural capacity of a crane/LARS and its components shall not be exceeded more often than 1 per 10 000 operations (DNV-OS-H101, 2011, Section 1, A201):

$$F_{max,\,dyn\ (p=0.9999)} < F_{crane\ components,max\ structural\ capacity}$$

   It is noted by DNV-OS-H101 (2011, Section 1, A202) that the intention of the load-, safety- and material factors in the VMO Standard is to ensure a probability for structural failure less than 1/10 000 per operation. Anyway, when also considering operational errors the total probability of failure may increase.

2. The most probable maximum dynamic tension in any lifting appliances for a safety level of x% shall not exceed the dynamic capacity of the crane, the design capacity of any lifting equipment, or the design capacity for the structure:

$$\begin{aligned} &F_{max,\,dyn(p=XX\%)} \\ &< F_{Crane\ dyn.capacity}\,;\, F_{Object\ design\ capacity};\, F_{Lifting\ equipment\ design\ capacity} \end{aligned} \tag{6}$$

   With regards to the safety level, research is performed in chapter 8 to give a conclusion on a suitable level.

3. The most probable minimum dynamic tension in the crane wire/rigging shall be larger than 10% of the static tension in the crane wire/rigging in air (DNV-RP-H103, 2014, 4.4.3.3):

$$F_{min\,crane} \geq 0.1 \times F_{static\ crane}$$

4. For deck operations, the pendulum motion (Δ_x) and motion amplitude (Δ_y) shall be within safe limits (Δ_{Lim}) (Sandvik and Kopsov, 1995, 5c):

$$\Delta_x \Delta_y < \Delta_{Lim}$$

   This criterion may be addressed by using preventive measures as bumper frames, tugger winches, or manually handling by ropes.

5. If heave compensation is used during the operation, the limiting wave height, H_s, shall be less than the limiting design wave height $H_{s,lim}$ for the heave compensation system (Sandvik and Kopsov, 1995, 5e):

$$H_s > H_{s,lim}$$

As this criterion is a very general recommendation usually not specified for more than a few wave periods/heights, a more detailed analysis covering the system limitations (max allowable crane tip amplitude, velocity and acceleration) should be performed.

6. During operations with long duration and many lifts, the number of force variation cycles shall be within any limits determined from low cycle fatigue analysis of the main load carrying elements (crane, structure and installation equipment) (Sandvik and Kopsov, 1995, 5d):

$$N < N_{Lim}$$

2.3 The Alfa factor criterion

From the limiting criteria described in the last chapter, limiting wave conditions are found. Before a lifting operation is to be carried out offshore, a wave forecast and, if possible, wave monitoring shall be considered. But, as a wave forecast/monitoring does not include uncertainties in the data, DNV-RP-H101 (2011) states that an Alfa-factor should be applied to cover for any deviates between the forecasted and the real ocean waves, meaning:

$$\alpha = \frac{H_{max}}{H_{\max\_WF}} \tag{7}$$

Where $H_{\max\_WF}$ is the maximum forecasted wave height, and $H_{\max}$ is the maximum wave height with a 10^{-4} probability for exceedance during the period under consideration. Generally, the α-factors are applicable for weather restricted operations, meaning operations with a reference period (T_R) of less than 96 hours, and a planned operational period (T_{POP}) of less than 72 hours:

$$T_R = T_{POP} * T_C \tag{8}$$

Where T_C is the contingency time to cover for uncertainties done during the assessment of T_{POP}, see DNV-RP-H101 (2011).

Further, as the waves/weather is hard to predict 100% accurate, restrictions must be applied to the operational limit criterion (OP_{lim}) found from analysis:

$$OP_{WF} = \alpha * OP_{lim} \tag{9}$$

Or in wave terminology as:

$$H_{s,OP} = \alpha * H_{S,Design} \tag{10}$$

Where $H_{S,OP}$ is the maximum significant operational wave height to be allowed during operation, and $H_{S,Design}$ is the significant design wave height found from analysis.

Some of the factors that are proposed by DNV-RP-H101 (2011) for use in the Norwegian Sea area are shown in Table 2 below:

Table 2: Norwegian Sea alpha factors based on one forecasting source and no meteorologist on site (DNV-RP-H101, 2011)

Operational Period [hours]	*Design Wave Height [m]*						
	$H_S = 1$	$1 < H_S < 2$	$H_S = 2$	$2 < H_S < 4$	$H_S = 4$	$4 < H_S < 6$	$H_S \geq 6$
$T_{POP} \leq 12$	0.65	Linear Interpolation	0.76	Linear Interpolation	0.79	Linear Interpolation	0.80
$T_{POP} \leq 24$	0.63		0.73		0.76		0.78
$T_{POP} \leq 36$	0.62		0.71		0.73		0.76
$T_{POP} \leq 48$	0.60		0.68		0.71		0.74
$T_{POP} \leq 72$	0.55		0.63		0.68		0.72

It should however be noted that these factors may be increased by having either (1) more forecasting sources and inputs, meteorologist(s) on site, or (3) monitoring instruments or sources that can measure the weather condition and thereby cope with uncertainties. For more information, reference is made to DNV-RP-H101 (2011).

3. Statistics

3.1 Statistical distributions

In order to describe different stochastic and ergodic phenomena, statistics are used to summarize available data sets. This is done by a statistical function which according to Investopedia (2016) is:

"*A function that describes all the possible values and likelihoods that a random variable can take within a given range. This range will be between the minimum and maximum statistically possible values, but where the possible value is likely to be plotted on the probability distribution depends on a number of factors, including the distribution mean, standard deviation, skewness and kurtosis".*

Different statistical functions may be used to represent data sets (Figure 3). However, some of them are known to be more representative for cases involving wave heights and corresponding wire forces. A few of them will briefly be introduced below.

3.1.1 Continuous value distributions

When evaluating a wave process in the time domain, one often assumes that it follows a Gaussian distribution when a stationary random stochastic and ergodic process goes towards infinity. In a Gaussian process, every instance of a wave elevation may be assumed to be normally distributed. A normal distribution (Figure 2) has the following probability density function (PDF):

$$f(x) = \frac{1}{\sigma\sqrt{2\pi}} e^{-\frac{(X-\mu)}{2\sigma^2}} \tag{11}$$

Where μ represents the mean expectation of the distribution, and σ is the standard deviation of the process. If $\mu = 0$ and $\sigma = 1$, the distribution is called a standard normal distribution. The standard normal distribution has skewness (β_1) and kurtosis (β_2) values equal to 0.

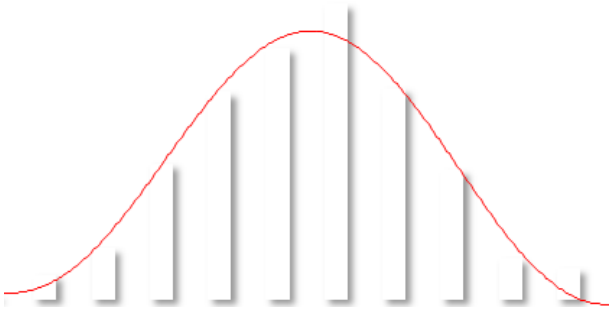

Figure 2: Probability density function (PDF) given a normally distributed data set

3.1.2 Peak value distributions

In this thesis, the maximum wire tension is the quantity of interest. The wire tension is assumed to be a stochastic process. Summarizing all global maximums in the wire over a sufficient time period, the statistical distribution may be assumed to follow the same distribution as the wave height process, namely a Weibull distribution (Myrhaug, 2014). This is based on the assumption that the wire follows the wave process, and other phenomena such as snatch forces or quadratic damping are not present or negligible.

The Weibull distribution is a continuous probability distribution, meaning that variables can take any value. The Weibull distribution is also commonly used in reliability and life data analysis due to its adaptability. The adaptability for a three-parameter Weibull distribution is created by adjusting the shape (k), scale (β), and γ_1-parameter values. The probability density function reads:

$$f(x;\beta,k) = \frac{k}{\beta}\left(\frac{x-\gamma_1}{\beta}\right)^{k-1} e^{-\left({}^{(x-\gamma_1)}/_{\beta}\right)^{k}}, \quad x \geq 0 \tag{12}$$

Integrating the Weibull PDF function, the cumulative distribution function (CDF) reads:

$$F(x;\beta,k) = 1 - e^{-\left({}^{(x-\gamma_1)}/_{\beta}\right)^{k}}, \quad x \geq 0 \tag{13}$$

The Weibull distribution is from here commonly adapted to form either the exponential distribution ($k = 1$), or the Rayleigh distribution ($k = 2$). When one considers individual wave heights/wire tension in a stochastic process, the minimums/maximums are assumed to be statistically independent, and follow a Rayleigh distribution (Myrhaug, 2014).

3.1.3 Extreme value distributions

When considering a stochastic process over a longer time period, the smallest/largest among all outcomes in that process is considered to be an extreme value. Summing up many extreme values in with the same distribution, the data set can be described one of the following generalized extreme value distributions (Haver et. al, 1980):

1. Exponential type distributions which results in a Gumbel extreme value distribution. A perfect Gumbel distribution has skewness, $\beta_1 = 1.3$ and kurtosis, $\beta_2 = 5.4$. Examples of exponential type distributions are the normal, the log-normal, and the Rayleigh.
2. Distributions with finite moments (i.e. the Cauchy distribution) resulting in a Frechet extreme value distribution.

Bounded distributions (i.e. the beta distribution) resulting in a Weibull extreme value distribution.

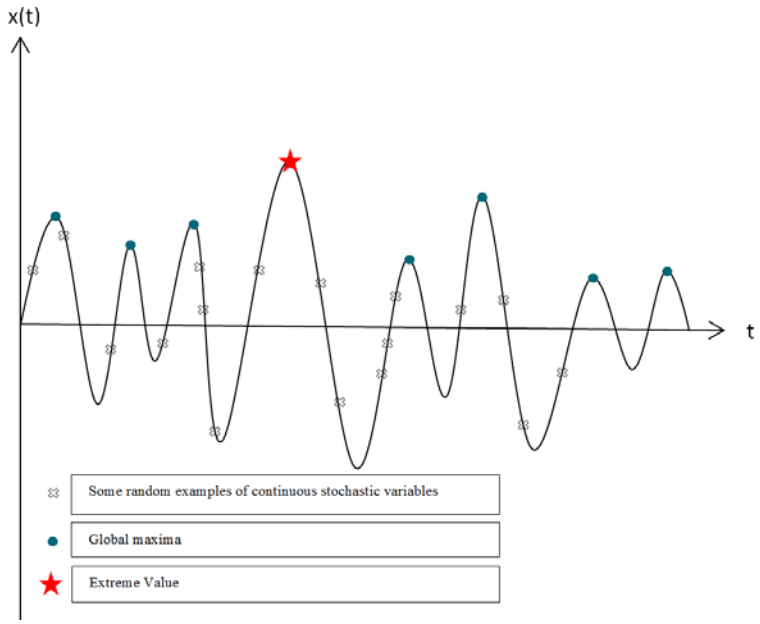

Figure 3: Illustration of an irregular stochastic process for a given time unit

3.2 Sea State Specifics

As an ROV launch often is done through the splash zone usually is done in 10-20 seconds, a short term wave condition applies. The DNV-RP-C205 (2010, 3.5.1) defines a short term wave conditions as an assumption that a sea state is stationary for a duration of 20 minutes to 3-6 hours. By having a stationary sea surface one may find a characteristic set of environmental parameters such as the significant wave height (H_s) defined as the average of the highest third waves, and the peak period (T_p) which is the wave period with the highest energy.

3.2.1 Wave spectra

Real sea water is compressible and inhomogeneous. However, this and some other features have only minor impact on an object during the splash zone lifting phase. Therefore, the potential flow theory basis for Orcaflex calculations is based on some simplifications of the real environment (Gudmestad, 2015):

i. The seawater is incompressible and homogeneous, $\nabla * \vec{V} = 0$.
ii. Non-rotational flow, $\nabla \times \vec{V}(x, y, z, t) = 0$, where $\vec{V}(x, y, z, t)$ is the velocity vector of the water particle at time t at the point (x, y, z) and ∇ is the Laplace operator. This is an ideal fluid with no shear forces between particles.
iii. No water flow through the bottom, $W|_{z=-d} = \left.\frac{d\varphi}{dz}\right|_{z=-d} = 0$, where d is water depth in negative z-direction.
iv. A water particle at the surface will always remain at the surface, $\xi = \xi(x, t)$.

v. The pressure at the surface is constant and equal to the atmospheric pressure, $p = p_0$ for all $z = \xi(x,t)$.
vi. Wave form invariant in time and space.
vii. Coriolis effect neglected

In order to check that these assumptions are correct, one should optimally use real data to solve the equations. If the error between the calculated and measured data is negligible, the approximation is correct. Next, data from open sea is obtained and the equations are solved to establish under what conditions our approximations are still valid.

According to these simplifications, the wave specifics of long crested sinusoidal waves (Figure 4) given an airy/linear wave theory on deep water ($\lambda < 2d$) may be taken as in Table 3.

Table 3: Description of regular long crested waves on deep water (Gudmestad, 2015)

	Deep water ($\lambda < 2d$)
Wave number	$k_i = {2\pi}/{\lambda}$
Wave angular frequency	$\omega = {2\pi}/{T}$
Wave frequency	$f = {1}/{T}$
Velocity potential	$\varphi = \frac{g\xi_0}{\omega} e^{k_i z}\cos(\omega t - k_i x)$
Connection between wave number k_i and circular frequency ω	$\frac{\omega^2}{g} = k_i$
Connection between wavelength λ and wave period T (Dispersion relation)	$\lambda = \frac{g}{2\pi} T^2$
Wave profile	$\xi = \xi_0 \sin(\omega t - k_i x)$
Dynamic pressure	$p_d = \rho g \xi_0 e^{k_0 z} \sin(\omega t - k_i x)$
Phase velocity	$v = {\lambda}/{T} = {\omega}/{k_i}$
x-component of velocity	$v_x = \omega \xi_0 e^{k_i z} \sin(\omega t - k_i x)$
z-component of velocity	$v_z = \omega \xi_0 e^{k_i z} \cos(\omega t - k_i x)$
x-component of acceleration	$a_x = \omega^2 \xi_0 e^{k_i z} \cos(\omega t - k_i x)$
z-component of acceleration	$a_z = -\omega^2 \xi_0 e^{k_i z} \sin(\omega t - k_i x)$

Wave Length (λ): The wave length λ is the distance between successive crests.
Wave Period (T): Time for two successive crests to pass a particular point.
ξ_0: Wave amplitude
g: Acceleration of gravity
t: Time variable
x: Direction of wave propagation
z: Vertical coordinate with positive upwards
$p_d - \rho g z + p_0$: Total pressure in the fluid
p_0 : Atmospheric pressure
p_d: Pressure at depth (d)

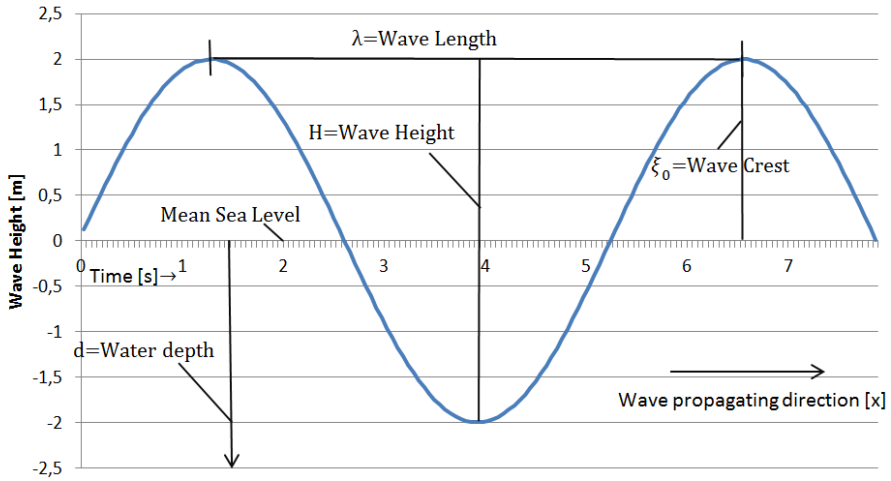

Figure 4: Illustration of some wave parameters of a regular sinusoidal wave profile

Whereas long crested waves are based on linear theory, the real ocean environment is irregular and random in nature. If one assumes that waves are propagating in the same direction, the real sea surface can be expressed by a linear superposition of a series of regular sinusoidal waves. This is called short crested waves and can be described as (Faltinsen, 1990):

$$\xi = \sum_{i=1}^{n} \xi_{0i} \sin(\omega_i t - k_i x + \varepsilon_i) \tag{14}$$

Where n is the number of regular wave components.
ε_i is the random phase angle considered to be uniformly distributed between 0 and 2π.

Wave elevation is commonly assumed Gaussian distributed with a mean value of 0 and variance σ^2. Looking at a shorter time frame, usually 3 hours, the wave process may be considered stationary, meaning that within this period the mean value and variance of the process will remain constant.

When evaluating the force response of a structure, an appropriate method for finding a correct value must be established. For simplicity, a regular sinusoidal wave with a given period and height may be used when assessing the extreme response. However, more accuracy may be needed. Therefore, for short term sea states, a random irregular ocean wave can be described by an energy density spectrum where statistical parameters are present. A wave spectrum may be given in a table form, or as a parameterized analytic formula. The wave spectrum ($S_{\Xi\Xi}$) can then be used to describe the energy content of a wave and its distribution over a frequency range of the random wave.

In order to decide on a suitable spectra, information on the geographical area, local bathymetry, and environmental conditions (wind, current, tides and general weather considerations) contributing to the sea state characteristics needs to be assessed (DNV-RP-C205, 2010, 3.5.2.2).
A wave spectrum is defined in such way that (Haver, 2015):

$$S_{\Xi\Xi}(\omega_i) = \frac{\xi_{0,i}^2}{2\Delta\omega} \tag{15}$$

Where $\xi_{0,i}$ and ω is the amplitude and angular wave frequency in rad/s of wave component *i*, whereas $\Delta\omega$ is the difference between successive wave frequencies:

$$\Delta\omega = \frac{\omega_n - \omega_1}{n-1} \tag{16}$$

Or as a frequency wave spectrum in Hertz as:

$$S_{\Xi\Xi}(f_i) = S_{\Xi\Xi}(\omega_i) * 2\pi \tag{17}$$

The variance of the sea state is equal to the first order moment:

$$M_0 = {\sigma_{\Xi\Xi}}^2 = \int_0^\infty \omega^0 S_{\Xi\Xi}(\omega) d\omega = \sum_{i=1}^{n} S_{\Xi\Xi}(\omega_i) * \Delta\omega \tag{18}$$

Several ocean spectrums are created and used to cope with different scenarios. They all build on observed properties of ocean waves, and are therefore empirical in nature. In Orcaflex, five different spectrums can be used to describe irregular waves: JONSWAP, the ISSC model, Ochi-Hubble, Torsethaugen, and Gaussian swell. Other common spectrums are the Pierson-Moskowitz and the Brethschneider. The main difference between these is that for a given energy content, the frequency band distributes the energy unequally. This means that different spectrums give different responses of a structure/object for the same wave energy.

Before going in depth on some of the most commonly used spectrums for lifting applications offshore, some relevant definitions must be established to understand the models fully.

Wind sea: A wind sea refers to a sea state developed by a local wind field. A wind sea may be further divided into either a growing wind sea or fully developed wind sea. A growing wind sea starts when turbulence in the wind produces random pressure fluctuations at the sea surface, thereby producing small waves. These small waves will eventually grow as the wind continues to produce pressure differences along the wave profiles. A fully developed wind sea is a condition where the wind has blown steadily for a long time ($Time > 10000\ wave\ periods$) over a large area ($Area > 5000\ wave\ lengths$), and equilibrium of the sea state has been reached. The spectrum form will then not change (Gudmestad, 2015).

Swell sea: A swell sea can be viewed as the period after a wind sea has been generated, and the local wind strength is reduced or moved to another area. Often, this type of sea state is characterized by low frequencies and long wave periods compared to the height of the corresponding waves. The dispersion relationship (Table 3) gives that swell waves are traveling faster than wind generated waves.

Combined sea: A combined sea state is a combination between wind- and swell sea. This sea state is most often the case and should be used for most problems under consideration.

3.2.1.1 Pierson-Moskowitz spectrum

The *Pierson-Moskowitz* spectrum is developed by Pierson and Moskowitz (1964). The spectrum is derived from data collection in the North Atlantic Ocean, and is representative for fully developed sea states in an open sea condition. To check whether the sea state is fully developed or not, Haver (2013, p.149) proposed the following formula for checking if the spectrum is suitable:

$$t_p \approx 5\sqrt{h_s} \tag{19}$$

The Pierson-Moskowitz spectrum has the shape (DNV-RP-H103, 2014, 2.2.6.2):

$$S_{PM}(\omega) = \frac{5}{16} * H_s^2 {\omega_p}^4 * \omega^{-5} * exp\left(-\frac{5}{4}\left(\frac{\omega}{\omega_p}\right)^{-4}\right) \tag{20}$$

Where ω is the wave angular frequency in rad/s, and ω_p is the angular spectral frequency in rad/s ($^{2\pi}/_{T_p}$).

The relation between T_z and T_p can be taken as $T_p = 1.4T_z$ (DNV-RP-H103, 2014, 4.3.2.1).

3.2.1.2 JONSWAP spectrum

The JONSWAP spectrum (Joint North Sea Wave Observation Project), where theory is proposed by Hasselman (1973), is at present time the most commonly used spectrum for the North Sea area. The spectrum is formulated as a modification of the Pierson-Moskowitz spectrum for a developing sea state in a fetch limited situation (Figure 5). The difference is that in the JONSWAP spectrum waves continue to grow with distance (or time), given by the A_γ-term. Also, the peak (γ_2) is more pronounced and leads to nonlinear interactions (Gudmestad, 2015). It is described using five parameters, where only two of them, ω_p and H_S, varies when the spectrum has been applied to a location. The spectrum is modified from the PM spectrum as (DNV-RP-H103, 2014, 2.2.6.2):

$$S_J(\omega) = A_\gamma * S_{PM}(\omega) * {\gamma_2}^{exp\left\{-0.5\left(\frac{\omega-\omega_p}{\omega_p\sigma}\right)^2\right\}} \tag{21}$$

Where σ is given as (Hasselmann, 1973):

$$\sigma = \begin{cases} 0.07\ for\ \omega \leq \omega_p \\ 0.09\ for\ \omega \geq \omega_p \end{cases} \tag{22}$$

If no particular peak value has been applied, the peak enhancement factor can be calculated from DNV-RP-H103 (2014, 2.2.6.9):

$$\gamma_2 = \begin{cases} 5 & for\ \frac{t_p}{h_s} \leq 3.6 \\ exp\left\{5.75 - 1.15\frac{t_p}{\sqrt{h_s}}\right\} & for\ 3.6 < \frac{t_p}{\sqrt{h_s}} < 5 \\ 1 & for\ \frac{t_p}{\sqrt{h_s}} > 5 \end{cases} \quad (23)$$

A_{γ_2} in a normalizing factor taken as $1 - 0.287\ln(\gamma_2)$.

Further, T_z is related to T_p by the following relation (DNV-RP-H103, 2014, 2.2.6.8):

$$\frac{T_z}{T_p} = 0.6673 + 0.0503\gamma_2 - 0.006230{\gamma_2}^2 + 0.0003341{\gamma_2}^3 \quad (24)$$

Based on Haver (2013, p.118), the JONSWAP may be applicable for sea states not far from the relation given by Torsethaugen (2004):

$$t_{p0} = 0.78 f_e^{\frac{1}{6}} h_s^{\frac{1}{3}} \quad (25)$$

Where f_e is the effective fetch length.

Typically, the JONSWAP is applicable for (DNV-RP-H103, 2014, 2.2.6.7):

$$3.6 < {T_p}/{\sqrt{H_s}} < 5 \quad (26)$$

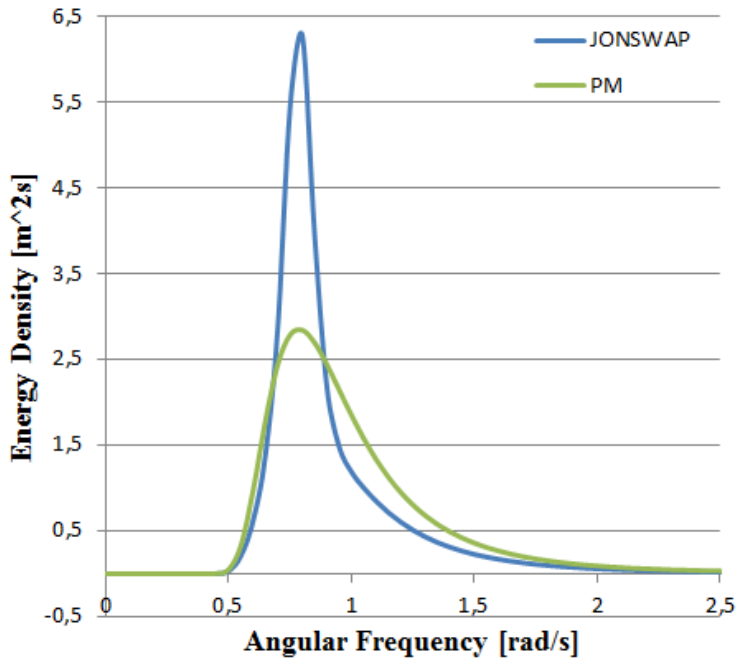

Figure 5: PM and JONSWAP wave spectrums for H_s=3m and T_p=5s

3.2.1.3 Torsethaugen spectrum

The Torsethaugen spectrum, developed by Torsethaugen (2004) is based on measurements from the Norwegian Continental Shelf (Statfjord and Haltenbanken). The spectrum is based on a superposition of two JONSWAP spectra fitted together; one representing wind sea while the other is representing swell sea. These two spectra are then divided by the spectral peak period (T_{PF}) to form a fully developed sea at the location under consideration.

One has that for:

- Wind dominating sea: $T_P < T_{PF}$
- Swell dominated sea: $T_P > T_{PF}$

This spectrum is dependent upon the significant wave height (H_S) and the spectral peak period (T_P). There is also need for complex residual parameters. In order to avoid this complexity, Torsethaugen and Haver (2004) developed a new spectral model sumarized in Appendix 1. The reason for this simplified model was to reduce the use of free parameters only of concern at lower sea states, thereby not applicable for design loads. Therefore, the spectrum proposed was only defined by H_S and T_P, parameterized by regression analysis and curve fitting.

When analysing a sea state using a spectrum, a long crested sea state may be used with good results. Anyway, the effects of short crested waves where different wave directions are taken into accounted may be important and affect the results obtained in a time domain analysis (DNV-RP-H103, 2014, 4.3.3.8). A uni-directional spectra reads (DNV-RP-H103, 2014, 2.2.7.1):

$$S(\theta,\omega) = S(\omega)D(\theta,\omega) = S(\omega)D(\theta) \tag{27}$$

Where θ is the angle between the direction of elementary wave trains and gives the main direction of the short crested wave system.

A double peaked wave spectrum are then taken as (DNV-RP-H103, 2014, 2.2.7.1):

$$S(\theta,\omega) = S_{wind\ sea}(\omega)D_{wind\ sea}(\theta) + S_{swell}(\omega)D_{swell}(\theta) \tag{28}$$

Where:
$S_{wind\ sea}(\omega)$: Wave spectrum for pure wind sea
$S_{swell\ sea}(\omega)$: Wave spectrum for pure swell sea

The directional spreading of the spectrum is:

$$D(\theta) = \frac{\Gamma\left(1+\frac{n}{2}\right)}{\sqrt{\pi}\Gamma\left(\frac{1}{2}+\frac{n}{2}\right)} cos^n(\theta-\theta_p) \tag{29}$$

Where Γ is the Gamma function, and $\left|\theta - \theta_p\right| \leq \frac{\pi}{2}$. The constant n is typically 2 or 4 for wind sea, wheras for swell it is to be taken as equal to or greater that 6 (DNV-RP-C205, 2010, 3.5.8.6).

4. Extreme loads and responses

When considering responses in a given sea state, separate analysis from repeated simulations should be carried out to determine the conditional distribution of the maximum responses. Using the analogy of continuous probability distributions, the cumulative density function of the extreme response for an irregular short term sea state can be expressed as (Cheng, 2002):

$$F(x) = \iint_{H_S,T_Z,\overline{U}} F(x|\overline{U},H_s,T_z) * f(\overline{U},H_s,T_z) d\overline{U} dH_s dT_z \quad (30)$$

Where:
x is the response variable
$f(\overline{U},H_s,T_z)$ is the joint probability density for the parameters; and
$F(x|\overline{U},H_s,T_z)$ is the conditional distribution of the maximum response.

As some operations may last for a long-term period (i.e. more than 3 hours), it can be assumed that the different (stationary) sea states are independent and the probability of non-exceedance for a maximum response in a number of sea states is therefore:

$$F(x) = (F(x))^N \quad (31)$$

Where N is the number of independent sea states in a period of time and x is the maximum response in N number of sea states.

4.1 Characteristic Most Probable Largest Load

When evaluating the characteristic largest load, the total load is either a combination of a static and a dynamic force component (where no slack in wire), or a combination of static- and snap forces from a wire that has undergone slack. According to DNV-RP-H103 (2014, 3.4.3), by assuming that incoming waves and the resulting dynamic peak loads follows a Rayleigh distribution, the most probable largest maximum load, R_{max}, may be found by the following calculation:

$$R_{max} = \sigma_r \sqrt{2ln\left(\frac{t}{T_z}\right)} = \sigma_r \sqrt{2ln(\overline{n})} \quad [N] \quad (32)$$

Where t is the time under consideration in seconds and $\overline{n}$ is the number of maxima observed. σ_r is the standard deviation of the load responses (x_i):

$$\sigma_r = \sqrt{\frac{1}{N}\sum_{i=1}^{N}(x_i - \bar{x})^2} \quad (33)$$

The average zero-up-crossing period T_z represents the average time interval between two successive up-crossings of the load process:

$$T_z = 2\pi * \sqrt{\frac{m_0}{m_2}} \tag{34}$$

Where the moments of the load spectrum reads:

$$m_n = \int_0^\infty \omega^n S(\omega) d\omega_n = \int_0^\infty f^n S(f) df\,, \quad n = 0,1,2,\ldots. \tag{35}$$

Anyway, DNV-RP-H103 (2014, 3.4.3.5) also gives us the guidance note that:
"In most dynamic non-linear cases the response does not adequately fit the Rayleigh distribution. The estimated maximum load should therefore always be compared with the largest observed load in the simulation".

4.2 Study of Most Probable Largest Load

To evaluate the most probable largest load as described by DNV, one can consider that a variable is of an additive nature, meaning that several sources of similar effect contribute to its value. A Gaussian model would then be a reasonable choice. Therefore, with the assumption of linearity, a response process can be modeled as a Gaussian stochastic process since the sea surface elevation process is Gaussian (Haver, 2015).

Further, as a linear system's global maximum amplitude for an narrow banded process (i.e. narrow banded wave spectrum), meaning the largest response maxima between two adjacent up-crossings may be reasonably well modeled using a Rayleigh distribution (Haver, 2015):

$$f_x(x) = \frac{x}{{\sigma_r}^2} exp\left\{-\frac{1}{2}\left[\frac{x}{\sigma_r}\right]^2\right\} \tag{36}$$

Where the cumulative distribution function is:

$$F_x(x) = \int_0^x \left(f_x(x)\right) dx = 1 - exp\left\{-\frac{1}{2}\left[\frac{x}{\sigma_r}\right]^2\right\} \tag{37}$$

By assuming Rayleigh distributed and $\bar{n}$ global maxima, the characteristic largest value in a stationary sea state which is expected to be exceeded on average once every d-hour is equal to $1/\bar{n}$. The most probable largest characteristic response amplitude x is then given by:

$$1 - F_x(x) = \frac{1}{\bar{n}} \tag{38}$$

$$exp\left\{-\tfrac{1}{2}\left[\tfrac{x}{\sigma_r}\right]^2\right\} = \tfrac{1}{\bar{n}} \;\rightarrow \boldsymbol{x = \tilde{r}_{max} = \sigma_r\sqrt{2ln\bar{n}}} \tag{39}$$

This means that the level of not exceeding the given characteristic value is a factor depending on the period and corresponding global maxima number.

As the surface elevation process can be modeled as a Gaussian process, then $H_s = 4\sigma_r$. The corresponding H_s may then be calculated based on the characteristic largest ocean response amplitude (ξ) where $x = \xi$:

$$\xi = \frac{H_s}{4}\sqrt{2\ln \bar{n}} \rightarrow H_s = \frac{4\xi}{\sqrt{2\ln \bar{n}}} \tag{40}$$

In simulation software, one will be able to observe a number of realizations of the same short term sea state. Due to fluctuations in the sum given by probability density function (equation 36), the maximum value will vary. This means that the largest value observed is a variable of randomness. Assuming independent and identically distributed, the cumulative distribution function for the d-hour maximum ($x_{dh,max}$) can then be found by (Haver, 2015):

$$\begin{gathered} F_{\Xi zh}(x_{dh,max}) = \left[P(x_1 \leq x_{dh,max}) \cap (x_2 \leq x_{dh,max}) \cap \ldots \cap (x_n \leq x_{dh,max})\right] \\ F_{\Xi 3h}(x_{dh,max}) = F_x(x_{dh,max}) * F_x(x_{dh,max}) * \ldots * F_x(x_{dh,max}) \\ F_{\Xi nh}(x_{dh,max}) = \left\{F_{\Xi 3h}(x_{dh,max})\right\}^{\bar{n}_{dh}} \\ F_{\Xi 3h}(x) = \left\{1 - exp\left\{-\frac{1}{2}\left[\frac{x}{\sigma_r}\right]^2\right\}\right\}^{\bar{n}_{dh}} \\ = \left\{1 - exp\left\{-\frac{1}{2}\left[\frac{\sigma_r\sqrt{2ln\bar{n}_{dh}}}{\sigma_r}\right]^2\right\}\right\}^{\bar{n}_{dh}} \end{gathered} \tag{41}$$

$$\lim_{\bar{n}\to\infty}\left(1 - \frac{1}{n}\right)^{\bar{n}_{dh}} = e^{-1} \approx 0.3678$$

Meaning that the probability of a value above $x_{dh,max}$ can be approximated to 0.6321 as $\bar{n} \rightarrow \infty$.

The *most probable largest* value for a period of d-hour is the value with largest density, i.e. the top point in the given d-hour extreme value density function (Rayleigh^n). The value is found as:

$$f_{\Xi dh}(x) = \frac{df(F_{\Xi dh})}{dx_s} = 0$$

$$f_{\Xi dh}(x) = \frac{\bar{n}_{3h}x_s}{{\sigma_r}^2} exp\left\{-\frac{1}{2}\left[\frac{x_s}{\sigma_r}\right]^2\right\}\left\{1 - exp\left\{-\frac{1}{2}\left[\frac{x_s}{\sigma_r}\right]^2\right\}\right\}^{\bar{n}_{dh}} = 0 \tag{42}$$

Which gives the function also given in DNV-RP-H103 (2014, 2.2.8.1) as:

$$x_{MPL} = x_s * \sqrt{\frac{1}{2}ln(\bar{n}_{dh})} \tag{43}$$

Where x_s here is the significant peak response equal to $2\sigma_r$.

This means that the most probable largest value (x_{MPL}) is equal to the characteristic largest value ($\tilde{x}_{dh}$):

$$x_s * \sqrt{\frac{1}{2} ln(\bar{n}_{dh})} = \sigma_r \sqrt{2ln(\bar{n}_{dh})} \rightarrow \sigma_r \sqrt{2} \sqrt{ln(\bar{n}_{dh})} = \sigma_r \sqrt{2} \sqrt{ln(\bar{n}_{dh})} \quad (44)$$

From the probability function, an expected extreme value may be found as:

$$E[x_{max}] = \int_0^\infty x f_x(x) dx \quad (45)$$

Which after progressing the formula becomes:

$$E[x_{max}] = x_s * \sqrt{\frac{1}{2} ln(\bar{n}_{dh})} * \left(1 + \frac{0.5772}{lnN}\right)^{0.5} \quad (46)$$

The expected extreme value from equation 46 is then $\left(1 + \frac{0.5772}{lnN}\right)^{0.5}$ larger than the characteristic value determined in equation 39. The probability of exceeding this value may be determined from the CDF function, and is on average about 43% (Haver, 2016).

Conclusion:
To conclude, the probability of exceeding a given value should be taken into account when considering design values for a specific case. This should be chosen based on consequence- and safety factors from the specific case.

Given the use of a Rayleigh distribution for analyzing lifting operations through the splash zone, a long term analysis of at least 30 minutes (optimally 3 hours) has to be performed for a maximum load to be extracted correctly. For repeated lifting operations through the splash zone where an analysis last for a realistic duration (i.e. 30 $\frac{\text{second}}{\text{simulation}}$) and the maximum load is extracted from each of these simulations, a criterion of not exceeding a given upper fractile in the distribution function should be applied.

4.3 Generalized Extreme Value distribution

As stated, for a Rayleigh^n-distributed d-hour maximum:

$$f_{\Xi dh}(x) = \frac{\bar{n}_{dh} x}{{\sigma_r}^2} exp\left\{-\frac{1}{2}\left[\frac{x}{\sigma_r}\right]^2\right\}\left\{1 - exp\left\{-\frac{1}{2}\left[\frac{x}{\sigma_r}\right]^2\right\}\right\}^{\bar{n}_{dh}} \quad (47)$$

As $\bar{n} \rightarrow \infty$ and x increases, $f_{\Xi dh}(x)$ is normally decaying exponentially. The distribution of the maximum will then be characterized by a generalized extreme value probability function with a shape parameter (k) of 0:

$$f(x) = \frac{1}{\hat{\beta}}\left\{1 + k\left\{\frac{x-\hat{\mu}}{\hat{\beta}}\right\}\right\}^{-\left(\frac{1}{k+1}\right)} * exp\left\{-\left[1 + k\left(\frac{x-\hat{\mu}}{\hat{\beta}}\right)\right]\right\}^{-\left(\frac{1}{k}\right)} \quad (48)$$

Whereas the cumulative distribution function reads:

$$F(x) = 1 - \left\{1 + k\left(\frac{x-\hat{\mu}}{\hat{\beta}}\right)\right\}^{-\left(\frac{1}{k}\right)} = exp\left\{-\left[1 + k\left(\frac{x-\hat{\mu}}{\hat{\beta}}\right)\right]\right\}^{-\left(\frac{1}{k}\right)} \quad (49)$$

Where $\hat{\beta}$ is the scale parameter, $\hat{\mu}$ is the (mode) location parameter, and k is the shape parameter determining the rate of tail decay (Figure 6), with:

- $k > 0$ giving a heavy tail (Fréchet)
- $k = 0$ giving a light tail (Gumbel)
- $k < 0$ giving a short tail (Negative Weibull)

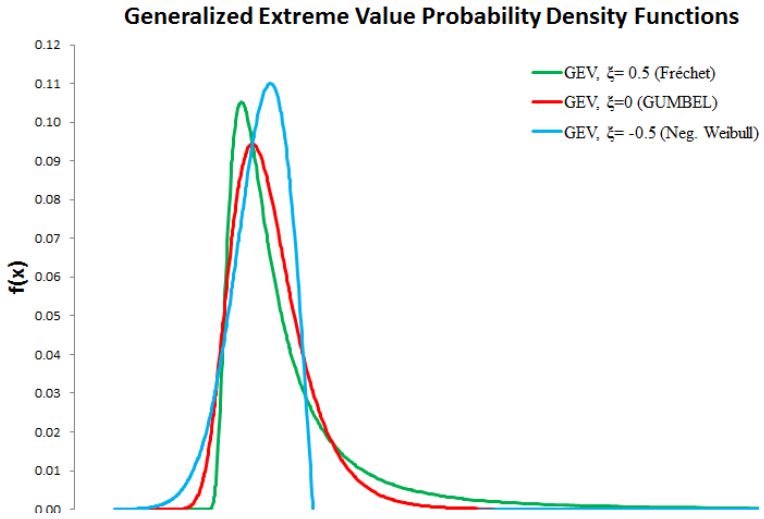

Figure 6: Typical generalized extreme value densities for different shape parameters

The inverse distribution gives the return level associated with the return period:

$$x_{p,max} = \hat{\mu} - \frac{\hat{\beta}}{k}\left[1 - \left(-lnF(x)\right)^{-k}\right] \quad (50)$$

The maximum value expected for every $\bar{n}$ global maximum is then calculated as:

$$1 - F(x) = \frac{1}{\bar{n}} \quad (51)$$

Rewriting the full term gives:

$$x_{p,max} = \hat{\mu} - \frac{\hat{\beta}}{k}\left[1 - \left(-ln\left(1 - (1/\bar{n})\right)\right)^{-k}\right] \quad (52)$$

Where the return level is given as:

$$T_R = \frac{1}{1 - F(x)} \quad (53)$$

As the shape parameter (k) for a maximum given a Gumbel distribution can be equaled to zero, the Gumbel probability function applies as:

$$f_x(x) = \frac{1}{\hat{\beta}} exp\left\{-\frac{x-\hat{\mu}}{\hat{\beta}} - exp\left\{-\left[\frac{x-\hat{\mu}}{\hat{\beta}}\right]\right\}\right\} \tag{54}$$

The Gumbel cumulative distribution functions for maximum and minimum values are then given by:

$$\begin{aligned} CDF_{max} = F_x(x) &= \int_0^x f_x(x)dx = exp\left\{-exp\left\{-\left[\frac{x-\hat{\mu}}{\hat{\beta}}\right]\right\}\right\} \\ &= exp\left\{-exp\left\{-\left[\frac{x-\sigma_r\sqrt{2\ln(n_{3h})}}{\frac{\sigma_r}{\sqrt{2\ln(n_{3h})}}}\right]\right\}\right\} \end{aligned} \tag{55}$$

$$\begin{aligned} CDF_{min} = 1 - F_x(x;\mu,\beta) &= 1 - \int_0^x f_x(x)dx \\ &= 1 - exp\left\{-exp\left\{-\left[\frac{x-\hat{\mu}}{\hat{\beta}}\right]\right\}\right\} \end{aligned} \tag{56}$$

By using moments estimators $(\hat{\mu}, \hat{\beta})$, the mean $(\bar{x})$ and standard deviation (σ_r) of the force responses are used to determine these parameters. The mode parameter is determined from:

$$\hat{\mu} = \bar{x} - C_2\,\hat{\beta} \overset{\bar{n}\to\infty}{\cong} \bar{x} - \gamma\hat{\beta} \tag{57}$$

Where γ is the Euler-Mascheroni constant which is equal to 0.5772 when the selection $(\bar{n})$ goes towards infinity. When limited sample size, the constant C_2 should be used (Table 4).
$\bar{x}$ is here the expected extreme value from a set of extremes (x_i):

$$\bar{x} = \frac{\sum_{i=1}^{n} x_i}{\bar{n}} \tag{58}$$

While the estimated β-dispersion relation reads:

$$\hat{\beta} = \frac{\sigma_r}{C_1} \overset{\bar{n}\to\infty}{\cong} \frac{\sigma_r * \sqrt{6}}{\pi} \tag{59}$$

Where C_1 is a constant given in Table 4.

The standard deviation (σ_r) of the extreme wire tensions can be calculated by:

$$\sigma_r = \sqrt{\frac{1}{N}\sum_{i=1}^{N}(x_i - \bar{x})^2} \tag{60}$$

Table 4: Gumbel constants given by Moan, Spidsøe and Haver (1980)

$\bar{n}$	C_1	C_2	$\bar{n}$	C_1	C_2
10	0.9497	0.4952	**80**	1.19382	0.55688
20	1.06283	0.52355	**100**	1.20649	0.56002
30	1.11238	0.53622	**250**	1.24292	0.56878
40	1.14132	0.54362	**500**	1.25880	0.57240
50	1.16066	0.54854	**1000**	1.26851	0.57450
60	1.17467	0.55208	**Infinity**	1.28255	0.57722

To estimate the maxima with a given probability of occurrence p, one may utilize the equation for a Gumbel cumulative distribution function:

$$F_x(x_p) = exp\left\{-exp\left\{-\left[\frac{x_p - \hat{\mu}}{\hat{\beta}}\right]\right\}\right\} = 1 - p$$

$$\left\{-exp\left\{-\left[\frac{x_p - \hat{\mu}}{\hat{\beta}}\right]\right\}\right\} = \ln(1-p)$$

$$\left[\frac{x_p - \hat{\mu}}{\hat{\beta}}\right] = -\ln(-\ln(1-p))$$

$$x_{p,max} = \hat{\mu} - \hat{\beta}\left[ln\left(-ln(1-p)\right)\right] \quad (61)$$

One may also establish a characteristic value which is not exceeded with a probability p during a sea state of n-hours. From the formula (41) one gets:

$$F_{\Xi nh}(x_p) = \left\{1 - exp\left\{-\frac{1}{2}\left[\frac{x_p}{\sigma_r}\right]^2\right\}\right\}^{\bar{n}} = p \quad (62)$$

$$x_p = \sigma_r\sqrt{\left[-2ln(1-p)^{1/\bar{n}}\right]} \quad (63)$$

If the acceptance probability is p for every z-hour event, the return period (T_R) of the maximum allowable value is:

$$T_R = \frac{1}{p} * (\frac{\mathrm{t}}{3600}) \quad (64)$$

Where t is given in seconds.

The probability of exceeding the return crest height is given by:

$$P\left(x \le x_{T_R}\right) = 1 - P\left(x > x_{T_R}\right) = 1 - p^{\bar{n}} \quad (65)$$

$$\rightarrow P\left(x > x_{T_R}\right) = 1 - [(1-p)^{\bar{n}}] \quad (66)$$

5. Lifting operation through the splash zone

In a lifting phase offshore, the lifted object is exposed to dynamic loads due to incoming waves and motions of the vessel and crane tip. A general offshore lift will consist of (1) liftoff from deck and over the vessel side, (2) lowering through the splash zone, (3) further lowering through the water columns, and commonly (4), landing of the object where applicable. Although the liftoff phase may cause a pendulum motion of the structure and therefore very often be a limiting criterion for large structures due to deck handling constrains, focus in this thesis will be on the extreme direct wave loading forces experienced in the splash zone due to significant water particle velocities and accelerations. As the lifting phase through the splash zone only lasts for a shorter timeframe, the hydrodynamic forces are highly dependent upon the incoming wave(s). The following sections in chapter 5 will therefore give a representation of some of the physical phenomena expected during a splash zone lift, and how they will affect a lifted object.

5.1 Splash zone loads

When lifting an object from the vessel deck and through the splash zone, large forces may occur depending on the size and steepness of the waves present, and where the object hits the incoming wave(s). The corresponding forces from irregular waves determine the operational wave height criteria to be set. These forces also contribute to a characteristic load condition which is the basis for dimensioning and design of the object, the crane/LARS and its fundament, and the wire used for lifting. It is therefore of high priority to establish these forces as accurately as possible in order to reduce downtime of the vessel, and increase the safety of lifting operations.

5.1.1 Weight of Structure

According to DNV-RP-H103 (2014, 3.2.3.6), the weight of an object submerged can be taken by the weight of a structure in air (W_0) and subtracting the buoyancy force (F_B).

$$W = W_0 - F_B = (M - \rho V)g \tag{67}$$

Where M is the total mass of the object, V is submerged volume, ρ is the density of salt water and g is the acceleration of gravity.

5.1.2 Hydrodynamic forces

Hydrodynamic loads relevant for the splash zone area are by Faltinsen (1990) categorized into two separate problems; (1) radiation, and (2) wave excitation. Both of these problems are described by linear dynamic loads and motions in regular waves. The radiation problem represents the waves generated by the vessel due to its motions. Radiation effects can be considered both negative and positive. Positive if radiated waves are far from the phase of

any incoming waves, providing neutralizing effects. Negative if they are close to the natural frequency, thereby increasing the amplification and corresponding motions. Effects caused by radiation can be reduced by forcing the vessel to oscillate in all 6 degrees of freedom (DOF) without incident waves. The hydrodynamic loads in the radiation scenario are the added mass, damping, and restoring forces.

The wave excitation problem is represented by the Froude-Kriloff and diffraction forces. The Froude-Kriloff forces represent the forces acting on the structure from wave propagating pressure. The diffraction forces recover impermeability and cause a flow due to the presence of the structure.

Due to linearity, the excitation and the diffraction problems may be added together as a representation of the hydrodynamic force F_H. The total time domain force in vertical direction can then be taken as (Sandvik and Kopsov, 1995):

$$F_H + F_L - W = F_R \tag{68}$$

Where F_H is representing the hydrodynamic forces and F_L is the main lift line forces.

The issue of excitation can be solved by restraining the object from oscillatory motions, and allowing for incoming waves to interact with the object. Analysis performed in Orcaflex is based on the assumption that the lifted object is small compared to the wave length and that wave diffraction can be ignored for most structures. However, as some structures have a size comparable to the relevant wave lengths, a small body assumption may give conservative lift line forces in the splash zone (Sandvik and Kopsov, 1995).

The radiation force F_R is determined from the velocity ($\dot{x}$) and acceleration ($\ddot{x}$) of the object. Due to the proximity to the free surface, the hydrodynamic forces will be dependent upon the distance to the free surface (Sandvik and Kopsov, 1995):

$$F_R = \frac{d}{dt}(M\dot{x}) + B_1\dot{x} + B_2\dot{x}|\dot{x}| \tag{69}$$

Where $\dot{x}$ is the relative velocity of the object, and M is here the sum of structural and added mass:

$$\begin{aligned} M &= M_s + A_{33} \\ &= M_s + \rho V C_a \end{aligned} \tag{70}$$

B_1 and B_2 is the linear and quadratic drag constants representing hydrodynamic damping in an oscillatory flow. These are further discussed in section 5.1.4.

The mass variations with time can be represented as (Sandvik and Kopsov, 1995):

$$\frac{d}{dt}(M\dot{x}) = M\ddot{x} + \rho\dot{x}\frac{d(C_a V)}{dt} = M\ddot{x} + \frac{dA_{33}}{dt}\dot{x} \tag{71}$$

M coupled with acceleration ($\ddot{x}$) gives the inertia term. The mass variations with time are then calculated from the position dependent added mass representing vertical slamming forces.

The wave forces (F_W) is dependent upon water particle velocities (v_w) and accelerations (a_w). The equation is given as:

$$F_W = \rho V a_w + \frac{d}{dt}(A_{33} v_w) + F_{HD} \tag{72}$$

$$= (\rho V + A_{33}) a_w + \frac{dA_{33}}{dz}\frac{dz}{dt}(a_w) + F_{HD} \tag{73}$$

The first part of the wave force equation is the pressure gradient due to the waves, whereas the second equation is the change of fluid momentum. The second part is also associated with the slamming force. The last part of the equation (F_{HD}) is the hydrodynamic drag (or damping) and is expressed in the same manner as the damping terms in equation (69), but also dependent on the water particle velocity (v_w).

The general time-domain representation of the total hydrodynamic forces acting on a lifted object offshore may then be taken as a combination of the body reaction- and wave forces (Øritsland and Lehn, 1989):

$$\underbrace{(M_s + A_{33})\ddot{x}}_{Inertia\ force} = \underbrace{B_1 v_r}_{Linear\ damping} + \underbrace{B_2 v_r |v_r|}_{Quadratic\ damping} + \underbrace{(\rho V + A_{33}) a_w}_{Wave\ forces} + \underbrace{\frac{dA_{33}^{\infty}}{dt} v_r}_{Slamming} - \underbrace{W}_{Weight} + \underbrace{F_L(t)}_{Line\ force} \tag{74}$$

Here, v_r is the characteristic vertical velocity between the object system and the water particles. The added mass A_{33}^{∞} in the slamming equation is an expression of the high-frequency limit added mass, which assumes that the water particle accelerations due to the slamming effects are much larger than the acceleration of gravity.

The slamming force may also be taken as (DNV-RP-H103, 2014, 3.2.9):

$$F_s = \frac{d(A_{33}^{\infty} v_s)}{dt} = \frac{1}{2}\rho C_s A_p v_r^2 \tag{75}$$

Where A_{33}^{∞} is the instantaneous high-frequency limit heave added mass, and A_p is the horizontal projected area of the object.

The slamming coefficient (C_s) may be taken as a function of the rate of change of the sectional added mass (A_{33}^0) with submergence z:

$$C_s = \frac{2}{\rho A_p}\frac{dA_{33}^0}{dz} \tag{76}$$

For cases where an object is lifted through the upper water columns, the slamming force can be taken as:

$$F_s = \frac{1}{2}\rho C_s A_p(\dot{\varsigma} - \dot{\eta}) \tag{77}$$

$\dot{\varsigma}$ is the vertical velocity of the sea surface, and $\dot{\eta}$ is the vertical motion of the object.

Another force present during recovery of a structure is the water exit force F_e:

$$F_e = -\frac{1}{2}\rho C_e A_p v_e^2 \tag{78}$$

v_e is the water exit velocity.

This force is a function of the water exit coefficient C_e:

$$C_e = -\frac{1}{\rho A_p}\frac{dA_{33}^0}{dz} = \frac{C_s}{2} \tag{79}$$

It should also be noted that other phenomenon's like vortex shedding and air-cavity entrapment can occur dependent on how the structure and the waves interact.

5.1.3 Slamming forces

During lifting operations offshore, the resulting hydrodynamic forces are highly dependent upon the incoming wave(s). Therefore, nonlinear effects from slamming and drag may vary significantly from lift to lift in quite similar wave conditions. Slamming loads will appear in milliseconds as vertical impulse loads on the object with corresponding high pressure peaks. Therefore, as the relative velocity between the object and the fluid flow increases, the slamming impact increases too. Also, slamming increases as the impact angle (θ) decreases. The resulting slamming impact on an object will be determined from the structure water absorption capabilities. Slamming forces will generally decrease as the object moves through the water columns (Faltinsen, 1990).

When lifting an object, the payout rate remains constant. As an impulse load strikes the object in positive upwards direction, a decrease in wire tension and vertical speed causes a peak load to occur. Worst case scenario would be if the wire goes slack, causing snap loads critical to the capacity of the lifting system/object. The number of cases where a slack in the wire occurs is expected to increase with decreasing weight of the object and with rapid/large vessel motions. Also, the severity usually increases with the duration of slack. Cases involving slack is hard to predict accurately due to the nonlinearities present, but can be predicted using statistical methods as discussed throughout this thesis.

5.1.4 Drag forces

When incoming waves gets in contact with an object, linear drag forces result onto the object. A representative formula for viscous drag force can be expressed by the Morison equation (DNV-RP-H103, 2014, 3.2.8.1):

$$F_d = \frac{1}{2}\rho C_D A_p v_r |v_r| \tag{80}$$

By introducing the Keulegan-Carpenter number (N_{K-C}) for irregular wave conditions one may further evaluate this definition in relation to lifting operations (DNV-RP-H103, 2014, 3.2.8.3):

$$N_{K-C} = \frac{(\sqrt{2}\sigma_w)T_z}{D} \tag{81}$$

Where T_z is the zero up-crossing period, σ_w is the standard deviation of water particle velocity, and D is the characteristic dimension of the structural member.

The N_{K-C} number is a representation of how the flow acts. Low numbers of N_{K-C} means that the flow oscillates fast. For lifting operations offshore, the Keulegan-Carpenter number can usually be taken as lower than 10. This means that flow particles travel less than 10 times the characteristic length of the body during one oscillation. In such cases, the drag and damping terms may instead be taken as the sum of a linear and quadratic term, B_1 and B_2 respectively (DNV-RP-H103, 2014, 3.2.8.2). In oscillatory flow with low KC numbers, the drag coefficient is typically in the order of 2-3 times the steady state drag coefficient C_{DS} (Øritsland and Lehn, 1989). Therefore, by ignoring oscillatory flow, underestimation of the damping and overestimation of resonant motions is likely (DNV-RP-H103, 2014, 4.6.2.2).

By considering a linear and quadratic drag term, coefficients dependent on wave amplitudes may be replaced. The linear and quadratic damping coefficients can be taken as (DNV-RP-H103, 2014, 3.2.8.8):

$$B_1 = \frac{2\rho A_p \sqrt{2gD}}{3\pi^2} b_1 \tag{82}$$

$$B_2 = \frac{1}{2}\rho A_p b_2 \tag{83}$$

Where b_1 and b_2 are non-dimensional damping coefficients. By assuming that the damping energy is dissipated throughout the quadratic term, B_1 and B_2 can be simplified to form the drag term of Morison`s formula (DNV-RP-H103, 2014, 3.2.8.7):

$$C_d = \frac{b_1}{\omega'} + b_2 \tag{84}$$

Where ω' is the non-dimensional frequency of oscillations:

$$\omega' = \omega\sqrt{\frac{D}{2g}} \tag{85}$$

6. Analysis of ROV lift operation

6.1 Orcaflex theory

Orcaflex, developed by Orcina, is a world leading time- and frequency domain element program serving the global offshore market. It`s main use lies within static and dynamic analysis of offshore systems as risers, mooring systems, towing systems, and installation/lifting cases. This section will describe the program as represented in the OrcaFlex User Manual, (Orcina, 2015).

In order to provide a start configuration for a dynamic simulation as well as determine the conditions of equilibrium of the system under weight, buoyancy, hydrodynamic drag, etc. in a dynamic analysis; a static analysis is performed in three iterative steps (Orcina, 2015, Section 5.5). First, a dynamic analysis over a preset time period is initiated from the initial conditions calculated by the static analysis. The dynamic analysis is then separated into two steps; the build-up and the simulation period. The build-up period is where the waves and the system under consideration are developed from a static state to a fully developed dynamic condition. This step helps to reduce transients when changing from a static position to a dynamic motion. The final simulation step is directed towards solving the dynamic equations in the time domain.

6.2 Dynamic time domain analysis

Although some hydrodynamic loads not influenced by the proximity of boundaries (i.e. seabed and water surface) can be described by linear wave theories in a frequency domain approach, this is not always the case. In the splash zone, large nonlinearities are present causing a linear approach to be inaccurate. Therefore, non-linear waves and extreme load effects are preferably handled in time-domain using step-by-step integration methods (DNV-RP-H103, 2014, 2.3.6.1). A wave spectrum is then used to simulate irregular wave kinematics by generating random time series.

An object will during a lift be exposed to the direct wave loading, but also some load caused by vessel motions. A time-domain analysis is able combine these loads, and handles non-linear hydrodynamic load effects and force coefficients that occurs through a wave period. It will also cover non-linear interaction effects such as transient response after slamming or snatch loading. Also, such an analysis would give the response statistics without making assumptions regarding the response distribution (DNV-RP-H103, 2014, 2.3.6.2).

Let us consider the case of a single degree of freedom (SDOF) system:

$$F(t) = M\ddot{x}(t) + C\dot{x}(t) + Kx(t) \tag{86}$$

Where M is the system mass, C is the system damping, K is the system stiffness, and F is the external loads in the time domain.

The differential relations between acceleration $\ddot{x}(t)$, speed $\dot{x}(t)$, and velocity $x(t)$ is given as:

$$\ddot{x}(t) = \frac{d\dot{x}(t)}{dt} \tag{87}$$

$$\dot{x}(t) = \frac{dx(t)}{dt} \tag{88}$$

Assuming that one knows the motion quantities at time t and the acceleration of motion over the time interval $t + h$, one can determine the speed and displacement by:

$$\dot{x}(t+h) = \dot{x}(t) + \int_0^h \ddot{x}(t)d\tau \tag{89}$$

$$x(t+h) = x(t) + \int_0^h \dot{x}(t)d\tau \tag{90}$$

In Orcaflex, two complementary dynamic integrations methods may be used to solve the dynamic equation, either explicit or implicit. The implicit method uses a generalized α integration, while the explicit is a forward Euler integration. Both of these methods are generalizations of the Newmark-beta method (Newmark, 1959):

$$\dot{x}(t+h) = \dot{x}(t) + (1-\gamma)\ddot{x}(t) + \gamma\ddot{x}(t+h) \tag{91}$$

$$x(t+h) = x(t) + h\dot{x}(t) + \left(\frac{1}{2} - \beta\right)h^2\ddot{x}(t) + \beta h^2\ddot{x}(t+h) \tag{92}$$

Further, a simplification based on a constant acceleration over the time interval means that $\gamma = \frac{1}{2}$ and $\beta = \frac{1}{4}$:

$$\ddot{x}(\varepsilon) = \frac{1}{2}\big(\ddot{x}(t) + \ddot{x}(t+h)\big), \qquad t \le \varepsilon \le t+h \tag{93}$$

Putting equation 93 into equation 90 gives:

$$\begin{aligned} \dot{x}(t+h) &= \dot{x}(t) + \frac{1}{2}\big(\ddot{x}(t) + \ddot{x}(t+h)\big)\int_0^h d\tau \\ &= \dot{x}(t) + \frac{1}{2}h\big(\ddot{x}(t) + \ddot{x}(t+h)\big) \end{aligned} \tag{94}$$

$$\begin{aligned} x(t+h) &= x(t) + \int_0^h \left(\dot{x}(t) + \frac{1}{2}\varepsilon(\ddot{x}(t) + \ddot{x}(t+h))\right)d\varepsilon \\ &= x(t) + \dot{x}(t)h + \frac{1}{4}h^2\big(\ddot{x}(t) + \ddot{x}(t+h)\big) \end{aligned} \tag{95}$$

Next, one can calculate the state one step length ahead of the known state by taking h as equal to a step length. One can then use that $x_i = x(t),\ x_{i+1} = x(t+h),\ \dot{x}_i = \dot{x}(t),\ \dot{x}_{i+1} = x(t+h),\ \ddot{x}_i = \ddot{x}(t)\ and\ \ddot{x}(t+h)$. With these notations one denote a step by step method as:

$$\dot{x}_{i+1} = \dot{x}_i + \frac{1}{2}(\ddot{x}_i + \ddot{x}_{i+1})h \tag{96}$$

$$x_{i+1} = x_i + \dot{x}_i h + \frac{1}{4}(\ddot{x}_i + \ddot{x}_{i+1})h^2 \tag{97}$$

Rewriting equation (97):

$$\ddot{x}_{i+1} = \frac{4}{h^2}x_{i+1} - \frac{4}{h^2}x_i - \frac{4}{h}\dot{x}_i - \ddot{x}_i \tag{98}$$

Introducing equation (97) into equation (96) gives:

$$\dot{x}_{i+1} = \dot{x}_i + \frac{1}{2}h\left(\ddot{x}_i + \frac{4}{h^2}x_{i+1} - \frac{4}{h^2}x_i - \frac{4}{h}\dot{x}_i - \ddot{x}_i\right) = \frac{2}{h}x_{i+1} - \frac{2}{h}x_i - \dot{x}_i \tag{99}$$

The motion at step $i+1$ is thus:

$$M\ddot{x}_{i+1} + C\dot{x}_{i+1} + Kx_{i+1} = F_{i+1} \tag{100}$$

By putting equation (98) and (99) into equation (100):

$$M\left(\frac{4}{h^2}x_{i+1} - \frac{4}{h^2}x_i - \frac{4}{h}\dot{x}_i - \ddot{x}_i\right) + C\left(\frac{2}{h}x_{i+1} - \frac{2}{h}x_i - \dot{x}_i\right) + Kx_{i+1} = F_{i+1} \tag{101}$$

The motion one time step ahead is then expressed as:

$$x_{i+1} = \frac{F_{i+1} + M\ddot{x}_i + \left(\left(\frac{4M}{h} + C\right)\dot{x}_i - \left(\frac{4M}{h^2} + \frac{2C}{h}\right)x_i\right)}{\left(\frac{4M}{h^2} + \frac{2C}{h} + K\right)} \tag{102}$$

As the initial conditions $(x_0, \dot{x}_0)$ determined from the static analysis are known, formula (100) is used to obtain:

$$\ddot{x}_0 = \frac{F_0}{M} \tag{103}$$

When the initial acceleration are known, equation (102) are solved to find x_1. Next, $\dot{x}_1$ and $\ddot{x}_1$ are decided from equation (98) and (99). x_2 may then found from equation (102) again. So, by repeating these steps over and over again in time intervals (h) for each free body and line node in the model, a representation of the response in the time domain are created.

Looking at short term response problems, a wave spectrum over a given time period (d-hour) should first be used to generate a realization of the wave elevation process. The water particle speed and accelerations may then be calculated. Also, loads at each nodal point of an object and the equation of motion can be solved by a step-by-step numerical integration, resulting in time domain series of all nodal points' responses. The distribution of global response maxima may then be determined. So, by repeating the time domain simulations a sufficiently amount of times, a representation of the extreme value distribution is obtained.

6.2.1 Simulations in the time domain

DNV-RP-H103 (2014, 2.3.6.5) states that a time-domain analysis of structural response caused by non-linear load effects must be carried out long enough to obtain stationary statistics. When lifting an object through the splash zone in a defined sea state, the resulting hydrodynamic forces are highly dependent on timing with the incoming wave(s) due to a launch period of 10-20 seconds through the critical splash zone area. Therefore, several simulations of the same situations needs to be performed in order to see the resulting characteristic load based on statistics.

Wave simulations in Orcaflex uses regular sinusoidal waves, either long-crested or short-crested. As described earlier, short-crested waves are composite series of sine waves with constant amplitude but pseudo-random phases chosen by a random number generator. This results in similar wave trains given the same simulation setup.

As the linear wave theory only takes into account wave kinematics up to a mean water level and is proved to overestimate forces appearing at the surface. Orcaflex may compensate for this by stretching the wave kinematics either by vertically stretching, Wheeler stretching (Wheeler, 1969), or by extrapolation. This avoids unrealistic high velocities of the waves.

1. Vertical stretching takes the values above the mean water level ($z > 0$) and replace them with the given values for ($z = 0$).
2. Wheeler stretching stretches or compresses the water column kinematics at the original level z to a modified level z'. The corrected vertical coordinate is given as:

$$z' = \frac{z - \xi}{1 + \frac{\xi}{d}} \tag{104}$$

   Where d is the water depth, and ξ is the free surface elevation.
3. Extrapolation uses the tangent of the mean water level to linearly extrapolate the sea water characteristics for $z > 0$.

6.2.2 Coordinate systems

Two different coordinate systems can be utilized in Orcaflex. The first one is a global coordinate system which is denoted GXYZ, where G is the global origin surrounded by the global axes GX, GY, and GZ. For each modeled object, a local coordinate system (Lxyz) is used. The coordinate systems have positive rotations clockwise looking in the direction of the axis under consideration.

6.3 Objects

6.3.1 Vessel

The vessel is a system with six degrees of freedom, respectively three longitude motions (surge, sway and heave) and three rotated motions (roll, pitch and yaw). Such a system is frequently used for the modeling of ships, platforms, semisubmersibles and other floating structures. The motions of a vessel are described by the RAOs assigned to the vessels COG. These motions are categorized as either low or wave frequency. Both types of motions are usually present, but can be calculated separately where the wave frequency motions are what Orcaflex refer to as superimposed of the low frequency (primary) motions.

6.3.2 Buoys

Buoys are in Orcaflex combined to represent the body features of an object. In Orcaflex, one can choose to use either a six dimensional buoy or a three dimensional buoy. Further, three different types of 6D buoys can be used; the spar-, the towed fish-, and the lumped buoy. In this thesis, only 6D lumped buoys are used for modeling of the ROV system due to its geometrical flexibility. These rigid bodies have properties such as mass, size, moments of inertia and hydrodynamic properties such as drag and added mass. A 6D buoy is represented with a rigid body with six degrees of freedom, 3 along axis and 3 around axis. These motions are calculated by time domain integration in Orcaflex. The hydrodynamic loads are calculated from an extended Morison`s equation:

$$F_w = (\Delta a_w + C_a \Delta a_r) + (\frac{1}{2}\rho C_D A_p v_r |v_r|) \tag{105}$$

Where F_w is the fluid force defined as the sum of inertia- and drag forces. The inertia part is represented by Δ which is the mass of displaced water, a_w and a_r which is the fluid particle acceleration relative to the earth and body, whereas C_a is the added mass coefficient. The drag equation is dependent on the fluid particle (v_r) relative to the body with a projected area (A_p), and a drag coefficient (C_D).

Slamming loads are determined from the following equation:

$$F_s = \rho C_s A_w |v_r|^2 \vec{V} \tag{106}$$

Where C_s is the slamming coefficient, A_w is the slamming area, and $\vec{V}$ is the unit vector in the surface. The slamming force on a lumped buoy is calculated using fluid kinematics at the center of the wetted volume. The loads are then scaled by a scaling factor equal to the proportion wet of the buoy. For a spar buoy forces is calculated independently for each defined cylinder.

The lumped buoy is defined without a detailed geometry. This results in inaccuracy when modeling due to roll and pitch motions not being captured. Further, the buoyancy for a

lumped buoy is treated as a vertical element with length equal to the specified height of the buoy. The buoyancy force then changes linearly with the vertical submergence of the buoy.

6.3.3 Links

In Orcaflex, links used to connect two objects are mass-less and may be modeled as a tether or a spring-damper system. The difference lies in that the spring-damper can take both tension and compression, whereas the tether is an elastic tie that can only take tension (often used to model slings in lifting operations).

6.3.4 Winch

Two types of winches can be utilized in Orcaflex, either a simple or a detailed model. The simple winch used in this thesis is massless and connected between two or more points in the model. Further, the wire is given stiffness and a specified length, before a preset tension in the static analysis is decided from:

$$T = F_{winch} = \frac{(L - L_0)}{L_0} K_{wire} = K_{wire} * \epsilon \tag{107}$$

Where:
K_{wire}: Wire Stiffness
L: Total length of the winch wire path
L_0: Un-stretched length of wire paid out
ϵ: Wire Strain

Inertia forces are in this model ignored. During a dynamic analysis, a specified length, velocity, acceleration controls the winch. Further, the dynamic tension is then taken as:

$$T = F_{winch} = \frac{(L - L_0)}{L_0} * C_{wire} = K\epsilon * B_{wire} * K_{wire} * \frac{d\epsilon}{dt} \tag{108}$$

Where:
B_{wire}: Wire Damping
$\frac{d\epsilon}{dt}$: Wire strain rate

As seen from the above equation, compression is not possible in the winch wire if T calculated is negative. If $T \leq 0$, the wire is in slack.

6.4 Installation Vessel

The specific vessel picked for use in this thesis is Rem Ocean (Figure 7). Rem Ocean is a construction vessel specifically suited to perform inspection-, maintenance- and repair (IMR)

work below the waterline. The selection of vessel type and size will often influence the limiting sea state, although the splash zone most often will determine the sea state limitation. In cases where wave forces on the structure are the main contribution to the experienced load, the limiting sea state will be independent of vessel type (Sandvik and Kopsov, 1995).

When performing IMR work one always uses ROVs to either get a visual view of situations subsea, or perform various tasks using their manipulators (commonly in combination with purpose made tools). Next to the use of ROVs; operation by either the crane and/or the module handling system (MHS) is commonly for maintenance, construction, and repair work.

Main characteristics of the vessel are presented in Table 5.

Figure 7: Photo of Rem Ocean taken by Valderhaug (2014)

Table 5: Rem Ocean main dimensions

Main dimensions – Rem Ocean	*Value*	*Unit*
Length w.l.	106.90	[m]
Length p.p.	100.45	[m]
Breadth	22.00	[m]
Max draft	7.15	[m]
Design/regular draft	5.18	[m]
Deadweight	6000	[Te]
Gross tonnage	7300	[Te]
Displacement	9018	[Te]

6.5 ROV, TMS and LARS

Rem Ocean is equipped with two Supporter MK2 working remotely operated vehicles (WROVs) (Figure 8) and one Sea Owl XTI Observation ROV (OROV). They are all situated in the hangar, and handled by a launch and recovery system (LARS). The tether management system (TMS) holds a drum with a tether for connecting the ROVs to the vessel system through a stiff umbilical going from the top of the TMS to the drum in the hangar.

The systems for the WROVs is launched and recovered by an A-frame of type FSM90 (LARS). Further, the TMS is connected to the ROV by a latch during the launch/recovery phase and is usually disconnected about 20-30 meters from the seabed. The TMS c/w a tether drum is a commonly used method today to ensure that the ROVs can work undisturbed by things as umbilical drag, movement restrictions, and (partly) the vessel location.

In this thesis, the Supporter WROVs onboard Rem Ocean is considered as the main case under consideration. The main dimensions of the ROV, TMS, LARS and the umbilical can be found in Table 6 below. Note that the mass of the ROV includes the bottom skid and its manipulators.

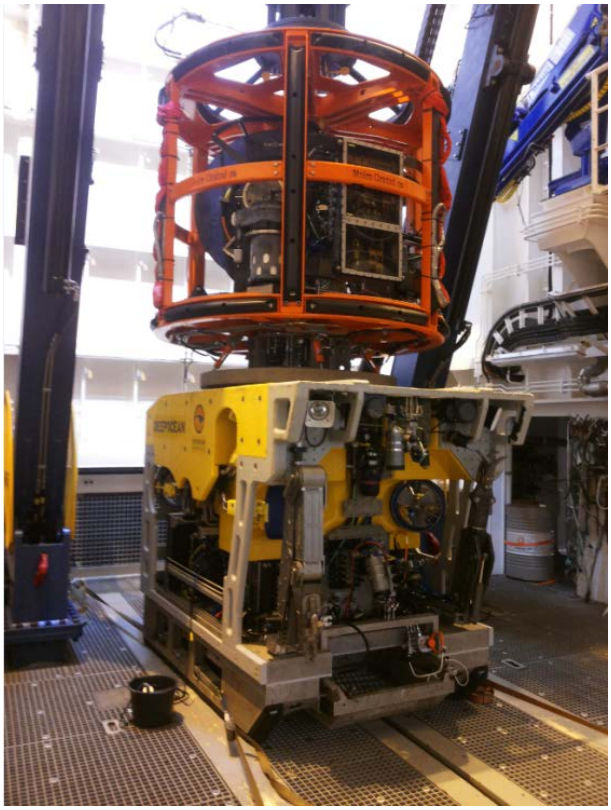

Figure 8: Picture of a Supporter Mk2 WROV onboard Rem Ocean taken by Aasen (2015)

Table 6: Main dimensions on the ROV system

Structural Input	Value	Unit
Constants		
Gravity	9.81	[m/s^2]
Seawater density	1027	[kg/m^3]
Steel density	7850	[kg/m^3]
Supporter MK2 WROV - Main dimensions		
Length	2.50	[m]
Width	1.70	[m]
Height	2.00 (skid included)	[m]
Displacement	3.46	[m^3]
Mass	3.62	[Te]
Weight	35.50	[kN]
Weight in water	0.00 (will vary, but assumed neutral)	[kN]
Max payload	0.40	[Te]
TMS with tether - Main dimensions		
Diameter	2.20	[m]
Height	2.13	[m]
Displacement	0.77	[m^3]
Mass	3.62	[Te]
Weight	35.50	[kN]
Weight in water	27.08	[kN]
ROV and TMS – Main dimensions		
Length	2.50 (modeled as an equivalent rectangular box)	[m]
Width	1.70	[m]
Height	3.07 (TMS height reduced 50% in Orcaflex due to the shape)	[m]
Displacement	4.24	[m^3]
Mass	7.19	[Te]
Weight	70.50	[kN]
Weight in water	27.08	[kN]
COB	0.2	[m]
COG	-0.2	[m]
Umbilical - Main dimensions		
Outer diameter	34.6	[mm]
Mass/unit length	4.2	[kg/m]
Mass in seawater/unit length	3.2	[kg/m]
Axial stiffness	44000	[kN]
Minimum Breaking Load (MBL)	620	[kN]
Damping ratio (C)	3	%

6.6 Crane/LARS capacity

A LARS/crane`s dynamic capacity is determined by the safe working load (SWL), Dynamic amplification factor (DAF), lifting height, and lifting sector ranges. The dynamic amplification factor (DAF) characterized by the dynamic capacity is defined as:

$$DAF = \frac{Static\ response + Dynamic\ response}{Static\ response} = \frac{1}{\left[\left(1-{\beta_0}^2\right)^2 + (2C\beta_0)^2\right]^2} \quad (109)$$

Where:
The frequency ratio, $\beta_0 = \frac{\omega}{\omega_n}$
And the damping ratio, $C = \frac{c\ (constant\ of\ damping)}{c_{crit}} = \frac{c}{2m\omega_n}$

Where m is mass of the object, ω and ω_n is the system- and natural frequency of the system respectively. c is a constant which is specific to the system under consideration.

The DAF factor can for a deck/sea lift be taken to be from 1.3 up to 2.0 based on the lifted object weight compared to the SWL (Safe Working Load). For lowering through the splash zone, the winch payout rate may have a significant influence on the value of the dynamic loading since it determines the period where the most extreme forces occurs (Sandvik and Kopsov, 1995).

6.7 Modeling in Orcaflex

As a basket/ROV lift operation is considered to be a light lift operation, the LARS/crane system may be modeled as rigid, hence the motions of the tip can be determined from the wave induced motions of the vessel (RAOs), meaning the transfer functions of the body motions. The RAOs are given as (Haver, 2015):

$$RAO_{\Xi X}(\omega_n) = h_{\Xi X}(\omega_n) = \frac{X_{0,n}}{\xi_{0,n}} \quad (110)$$

Where $h_{\Xi X}(\omega_n)$ is the transfer function, and $X_{0,n}$ is the response amplitude per unit wave amplitude $(\xi_{0,n})$.

The RAOs are given in six rigid degrees of freedom (surge, sway, heave, roll, pitch, yaw) defined numerically at the center of gravity (COG) of the vessel for a given load condition. The RAOs together with the crane tip are used to define the wave induced translational motion of the crane tip.

The displacement of the vessel (η_n) at the n^{th} degrees of freedom is then calculated by multiplying the RAO with respect to the relevant wave direction as well as the degree of freedom of the wave amplitude:

$$\begin{aligned}\eta_n(t) &= Re\left[h_{\Xi X}(\omega_n) * \xi_0 e^{i_0 \omega t}\right] \\ &= |h_{\Xi X}(\omega_n)| * \xi_0 \cos(\omega t + \varphi_n)\end{aligned} \tag{111}$$

Where $n = 1,2, \dots ,6$.

ω is the wave frequency given in rad/s, t is the time in seconds, φ_n is the phase angle in radians, and ξ_0 is the wave amplitude. i_0 is here an imaginary number.
It should be noted that the equations is meant for use when the vessel is in a lifting phase, i.e. floating on open sea without any thrusting or anchoring.

The dynamic tension in the wire cable (F_{Dyn}) may be developed from the dynamic transfer function in complex form (S.Rao, 2005):

$$h_{\Xi F dyn}(\omega_n) = \frac{F_{Dyn}}{\xi(t)} \tag{112}$$

The dynamic tension on the wire for an un-damped case where the frequency of the wire is smaller than the natural frequency of the lifting system is expressed from (S.Rao, 2005):

$$F_{Dyn} = -\omega^2 M e^{i_0 \omega t} \eta_{tz} \tag{113}$$

Where M is the mass of the lifted object plus wire weight, and the crane tip motion (η_{tz}) in this thesis is assumed to follow the vessel motions (η_n) converted from the COG of the vessel to the crane tip:

$$\begin{aligned}\eta_n(t) &= Re\left[h_{\Xi X}(\omega_n) * \xi_0 e^{i_0 \omega t}\right] \\ &= |h_{\Xi X}(\omega_n)| * \xi_0 cos(\omega t + \varphi_n)\end{aligned} \tag{114}$$

Where $n = 1,2, \dots ,6$.

A response spectrum for the dynamic tension in the wire is then obtained as:

$$S_{\Xi\Xi}(\omega_i) = S_{\Xi\Xi}(\omega_i) * |h_{\Xi X}(\omega_n)|^2 \tag{115}$$

While the combined response spectrum is then taken as (Haver et al., 2002):

$$S_{RS}(\omega) = |h_{\Xi wind}(\omega_n)|^2 * S_{wind\ sea}(\omega) + |h_{\Xi swell}(\omega_n)|^2 * S_{swell}(\omega) \tag{116}$$

Where:

$h_{\Xi wind}(\omega_n)$: Dynamic tension amplitude due to wind sea
$h_{\Xi swell}(\omega_n)$: Dynamic tension amplitude due to swell sea

6.7.1 ROV and TMS

The ROV are represented by a rectangular box reflecting the characteristic dimensions of the ROV with TMS. In Orcaflex, these objects are represented as 6 dimensional "*lumped buoys*" (meaning buoys that are combined in Orcaflex to represent the body features of an object).

6.7.2 LARS

Although the LARS (or crane if used) may be modeled as stiff; some stiffness data has been included to introduce some more elasticity to the hoisting system. This would reduce snatch loads, and be more representative for a real life case. The rest of the hoisting system has been conservatively modeled as infinitely rigid, although some elasticity is likely to be introduced by hydraulic cylinders, winch mechanisms, etcetera.

The deflection on the A-frame and its elements (i.e. crane wire, soft slings, master links, etc.) is assumed linear between applied force and deformation:

$$K = \frac{F}{\delta} \tag{117}$$

The stiffness contributions from the A-frame/crane are then combined with the wire and rigging stiffness to form the total stiffness:

$$\frac{1}{K} = \frac{1}{K_{rigging}} + \frac{1}{K_w} + \frac{1}{K_{comp.}} + \frac{1}{K_{block}} + \frac{1}{K_{boom}} + \frac{1}{K_{other}} \tag{118}$$

$K_{rigging}$ = Stiffness of rigging arrangement (i.e. shackles, softstrops, chains, etc.) [N/m]
$K_{comp.}$ = Stiffness of (active/passive) heave compensation system used [N/m]
K_{block} = Stiffness of multiple lines in a block if used [N/m]
K_{boom} = Stiffness of crane/LARS boom [N/m]
K_{other} = Stiffness of other contributions if any [N/m]
$K_{crane/A-frame}$ = Total crane stiffness [N/m]

The longitudinal wire stiffness is:

$$K_w = \frac{E_w A_w}{L_w} = \frac{E_w \pi d_w^2}{4 L_w} \tag{119}$$

Where E_w is the cross-sectional Young`s modulus, A_w is the circumscribed wire area, d_w is the wire diameter, and L_w is the wire length.

The eigenperiod which may cause resonant motions and corresponding load of the system in z-direction is then:

$$T_0 = \frac{2\pi}{\omega_0} = \sqrt{\frac{M}{K}} = \sqrt{\frac{M_{object} + M_{rigging} + M_{wire} + A_{33}}{K}} \quad (120)$$

Where M is representing the weight of the object, rigging, and the wire. A_{33} is the added mass term.

The stiffness of the LARS system (Figure 9) is taken as in Table 7.

Table 7: Stiffness of the LARS system

Umbilical - Main dimensions		
K - LARS	10117	[kN/m]
K – Umbilical	44000	[kN/m]
1/K - combined	0.00012	[1/kN]
K - combined	8225	[kN]

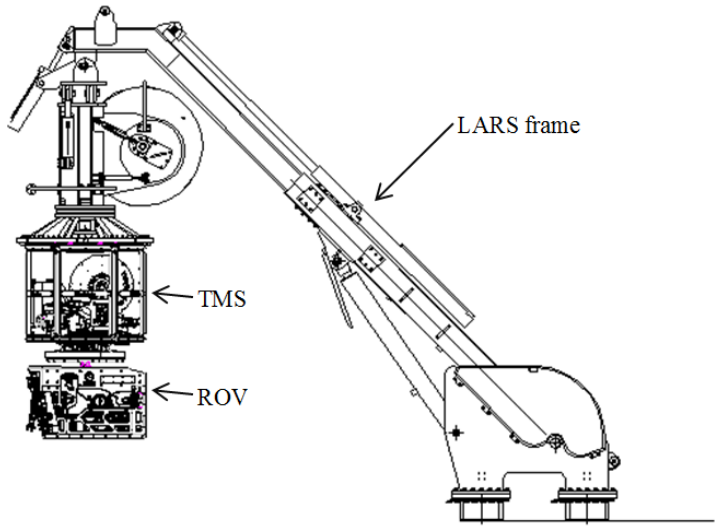

Figure 9: WROV system at Rem Ocean

The launch point has in Orcaflex been modeled with a fully extended A-frame in order to give a representative vessel motion.

6.7.3 Capacity check

As the capacity for the lifting wire on the LARS frame is known to be the limiting criterion for the cases discussed in this thesis, a safety factor must be found. The safety factor can be taken as (DNV Standard for certification No.2.22 (2011, ch.2, section 3, B505):

not less than 3 and:

$$S_F = \frac{10^4}{0.885 * SWL[kN] + 1910} \quad (121)$$

But not exceed 5.

As the SWL is not defined for a ROV umbilical, the minimum demand is used, giving a safety factor of 3.0. The maximum safe working load in the wire rope (S) is then:

$$S = \frac{B}{S_F} = \frac{620kN}{3.0} = 206.66kN \quad (122)$$

6.8 Hydrodynamic coefficients for the ROV system

In order to determine forces acting on an object and corresponding responses through the splash zone as accurate as possible, a proper evaluation of the hydrodynamic properties should be carried out as far as time and resources allows. This means either theoretically from design properties, empirically by i.e. CFD modeling, or by model tests. The hydrodynamic properties are dependent upon things as the geometry of the structure, weight, perforation, Reynolds number, and the Keulegan-Carpenter number. In addition, motion- and wave direction, wave frequency, and the vicinity to the surface will give contributions.

6.8.1 Added Mass

In fluid mechanics, the added mass term is a representation of inertia added to a system due to the fact that an accelerating or decelerating object will deflect some of the fluid volume surrounding it as it moves. This phenomena is a common issue because the object and the surrounding fluid can`t occupy the same physical space simultaneously.

The dimensionless added mass coefficient (C_{Ai}) is found by using the added mass in one direction and divide by the displaced fluid mass (DNV-RP-H103, 2014):

$$C_{Ai} = \frac{A_i}{\rho_w V_o} \qquad i = x, y, z \tag{123}$$

Where:
A_i: Uncoupled added mass in x/y/z-direction [kg]
ρ_w: Water density [kg/m^3]
V_o: Displaced volume of object in still water [m^3]

The Recommended Practice (DNV-RP-H103, 2014) proposes coefficients for simple 2- and 3- dimensional bodies. But due to the complexity of a ROV system, these cannot be used directly. A common way to find added mass properties of 3D bodies is to use the geometry of the structure and find the added mass of the non-perforated object. Then the perforation degree is used to find a reduction factor. A proposal of such a calculation can be found in either DNV-RP-H103 (2014) or in Sandvik (2007). A calculation using the Sandvik method can be found in Appendix 2.

The properties for the Supporter Mk2 based on calculations made in Appendix 2 gives:

- $A_x = 4.57\,Te$ and $C_{Ax} = 0.90$
- $A_y = 6.18\,Te$ and $C_{Ay} = 0.71$
- $A_z = 5.11\,Te$ and $C_{Az} = 0.84$

Model tests done by Sayer (2008) concludes that the inertia coefficient ($C_m = 1 + C_a$) lies in the range of 1.4-1.6 for a typical WROV, meaning added mass coefficients (C_A) of 0.4-0.6. Further, due to the effects of proximity of free surface, the coefficients may be increased

about 10%. But it should be noted that the Super Scorpio WROV used in these tests are smaller than the Supporter Mk2 that is being used in this thesis.

Taking into account the TMS system comes with the ROV, the following properties are derived:

- $A_x = 8.51\,Te$ and $C_{Ax} = 1.68$
- $A_y = 6.62\,Te$ and $C_{Ay} = 0.76$
- $A_z = 7.85\,Te$ and $C_{Az} = 1.29$

6.8.2 Drag Factors

The drag factor is a dimensionless quantity obtained from the resistance of an object towards any environmental fluid. Generally, low drag numbers corresponds with low drag forces onto an object. An example of how one can find simplified drag coefficients (C_{DS}) in steady state flow based on design values of an ROV without TMS can be found in Appendix 3. Factors range from 2 to 2.5 in X/Y/Z-direction. Anyhow, these numbers are only valid in steady state scenarios. Drag coefficient in an oscillatory flow (C_D) is likely to be higher. Therefore, DNV-RP-H103 (2014, 4.6.2.4) states that unless CFD studies or model tests have been performed, drag factors in an oscillatory flow should be equal to or higher than 2.5.

6.8.3 Slamming and Water Entry Factors

In order to represent slamming forces on the structure during the launching phase through the water columns, slamming buoys are added along the members subjected to slamming. According to DNV-RP-C205 (2010, 8.6.1.2), a slamming coefficient C_s for structures similar to smooth circular cylinders can be taken as 5.15 as the structure enters the fluid flow. This representative value may be used for the TMS. For other structures, the slamming force value should be taken as equal to or greater than 5 (DNV-RP-H103, 2014, 4.3.5.1).

The water exit force in still water can be expressed as the rate of change of fluid kinetic energy (DNV-RP-H103, 2014, 3.2.11.2):

$$F_e(t) = -\frac{1}{v_e}\frac{d}{dt}\left(\frac{1}{2}A_{33}^0 v_e^2\right) = -\frac{1}{2}\frac{dA_{33}^0}{dt}v_e = -\frac{1}{2}\rho C_e A_p(\dot{\varsigma} - \dot{\eta})^2 \tag{124}$$

Where $\dot{\eta}$ is the vertical velocity of the sea surface (positive upwards), and $\dot{\varsigma}$ is the vertical motion of the object. v_e is the water exit velocity. The water exit coefficients (C_e) may then be taken as:

$$C_e = -\frac{1}{\rho A_p}\frac{dA_{33}^0}{dh} = \frac{1}{2}C_s = 2.5 - 2.575 \tag{125}$$

7. Analysis

7.1 Hindcast data

When analyzing lifts to be performed at sea, baseline would be to choose the most suitable wave spectra and perform simulations in a stationary sea state for a set time period. The results obtained may then be fitted to a statistical distribution so that a representation of critical values can be established.

Another method to get these critical values more accurate would be if one has historical wave data of the location where the lifting operation would be executed. This is called hindcast data which is a way to test or verify a mathematical/statistical model. This method is based on the principle of feeding historical (known) data into the model used in order to see how accurate the output values matches current or near past known data. If the model correlates well with the given data, the model may prove reliable for the prediction of future unknown data. Drawing such conclusions based on data is called *statistical inference* (Haver, 2015). Statistical inference makes it possible to (1) draw conclusions regarding the choice of probabilistic models, (2) estimate parameters for the probabilistic distribution, and (3) test if our fitted model is in agreement with what data samples suggest (Haver, 2015).

The reason why the historical data rarely are used is the fact that the data needed are usually not available for the users, or that accurate measurements with good quality are not generated over a sufficiently long term history where also many extreme weather phenomena are present. Extreme weather such as wind, waves, current, and storm surge is needed for the estimation of the probability distribution which provides the basis for calculating design loads and events. Data samples should be sampled under identical boundary conditions and as far as possible be statistical independent. The sample size must also be large enough for estimating distribution parameters with sufficient accuracy (epistemic uncertainty reduction).

7.2 Uncertainties

7.2.1 Model uncertainty

As statistical methods are models built on observed quantities, statistical uncertainties will always be present. In general, two types of uncertainties may create misalignments and uncertainties in a model towards its true values. The first one is aleatory uncertainty which is uncertainty towards the random nature of a phenomenon. For instance, one cannot be certain about the largest observed annual wave height in the future due to the inherent random nature of waves, and therefore also wave induced loads and responses (Haver, 2015). A good description of this variability is therefore required, involving probabilistic methods.

The second uncertainty is epistemic where a deterministic phenomenon or parameter are uncertain and may vary due to lack of proper data and/or prior information (i.e. expert judgment, technical knowledge, data from similar cases, etc.). This type of uncertainty gives

uncertainty related to the choice of probabilistic distribution types for the stochastic variables. Epistemic uncertainty can be indicated by bootstrapping (Monte Carlo simulations). Anyway, a fitted model can never prove 100% correct. Only indications of whether or not a model is acceptable can be established. This can be accomplished by (1) gaining more data/knowledge, (2) executing research work regarding the underlying structure of the phenomenon, or (3) investigating in more accurate equipment for observing a phenomenon (Haver, 2015).

7.2.2 Chi-squared method

A way to verify that the deviation between a fitted model and available data is larger than what is likely to be a consequence of inherent randomness, is by doing a chi-squared (χ^2) test. This test gives us guidance on the suitability of a given probability model. First step of this test is to group the given sample space into m classes such that the class probability, $p_m, m = 1,2, \dots, N$ are more or less the same for all classes. As the class width will be narrow in the central part of the distribution and broader in the tail region, the expected number of observations should as guidance be at least 5 in each class (Haver, 2015). The target class probability thus becomes:

$$p = \frac{5}{n} \tag{126}$$

Also, the number of classes, m, should be large enough to get a reasonable resolution.

The steps of the χ^2-test is (Haver, 2015):

1. Class limits are determined such that the class probability of the fitted model is p for all classes.
2. Observations of the given phenomena are pooled into the various classes. The number of observations within each class no. i is denoted $o_i, i = 1,2, \dots, n$.
3. The error between observations and fitted model is then calculated as follows:

$$\chi^2 = \sum_{k=1}^{m} \frac{(o_i - np)^2}{np} \tag{127}$$

4. As o_i is unknown prior to the observations, this random variable will be the case for the sum.

Further, if it is given that:

i. The fitted model is the true model
ii. That $np \to \infty$ for all classes
iii. The parameters of the fitted distribution are estimated using the maximum likelihood method

It can be shown that χ^2 is a realization from a chi-square variable with $v = n - r - 1$ degrees of freedom, where r is the number of parameters estimated from the sample. But as seen, our minimum value for np is far from infinity and the parameters may be estimated by other techniques. Due to this, the test will be used by assuming that one can utilize the same probabilistic structure of the error variable.

5. From tables of the chi-square distribution, the value of exceeding $1 - \alpha$ is found as $\chi^2_{v,1-\alpha}$.
6. If the calculated error, χ^2, is larger than $\chi^2_{v,1-\alpha}$, the model will be rejected on significance level $1 - \alpha$. The probability of a rejected model thus becomes $1 - \alpha$.

7.2.3 Monte Carlo

When analyzing lifts that is to be performed offshore, one will often perform simulations in time domain software to get representative forces so that limiting wave conditions can be found. But, after generating n amount of simulations, the characteristic load that is extracted from a suitable statistical distribution will have uncertainties. To cover for this uncertainty, the confidence should be assessed. As performing many repeated simulations in Orcaflex is time consuming, the question thus becomes how one can numerically generate a value that is representative to a true observable value so that one can estimate the confidence/uncertainty in a distribution. This can be done using Monte Carlo simulation of a realization from a given distribution function with a set of estimated parameters.

First, the original data set is fitted to the most suitable probability model in i.e. a probability paper. Before the realization of the sample $x_1, x_2, \dots, x_n$ are known and the corresponding cumulative distribution function $F_x(x)$ is given as a random variable $R = F_x(x)$. No matter what the true distribution of x is, R is uniformly distributed between 0 and 1. The simulation is then performed by the following steps (Haver, 2015):

1. Generate a number of randomness between 0 and 1 by using a random number generator, denoted r_1.
2. The corresponding value of x is: $x_1 = {F_x}^{-1}(r_1)$.
3. Repeat step 1. and 2. y times in order to obtain a sample of n values from $F_x(x)$.
4. Fit the same type of probabilistic model used for the original data set to the y samples. One then gets y estimates for the distribution parameters.
5. Calculate the mean parameters of the y estimates and compare to the parameters of the (“true”) distribution used for the Monte Carlo simulations.

If the means of the y estimates is approximately equal to the background values, the estimation process indicates that unbiased estimates are being generated.

7.3 Extraction of data

When observing or simulating a value (i.e. H_s, T_p or wire tension) for a given case, not all values obtained are of interest. Therefore, if only the more extreme values are of interest, they may be extracted generally by using two methods.

1) MAX method

In the max method, the response maximum of each simulation is extracted. From the maximums of multiple simulations, the data can be fitted to an extreme value distribution. A limitation of this approach is that several simulations need to be performed (Gudmestad, 2015). Also, the method totally disregards the information in the remaining data.

2) Peak over threshold (POT)

In the peak over threshold (POT) approach, only peak values above a given threshold is extracted from the simulation(s). A process called de-clustering ensures that only successive peak observations are retained from the time series. It also ensures that only the peaks that are at a certain range of distance apart are taken into account in the POT. The obtained data points are assumed to follow some sort of a Generalized Pareto Distribution (GDP) (Gudmestad, 2015).

The POT method allows for more data points to be taken into consideration in statistical analysis than the MAX method. The threshold limit is a subjective choice, although a low threshold may result in a data set with high variance. The minimum required threshold to provide a reasonably good GPD model may be determined from the threshold stability property of the GPD (Gudmestad, 2015):

$$\hat{\beta}_u = \hat{\beta}_{u0} + k(u - u_0) \tag{128}$$

Where u_0 is the minimum threshold, u is the higher threshold, $\hat{\beta}$ is the scale parameter of the GDP, and k is the shape parameter.

The number of exceedances for u for a given period of time is assumed to follow a Poisson distribution, where the density function reads:

$$f(X = x) = \frac{\mu^x}{x!} e^{-\mu} \tag{129}$$

Where μ gives the expected frequency of occurrence, and x is the number of occurrences.

7.4 Fitting of data

As mentioned, a probability distribution may be determined by data analysis using a suitable wave spectrum and historical data if present. This can be done simply by looking at the probability density function for the present data, but can prove difficult in some scenarios. More often, the process of fitting a distribution to available data are done by plotting the empirical data distribution in probability papers. The aim of fitting data to a specific distribution is to predict the probability or to forecast the frequency of occurrence of the extent of a phenomenon in a certain time interval. Generally, a large data sample should be aimed for as a number of different probabilistic models may seem reasonable for smaller data sets. Especially the tail region should be of large concern as this area most often provides the extreme value predictions of interest.

In order to obtain an empirical/cumulative distribution function, various methods may be used. The most logic choice to select might be to take the sample distribution function:

$$\hat{F}(x) = \frac{n_i}{N} \quad n_i = 1,2,3,\dots.,N \tag{130}$$

Where n_i is the cumulative amount of observations and N is the total number of observations. This approach will provide wrong results when n_i goes equal to N. Therefore, the most common method (also used in this thesis) is:

$$\hat{F}(x) = \frac{n_i}{N+1}, \quad n_i = 1,2,3,\dots.,N \tag{131}$$

Or the more general method proposed by Blom (1958):

$$\hat{F}(x) = \frac{i - c_i}{N + 1 - 2c_i}, \quad 0 \leq c_i \leq 1 \tag{132}$$

Where i is the rank of the data point.

The last method might be able to put the points in a median position and thereby provide a very small bias when plotting data points.

After a probability distribution has been established, an estimate of the true parameters in the distribution function can be done. This can be done by various approaches (Haver, 2015, p.34):

1. *Method of moment:* Using the method of moment technique, more weight to the tail may be provided compared to the maximum likelihood method, but typically less than the least square approach used in the tail region.
2. *Least square fit:* In this approach, one uses the y-axis probability scale to draw/calculate the x-axis value based on a fitted line in the probability paper. Although the probability plot and/or the fitted line may be skewed so that slightly distorted values results, this method provides a fast and effective way to get the

wanted parameters with good accuracy. It may also be fitted to the tail region by excluding value below a set threshold.

3. *Method of maximum likelihood:* In this method, the parameters are estimated based on the fact that an observed sample is the most likely sample. For large sample sizes with good quality, this method provides most efficient if the chosen probability model is correct. For smaller sample sizes, this technique may not prove reliable.

7.4.1 Method of moments

The method of moment is a method for estimating parameters. It is very much used in the offshore industry as it gives much weight to the tail region and is easy to implement. It is to be noted that the method will only give estimates and not true values unless the sample size is unlimited. The Gumbel and the Weibull distribution will be used in the examples described below.

Weibull:

The 2-parameter Weibull distribution function is given as (Haver, 2015):

$$f(x;\beta,k) = \frac{k}{\beta}\left(\frac{x}{\beta}\right)^{k-1} e^{-\left({}^{(x)}/_{\beta}\right)^{k}} \tag{133}$$

The expected value and the variance may be given in terms of moments as:

$$\mu_x^{(n)} = E[X^n] = \int_0^{\infty} x^n f_x(x)dx = \hat{\beta}^n \Gamma\left(1+\frac{1}{\hat{k}}\right) \tag{134}$$

Giving:

$$E(x) = \hat{\beta}\Gamma\left(1+\frac{1}{\hat{k}}\right) \tag{135}$$

$$Var(x) = E(x^2) - E(x)^2 = \hat{\beta}^2\left(\Gamma\left(1+\frac{2}{\hat{k}}\right) - \Gamma^2\left(1+\frac{1}{\hat{k}}\right)\right) \tag{136}$$

Γ () represents the gamma function.

The moments may then be calculated by requiring:

$$\bar{x} = \hat{\beta}\Gamma\left(1+\frac{1}{\hat{k}}\right) \tag{137}$$

$$\sigma_x^2 = \hat{\beta}^2\left[\Gamma\left(1+\frac{2}{\hat{k}}\right) - \Gamma^2\left(1+\frac{1}{\hat{k}}\right)\right] \tag{138}$$

The shape estimator parameter $\hat{k}$/alpha is then estimated by equaling:

$$\frac{\left(\Gamma\left(1+\frac{2}{\hat{k}}\right)-\Gamma^2\left(1+\frac{1}{\hat{k}}\right)\right)}{\Gamma^2\left(1+\frac{1}{\hat{k}}\right)}=\left(\frac{\sigma_x^2}{\bar{x}}\right)^2 \tag{139}$$

A corresponding $\hat{\beta}$-value may then be found by introducing the estimated $\hat{k}$ into equation 137.

Gumbel:
For a Gumbel distribution, the usual moment of order r is obtained as (Mahdi & Cenac, 2004)

$$\mu_r = E(X^r) = \sum_{k=0}^{r}\binom{\hat{k}}{r}\hat{\beta}^{r-\hat{k}}\hat{\mu}^{\hat{k}}\int_R y^{r-\hat{k}}exp[y+exp(-y)]dy \tag{140}$$

In cases of order $r = 1$ and $r = 2$, we get after computation and simplification:

$$\hat{\mu}_1 = \hat{\beta}C_2 + \hat{\mu} \tag{141}$$

$$\hat{\mu}_2 = \hat{\beta}^2 J + 2\hat{\beta}\hat{\mu}C_2 + \hat{\mu}^2 \tag{142}$$

Where C_2 is a constant equal to $0.577215\, J \approx 1.978$ when the sample size goes large. From the above equation the method of moment estimates can be expressed as:

$$\hat{\beta} = \left[\frac{\overline{x^2}-\bar{x}^2}{J-{C_2}^2}\right]^{1/2} \tag{143}$$

$$\hat{\mu} = \bar{x} - C_2\hat{\beta} \tag{144}$$

Where $\bar{x}$ and $\overline{x^2}$ are the empirical moments of order 1 and 2 given from the sample.

7.4.2 Least square fit

As the method of moments is associated with uncertainties especially when applied to a small number of observations, other method may prove more accurate. One technique of indicating uncertainties in a fitted distribution is to use bootstrapping. Generally, two bootstrapping techniques are commonly used, parametric bootstrapping or classic bootstrapping.

Classic bootstrapping:
In classic bootstrapping, a sample of size n is used to produce a trend line fitted to data in the most suitable probability paper. As the nature is inherent random in nature, this data sample is just one of many possibilities. Other possible combinations may then be obtained by resample with replacements from the original data set. By producing multiple re-sampled

samples, a scatter in the fitted distributions will be present, indicating uncertainties. A disadvantage of using this method is the fact that no samples outside the original data set are obtained (Haver, 2015).

Parametric bootstrapping:
In parametric bootstrapping, one assumes the trend line fitted to the original data sample to be the true model. Then, Monte Carlo simulations are performed in order to generate new samples from the distribution fitted to the original sample (Haver, 2015).

7.4.3 Maximum Likelihood method

Another method often used to estimate parameters such that the observed such that the simulated/observed is the most likely sample, is the maximum likelihood method. This method uses obtained information in an efficient way, especially for larger sample sizes. For small/moderate sized samples, other methods may prove more accurate (Haver, 2015).

Given that $x_1, \dots, x_n$ are random samples following a Gumbel distribution, the likelihood function is given as (Mahdi and Cenac, 2004):

$$L(\hat{\mu}, \hat{\beta}) = \prod_{i=1}^{n} f(\hat{\mu}, \hat{\beta}) = \prod_{i=1}^{n} \frac{1}{\hat{\beta}} exp\left\{-\frac{x-\hat{\mu}}{\hat{\beta}} - exp\left\{-\left[\frac{x-\hat{\mu}}{\hat{\beta}}\right]\right\}\right\} \tag{145}$$

$$l(\hat{\mu}, \hat{\beta}) = lnL(\hat{\mu}, \hat{\beta}) = -nln\hat{\beta} - \sum_{i=1}^{n} \frac{x_i - \hat{\mu}}{\hat{\beta}} - \sum_{i=1}^{n} exp - \left[\frac{x_i - \hat{\mu}}{\hat{\beta}}\right] \tag{146}$$

This gives the partial derivatives:

$$\frac{dl(\hat{\mu}, \hat{\beta})}{d\hat{\beta}} = -\frac{n}{\hat{\beta}} + \sum_{i=1}^{n} \frac{x_i - \hat{\mu}}{\hat{\beta}^2} - \sum_{i=1}^{n} \left[\frac{x_i - \hat{\mu}}{\hat{\beta}^2}\right] exp - \left[\frac{x_i - \hat{\mu}}{\hat{\beta}}\right] \tag{147}$$

And:

$$\frac{dl(\hat{\mu}, \hat{\beta})}{d\hat{\mu}} = \frac{1}{\hat{\mu}}\left[n - \sum_{i=1}^{n} exp\left[\frac{x_i - \hat{\mu}}{\hat{\beta}}\right]\right] \tag{148}$$

For $\hat{\beta} \neq 0$, the system can be solved by $\frac{dl(\hat{\mu},\hat{\beta})}{d\hat{\beta}} = \frac{dl(\hat{\mu},\hat{\beta})}{d\hat{\mu}} = 0$. This yields the maximum likelihood (ML) estimates of the two estimators $(\hat{\beta}, \hat{\mu})$ as numerical solutions given by the following equations:

$$\hat{\mu} = \hat{\beta}\left\{\ln n - ln \sum_{i=1}^{n} exp - \left[\frac{x_i}{\hat{\beta}}\right]\right\} \tag{149}$$

$$\bar{x} = \hat{\beta} + \frac{\sum_{i=1}^{n} x_i * exp - \left[\frac{x_i}{\hat{\beta}}\right]}{\sum_{i=1}^{n} exp - \left[\frac{x_i}{\hat{\beta}}\right]} \tag{150}$$

Where $\bar{x}$ denotes the sample mean.

The estimate of $\hat{\beta}$ is explicitly obtained from equation (150), before the estimate of $\hat{\mu}$ is implicitly obtained from equation (149) after substitution of the estimate of $\hat{\beta}$.

7.5 Statistical confidence

When setting up a ROV model in a software program as Orcaflex, simplifications of the environment and wave processes must be done. One thereby gets uncertainties in the results obtained. To narrow the gap of uncertainty, DNV-RP-C205 (2010, 10.8.4) says that a repeatability of the specific case should be documented with a high level of confidence. From DNV-RP-C205 (2010, 10.7.3) one can further obtain that due to strongly nonlinear waves and statistical variability problems when running simulations, multiple realizations in the same wave spectrum may be needed to overcome some problems of the confidence accuracy.

When simulating in irregular sea states, statistical results will vary for each simulation. Therefore, many simulations must be run to obtain accurate and reliable results. In the following sections, some theory behind confidence levels is reviewed.

Given observations $X_1, \dots X_n$, one can estimate the mean by:

$$\hat{\mu} = \sum_{i=1}^{n} \left(\frac{X_i}{n}\right) \tag{151}$$

And the variance as:

$$VA = \frac{1}{N}\sum_{i=1}^{N} (x_i - \bar{x})^2 \tag{152}$$

The exact variable moments are given by Fisher (1928):

$$Var[\hat{\mu}] = \frac{\sigma^2}{n} \tag{153}$$

$$Var[VA] = \left(\alpha_4 - 1 + \frac{2}{n-1}\right)\frac{\sigma^4}{n} \approx (\alpha_4 - 1)\frac{\sigma^4}{n} \tag{154}$$

$$Cov[\hat{\mu}, VA] = \alpha_3 \frac{\sigma^3}{n} \tag{155}$$

As results often are derived using the standard deviation rather than the variance, a Taylor series for the standard deviation estimate ($\hat{\sigma}$) can be taken as Fisher (1928):

$$\hat{\sigma} = VA^{1/2} = \overline{VA}^{1/2} + \frac{1}{2}\overline{VA}^{1/2}(VA - \overline{VA}) \tag{156}$$

Where $\overline{VA} = E[VA] = \sigma^2$.

This results in the following equations:

$$Var[\hat{\mu}] = \frac{\sigma^2}{n} \tag{157}$$

$$Var[\hat{\sigma}] \approx \left(\frac{\alpha_4 - 1}{4}\right)\frac{\sigma^2}{n} \tag{158}$$

$$Cov[\hat{\mu}, \hat{\sigma}] \approx \frac{\alpha_3}{2}\frac{\sigma^2}{n} \tag{159}$$

The first moment reflects the uncertainty in the mean, the second the uncertainty in the standard deviation, whareas the last gives the correlation between these two estimates. These estimators are general, meaning they can be applied to any distribution. For a Gumbel model, the higher moments α_3 and α_4, are 1.14 and 5.4 respectively, while for a normal distribution, $\alpha_3 = 0$ and $\alpha_4 = 3$.

The first two moments are then used to predict the standard error $SE[x_p]$ of the simulations n as (Winterstein et al., 2001):

$$SE[x_p] = \frac{\sigma}{\sqrt{n}}\sqrt{1 + \alpha_3 * K_p + \left(\frac{\alpha_4 - 1}{4}\right) * K_p^2} \tag{160}$$

Where $K_p = {(x_p - \hat{\mu})}/{\sigma}$

Rewriting the term gives:

$$x_p = K_p\sigma + \hat{\beta} \tag{161}$$

In terms of a Gumbel standardized variable:

$$K_p = 0.78[-\ln(-\ln(p)] - 0.45 \tag{162}$$

The confidence intervals for the quantile estimate are then made using the standard error (SE[x_p]). The p% confidence level may then be expressed as:

$$\left(x_{p_L}, x_{p_H}\right) = \left[\bar{x}_p - z_{1-\frac{\alpha}{2}} * SE[x_p], \bar{x}_p + z_{\alpha/2} * SE[x_p]\right] = 1 - \alpha \tag{163}$$

$z_{1-\propto/2} = -z_{\propto/2}$ is the standard normal variable of a two tailored distribution for levels corresponding to the confidence interval $1 - \alpha$. z is here a confidence multiplier of a two tailed normal distribution. For a 90% confidence level, $z = 1.65$, for a 95% confidence level, $z = 1.96$, whereas a 99% level yields $z = 2.58$, etc.

Notice that x_L and x_H are stochastic variables. When the confidence interval is calculated, the resulting interval either contains the true value of x_p or not. Although when repeating an experiment/observation many times, the confidence interval should include the true value $(1 - \alpha) * 100\%$ of the times.

7.6 Limitations

For the specific lifting operation under consideration in this thesis, limitations and assumptions must be done:

1. The ROV model used in Orcaflex is a simplification of a real ROV. Even though the mass and volume is correct, uncertainties in buoyancy, COG, and simplifications regarding shape will affect the results slightly. Also, the hydrodynamic properties and distribution of drag and added mass are estimates and cannot be taken as 100% accurate unless model tests and/or CFD studies are carried out to confirm the values obtained.
2. The stiffness of the A-frame would be an estimate based on a simple "*Staad Pro*" software model. Also, the winch is simple and without any mass. The umbilical data are supplier specifications and should be fairly accurate.
3. Wind and current effects are not present in the analysis. The wind may cause a pendulum when using a vessel crane. When using a LARS frame, the TMS comes with the ROV gets fastened to the LARS tip prior to a launch, so neither the wind nor the vessel motions will have significant effects on the wire pendulum. Any current effects are neglected in the splash zone, although some horizontal forces may occur.
4. The main cases (Case 1a and 1b) under consideration handles a ROV launch with A-frame over the side of the vessel. Anyhow, the methodology discussed in this thesis would be the same for moonpool or crane operations.
5. Due to the complexity of phasing between incoming waves and lifting operation, the load case is investigated for a number of wave realizations. The operation is modeled as a "*blind*" lift, meaning that start of submergence/recovery is chosen arbitrary and no optimization has been applied with regards to timing of the lift. A winch speed of 1.0 m/s is used as base case.
6. Waves on the leeward side of the vessel would be dampened to some degree. But due to the fact that the motion of the vessel is only described by first order transfer functions, the presence of the vessel in the waves is not captured. Therefore, shielding- and radiation effects from vessel oscillation are not considered. Anyhow, shielding would not always be possible during a ROV/object launch/recovery. This goes especially for the two WROVs on Rem Ocean that is usually in operation simultaneously.
7. For simplification of the analysis, the crane/LARS tip motions are conservatively taken to represent the motion of the load. The crane/LARS motions are obtained from the COG of the vessel motions.

   Although these limitations and assumptions may have contributions when finding a characteristic load, the methodology suggested in this thesis will not suffer as a result.

7.7 Method for use in analysis

When performing analysis of lifting operations offshore, DNV-RP-H103 (2014, 3.4.3.7.) states:

"For lowering operations it is generally recommended to keep the object fixed in selected positions for minimum 30 min. If a continuous lowering of the object is simulated a large number of realizations is required in order to obtain a proper statistical confidence".

Also, from DNV-RP-C205 (2010, 10.7.2) one reads:

"For linear processes, the behaviors of the extremes are reasonably well known based on the standard deviation of the process, while for nonlinear processes it is essential to use and interpret measured extremes in a proper and consistent way. If only one sea state realization is run, it is better to use extreme estimates based on fitting of the tail of the peak distribution, rather than single sample extremes.

Further (DNV-RP-C205, 2010, 10.7.3):

"An extensive and accurate way to overcome the statistical variability problem is to run a large number of different realizations of the same spectrum, in order to obtain robust estimates. Strongly nonlinear processes exhibit a larger statistical scatter than weakly nonlinear processes, and the multiple realization approach is then often recommended. Sample extremes from each realization can be fitted to a Gumbel distribution, from which more robust extreme estimates can be estimated".

Two methods may then be applicable to use:

1. A stationary analysis where the object first is being stationed in some critical wave scenarios, or lowered slowly through the wave zone. This is done for some regular wave heights and wave periods to find the most critical situation and object position. Next, a stationary analysis in irregular waves based on a wave spectrum is performed while the object is placed in the most critical position. The analysis should last for 0.5-3 hours. Based on the results from analysis, extreme sea state/loads may be determined from statistical analysis.
2. Repeated lowering in critical irregular waves based on a wave spectrum where the object is lifted from air to well below surface in a short time frame (usually$<$ 1 minute). Different wave realizations then appear from each case. From the results in each case, the maximum forces, and if applicable, also minimum forces are extracted. These results may then be used in statistical analysis to study time series and estimate extreme sea state forces based on limiting criteria.

Method 1 will for cases involving lifting of light objects often give unrealistic values. This is partly due to the fact that a lift through the splash zone most often will be performed in less than1 minute, but also because waves interacting with a lifted object stationed in the wave

zone will cause a pendulum motion and thereby misaligned forces compared to a real splash zone lift will occur. Method 2 will therefore be preferred.

Based on chapter 2.2, the limiting criteria used in this thesis are the following:

1. The ultimate analysis states that the maximum structural capacity of the crane/LARS/object shall not be exceeded more often than in 1 per 10 000 operations (DNV-OS-H101, 2011, Section 1, A201):

$$F_{max\ (p=0.9999)} < F_{Crane/LARS/Object,max\ structural\ capacity}$$

2. The most probable maximum dynamic tension in any lifting appliances shall be lower than the lowest of either the SWL of the crane times the DAF used in the structural design, the wire design capacity, or the design capacity of the rigging.

$$F_{\max,dyn(p=X\%)} < min\left\{\begin{array}{c}(SWL_{crane} \times DAF) + W_{rigging} \\ F_{Lifting\ wire\ structural\ capacity}(MBL)\Big/\gamma_{sf} \\ F_{rigging\ structural\ capacity}(MBL)\Big/\gamma_{sf}\end{array}\right\} \quad (164)$$

Where SWL_{crane} is the safe working load for the crane at the given maximum radius used during the lift. $W_{rigging}$ is the summarizing weight of all rigging equipment. Also, a safety factor (γ_{sf}) is applied to the rigging equipment and lifting wire minimum breaking loads (MBL) to get the design load. The design load is representative to a safe working load (SWL) multiplied with the dynamic amplification factor (DAF). The required level of non-exceedance will be discussed in chapter 8 and 9.

The analysis performed in Orcaflex has been checked by zero-up crossing wave periods between (DNV-RP-H103, 2014, 4.3.2.1.):

$$8.9\sqrt{\frac{H_s}{g}} \leq T_z \leq 13 \quad [s] \quad (165)$$

The splash zone analyses are then run multiple times using different seed numbers for a target heading $\pm 15°$ of the wave direction (ref. DNV-RP-H103, 2014, 4.3.3.7), different wave periods (T_z), and significant wave heights to find the most critical scenario where snatch forces might occur. This critical scenario is then used as basis in this thesis for further statistical analysis. For the time-domain analysis, time steps (h) of 0.005s are used.

A spectrum covering a fully-developed sea state is used. The wave spectrum used in this thesis is based on DNV-RP-H103 (2014, 2.2.5.7) where a JONSWAP spectrum is proposed. The JONSWAP spectrum is covering fetch limited as well as the most critical sea states in relation to lifting operations in a good way, especially for the North Sea area (Gudmestad, 2015, p.352).

The maximum tensions from each simulation are then extracted and fitted to different distributions in probability papers. This is done to find the most suitable distribution for the prediction of maximum tensions.

To find the most suitable distribution, the least square error (R^2) function in excel has been used in the probability papers. The target is to get as close to 1 as possible, meaning the data follows a straight line perfectly. The least square error is defined as:

$$R^2 = \frac{\sum(y_i - \bar{y})^2 - \sum\left(y_i - y_{i_{calc}}\right)^2}{\sum(y_i - \bar{y})^2} \tag{166}$$

Where:
y_i is the extreme values ($i = 1,2, \dots n$) obtained from individual simulations
$\bar{y}$ is the average of all extreme values obtained
$y_{i_{calc}}$ for the given extreme value (x_i) is taken as:
$y_{i_{calc}} = mx_i + b$
Where m is the slope/gradient of the line, and b is the value of y when the line intersects with the x-axis.

8. Results

8.1 Linearization of non-linearized distributions in probability paper

When plotting on probability paper, a linearization of the non-linearized cumulative distribution function must be performed. The following Table 8 can be made, where $\hat{F}(x)$ represents the level of non-exceedance (Equation 133):

Table 8: Linearization of non-linear cumulative distributed functions (CDF)

Equation	Non-linear CDF equation, $F(x)$	Linearized equation	Linearized variables	
			x-axis	y-axis
Weibull	$F(x) = 1 - e^{-(x/\beta)^k}$	$\ln\left(-\ln\left(1-\hat{F}(x)\right)\right) = kln(x) - kln\beta$	$ln(x)$	$\ln\left(-\ln\left(1-\hat{F}(x)\right)\right)$
Exponential	$F(x) = 1 - e^{-((x)/\beta)}$	$\left[\left(-\ln\left(1-\hat{F}(x)\right)\right)\right] = \frac{x}{\beta}$	x	$\left(-\ln\left(1-\hat{F}(x)\right)\right)$
Gumbel	$F(x) = exp\left\{-exp\left\{-\left[\frac{x-\mu}{\beta}\right]\right\}\right\}$	$-\ln\left(-\ln\left(\hat{F}(x)\right)\right) = \frac{x-\mu}{\beta}$	x	$-\ln\left(-\ln\left(\hat{F}(x)\right)\right)$
Normal	$F(x) = \frac{1}{\sqrt{2\pi}}\int_{-\infty}^{z} e^{-x^2/2}dt = z_{1-\propto/2}$	$z_{1-\propto/2} = x$	x	$z_{1-\propto/2} = -z_{\propto/2}$
Log-normal	$F(x) = \frac{1}{\sqrt{2\pi}}\int_{-\infty}^{z} e^{-x^2/2}dt * \left[\frac{lnx-\mu}{\sigma}\right] = z_{1-\propto/2}$	$z_{1-\propto/2} = ln(x)$	$ln(x)$	$z_{1-\propto/2} = -z_{\propto/2}$

8.2 Case 1 – Supporter Mk2 WROV

In the first case, 500 simulations in a sea state with a significant wave height of 7.5 meter and zero up-crossing periods of 8 seconds are run (see Appendix 4 for data set values). The ROV is launched, and then recovered from 15m subsea in one continuous operation with a winch speed of 1 m/s. The largest observed wire tensions in each simulation are used to find a suitable distribution function. The distribution model generated from the given sample size (here 500 simulations) will then be assumed to be the "true" model.

It should also be noted that minimum values will not be considered here as occasions with no tension in the wire must be expected when evaluating objects with a relative low submerged weight.

8.1.1 Case 1a – Maximum forces during launch of a Supporter Mk2

Results using the best suited true distribution given all 500 simulation samples

Table 9 below illustrates the least square errors of 5 statistical distributions, and Figure 10 shows in probability paper the most suitable distributions for use when considering the 500 simulations generated in Orcaflex.

Table 9: R^2 values for different probability papers when considering all 500 simulations

Function	R^2
Weibull	0.3981
Exponential	0.8093
Gumbel	0.6815
Normal	0.4736
Log-normal	0.5887

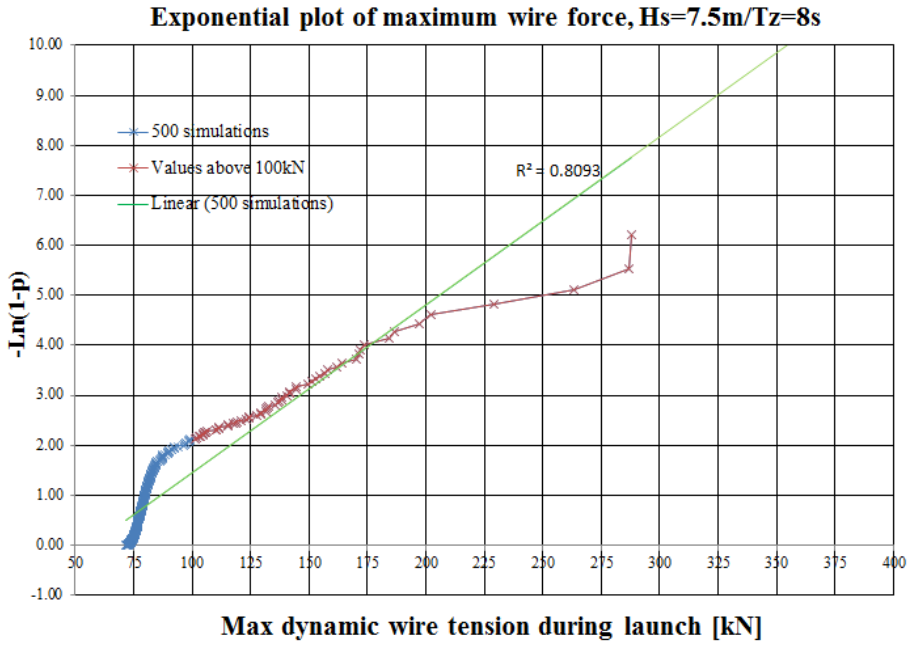

Figure 10: The Exponential distribution on probability paper using all 500 simulations when fitting the trend line

Considering the probability paper plots of the data simulations, one can see that the Exponential distribution seem to fit the data samples best in this case (Table 9). Based on the fact that the maximum in each simulation is extracted, a Gumbel extreme value distribution may in theory be assumed to be the most suitable for use (i.e. DNV-RP-C205, 2010, 3.7.3.2/ DNV-RP-C205, 2010, 10.7.3). Anyway, partly due to a limited number of wave crests during one simulation and thereby not extreme forces in each simulation, an exponential type of distribution seems reasonable for this case based on the probability paper plots (Table 9 and Figure 10).

From the true fitted line in the exponential plot where all 500 simulations have been taken into account, one can see that the 99.99% non-exceedance level equals:

$$-\ln(1-p) = x_p \tag{167}$$

$$-\ln(1-0.9999) = 9.21 \tag{168}$$

One sees from Figure 10 that the trend line at $y = 9.21$ intersects with the x-axis at about 330kN.

Results using the best suited distribution given simulation samples above 100kN

As the Exponential distribution in reality is poor when considering all 500 simulations performed, only values above a lower threshold value should be considered as it is the tail region that usually is of most importance. The lower threshold will here be set to 100kN based on the shape of the probability papers.

Table 10 below illustrates the least square errors of 5 statistical distributions, and Figure 11 and Figure 12 shows in a probability- and a CDF paper the most suitable distributions for use when considering the 59 samples with a value above 100kN. This lower value of 100kN might be adjusted down to about 90kN ($\mathrm{Ln}(90) = 4.5$) without large deviations in the results obtained. The important thing is to get a sufficient amount of the largest loads (i.e. more than 10% of the largest load), and that they all follow a given distribution quite well. Therefore, values below 90kN will cause larger deviations as the distribution for these values does not follow a Weibull well, see Figure 11.

Table 10: R^2 values for different probability papers when considering values above 100kN (59 simulations)

Function	R^2
Weibull	0.9815
Exponential	0.9724
Gumbel	0.9713
Normal	0.9511
Log-normal	0.9842

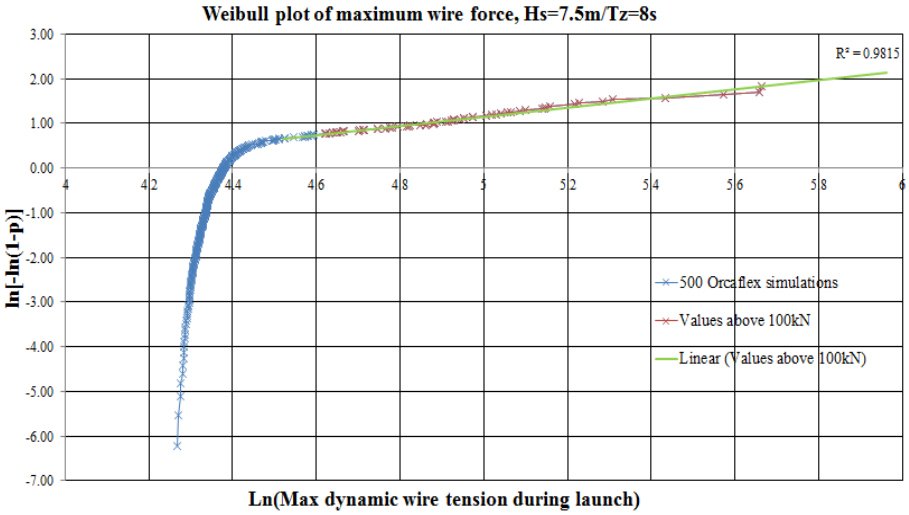

Figure 11: The Weibull distribution proves most suitable for use in this case

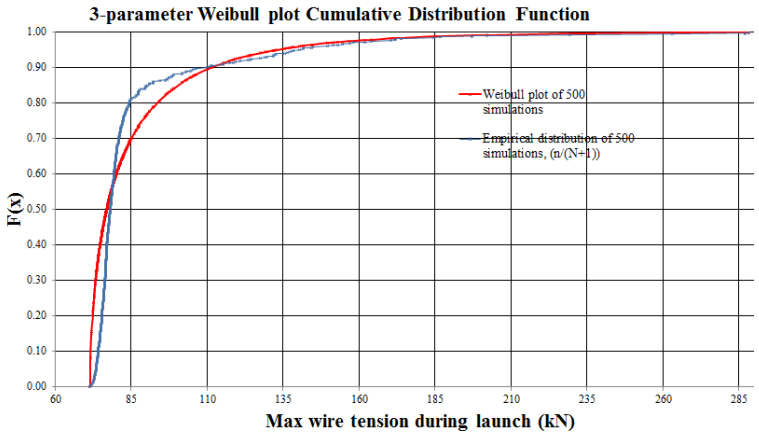

Figure 12: Illustration of the CDF by comparing the Weibull function with the empirical function, the parameters is k=0.6, β=10.0 and X=X-X_{min} (71.436kN).

As the tail region has more extreme values, a Gumbel distribution might prove more accurate for use when considering the most extreme values. However, as the least square test for values exceeding 100kN for the Gumbel distribution ($R^2 = 0.9713$) proves slightly less accurate than for the Weibull ($R^2 = 0.9815$), the Weibull distribution should prove reliable for this area as well. The lognormal may prove just as good, but as the Weibull distribution is an exponential type of distribution, which in theory follows the wave process, one may assume this to be a suitable model in this specific case.

To let the Weibull distribution start out from 0 and set a lower threshold value, a 3-parameter distribution with a γ_1-parameter is used to slide/straighten the Weibull function (Figure 13). This parameter is set to the lowest observation value among the 500 simulations, here 71.436kN equals x_{min}.

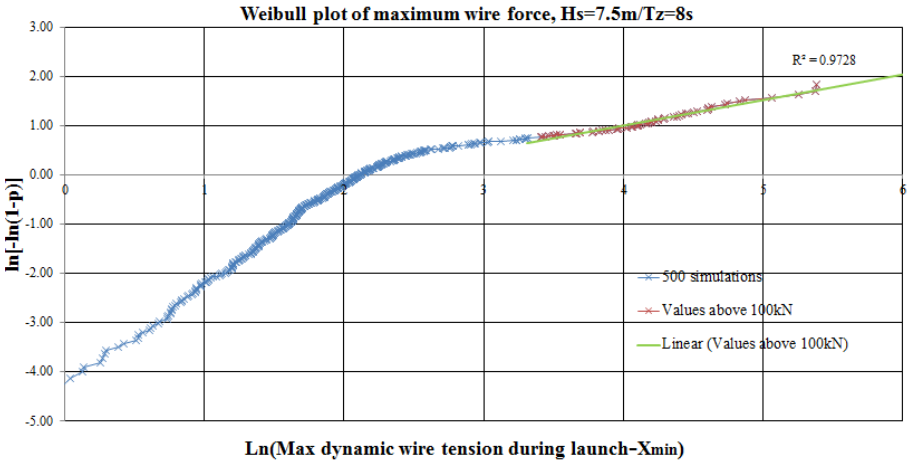

Figure 13: The Weibull probability plot adjusted with a minimum value, X_{min}=71.436kN

Limiting criteria #1, $p = 99.99\%$ non-exceedance

By using method of moments for estimating parameters of the Weibull distribution, one gets from the upper 59 simulations that:

$$\widehat{\boldsymbol{k}} = \mathbf{1.05}$$
$$\widehat{\boldsymbol{\beta}} = \mathbf{44.59}$$

Also, the γ_1-parameter is set to the lowest observation value among the 59 simulations, here 101.86kN equals $\gamma_1 = x_{min}$.

$$F(x) = 1 - e^{-\left(\left(x_p - x_{min}\right)/\hat{\beta}\right)^{\hat{k}}} \tag{169}$$

$$\ln\left(-\ln\left(1 - \hat{F}(x)\right)\right) = \hat{k}ln\left(x_p - x_{min}\right) - \hat{k}ln\hat{\beta} \tag{170}$$

$$x_p = e^{\left[\frac{\ln\left(-\ln\left(1-\hat{F}(x)\right)\right)}{\hat{k}}\right]} * \hat{\beta} + x_{min} \tag{171}$$

$$x_{0.9999} = e^{\left[\frac{\ln(-\ln(1-0.9999))}{1.05}\right]} * 44.59 + 101.86kN = \underline{473.58\ kN} \tag{172}$$

In this case, one has 441 values lower than the tailfitted line range. This means that the value of 486.00 kN actually corresponds to a higher probability of non-exceedance by the relation:

$$\begin{aligned} p_{non-exceedance,actual} &= p_{non-exceed} \\ &+ \left(p_{exceed} * \left(1 - \left[\frac{n_{values\ in\ range} - n_{values\ above\ range}}{N_{total}}\right]\right)\right) \end{aligned} \tag{173}$$

The 99.99% quantile for the tail fitted range therefore corresponds to:

$$\begin{aligned} p_{non-exceedance,actual} &= 99.99\% + \left(0.01\% * \left(1 - \left[\frac{59\ samples\ in\ range}{500\ total\ samples}\right]\right)\right) \\ &= 99.9988\% \end{aligned} \tag{174}$$

For the line fitted to the 59 simulations, a <u>99.914%</u> probability of non-exceedance then actually corresponds to a 99.99% level, meaning that:

$$x_{0.9999} = e^{\left[\frac{\ln(-\ln(1-0.99914))}{1.05}\right]} * 44.59 + 101.86kN = \underline{388.65\ kN} \tag{175}$$

$$\boldsymbol{MBL < F_{max}(x_{0.9999}) \rightarrow 388.65kN < 620kN \rightarrow OK} \tag{176}$$

F_{max} is the maximim load given a probability of non-exceedance (x_p).

Assessing the uncertainty:

In this case where a Supporter Mk2 is being launched, 500 simulations were performed. Due to long simulation time and the fact that results does not seem to converge to a specific value of non-exceedance, this approach is not feasible in the long run. In general, one will have two opposing pressures:

1. Generating too few simulations/samples resulting in low confidence, and therefore inaccurate outputs and graphs.
2. The generation of too many simulations/samples; resulting in long simulation time, and often even longer time to plot graphs, export and analyze data, etc. afterwards.

To get a representation of the confidence level of the results when having other sample sizes, a parametric bootstrapping method is used to get random numbers using excel. As the exponential distribution is suitable for use in the tail region ($k \approx 1$ and $R^2 = 0.9713$), the following equation will be generated in excel in order to create new samples:

$$\boldsymbol{x_{samples}} = \underbrace{[-\mathbf{ln}(\mathbf{1} - \boldsymbol{rand}())] * \widehat{\boldsymbol{\beta}} + \boldsymbol{x_{min}}}_{\boldsymbol{Exponential\ sample\ generation}} \tag{177}$$

Where $rand()$ give random numbers ranging from 0 to 1. It should also be noted that focus is put on the upper tail region, and to simplify, 50 generated samples (not 59) from the upper tail region will therefore correspond to 500 samples in the true distribution using $k = 1$, $\hat{\beta} = 42.12$, and $x_{min} = 110.41kN$.

Then, 1000 random groups of N samples are simulated to find a trend of the confidence level. A trend of the 90%, 95% and 99.99% (Figure 15) confidence interval levels can be drawn based on the fact that the limiting quantile of the 1000 groups are expected to be approximately normally distributed (Figure 14).

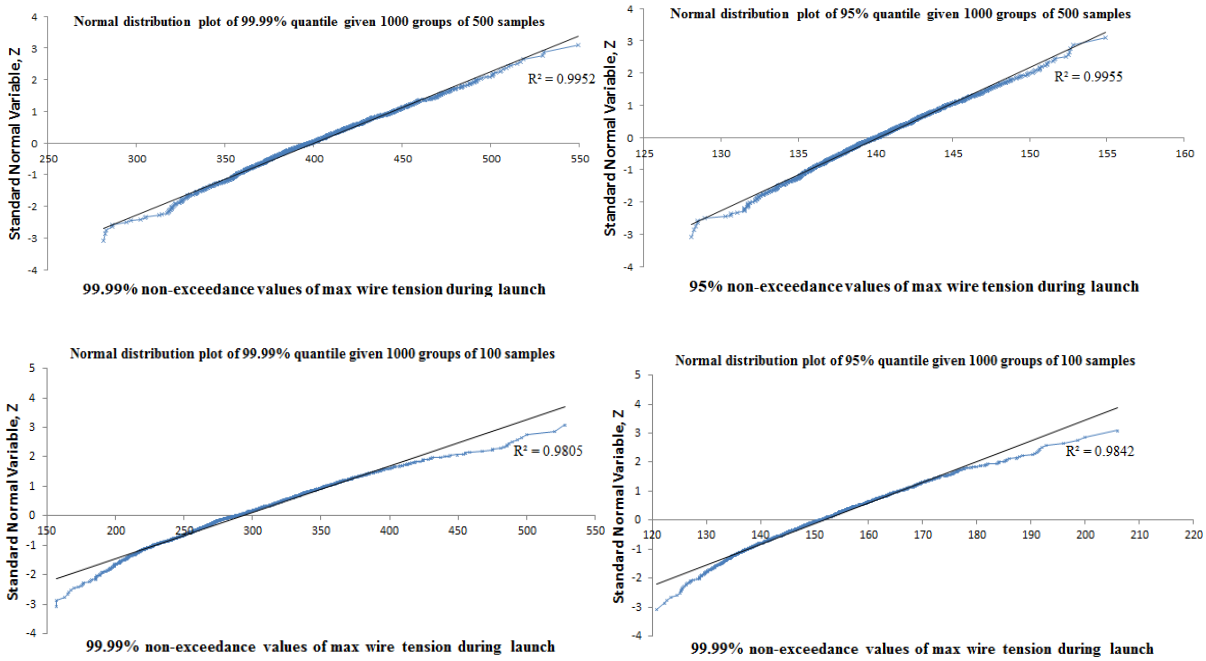

Figure 14: Some examples to prove that the x% level of non-exceedance follows a normal distribution quite well given 1000 groups of 100 (bottom) and 500 (top) samples. More accurate the more samples one has.

The formula used to produce the confidence level trend lines is then expressed as:

$$\left(x_{p_L}, x_{p_H}\right) = \left[\bar{x}_p - z_{1-\frac{\alpha}{2}} * SE\left[x_p\right], \bar{x}_p + z_{\alpha/2} * SE\left[x_p\right]\right] = 1 - \alpha \qquad (178)$$

$$\left(x_{p_L}, x_{p_H}\right) = \left[\bar{x}_p - z_{1-\frac{\alpha}{2}} * \sigma_p,\ \bar{x}_p + z_{\alpha/2} * \sigma_p\right] = 1 - \alpha \qquad (179)$$

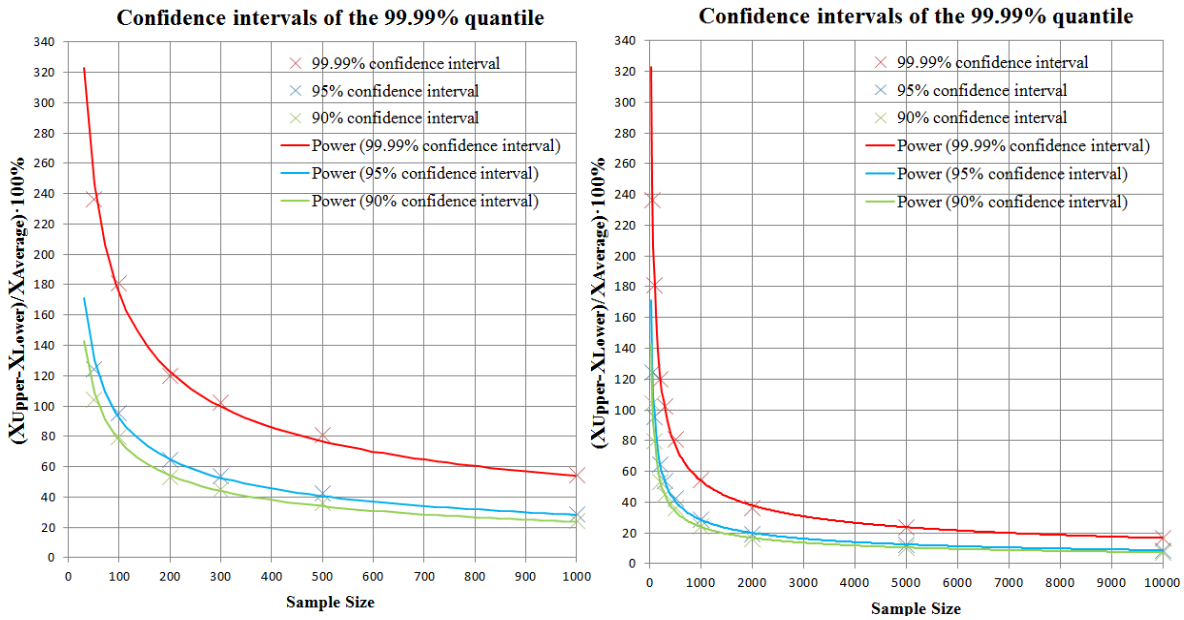

Figure 15: Confidence interval variations of the 99.99% quantile when considering the exponential distribution as "true" for the upper tail region; Left figure is up to 1000 samples; Right up to 10.000

By using the power trend line function in Excel, a curved line suited to compare measurements that decrease at a specific rate is being used as an indicator of the uncertainty. One can then see that the uncertainty/deviation from the assumed "true" model seems to stall somehow at about 1000 simulations, flattening at 10 000 simulations where 7.5% uncertainty is expected.

From the 99.99% confidence interval, one sees that a variation from the mean 99.99% quantile of about 80% may appear when generating 500 simulations. Meaning that this result may emerge:

$$\boldsymbol{F_{max}(x_{0.9999}) * 1.8 < MBL \rightarrow 700.57kN < 620kN \rightarrow NOT\ OK} \quad (180)$$

In order not to go beyond the minimum breaking load (MBL) of the lifting wire, one needs less than 55.70% uncertainty deviation from the (average) “true” distribution. To get this level of confidence, one should here have at least 1000 simulation samples. As a simulation size of 1000 is inefficient when finding the characteristic load criteria, a second more reliable criterion is needed. This criterion would then be used as a double check as the 10^{-4} probability of non-exceedance has a quite large variability, especially for smaller simulation sizes. It is therefore difficult to establish a sufficient reliable characteristic load based on extrapolating towards a value outside the value range given from repeated simulations in the time domain.

Additional research notes about the parametric bootstrapping method used:

As a note, the assumed "true" distribution model might in reality be offset compared to if new simulations are performed in Orcaflex; thereby skewing the uncertainty interval. Optimally, the uncertainty/confidence should be assessed by running multiple runs of simulations in Orcaflex to capture the physical parameter uncertainty (not only the statistical parameters) as well. But this procedure would be very time consuming.

By running 10 new sets of 500 simulations in Orcaflex, one may assume from Figure 16 that the outer deviations compared to the average would indicate a normally distributed 90% confidence interval. One then gets the 99.99% non-exceedance confidence interval by the relation:

$$\frac{(highest\ valued\ distribution - lowest\ valued\ distribution)}{average\ result\ of\ the\ 11\ distributions} = \left(\frac{439kN - 302kN}{374kN}\right) * 100\% = 36.54\%$$

Also here, the exponential distribution is used for the upper 50 values in each group. From (Figure 15), the parametric bootstrapping indicates an uncertainty of 36.07% given a 90% confidence interval of the 99.99% non-exceedance value.

Based on this, and checking other values of non-exceedance as well, it seems reasonable to assume/believe that Monte Carlo simulations by parametric bootstrapping in the tail region are effective when assessing the uncertainty although some variations are experienced for other values of non-exceedance. Parametric bootstrapping can never be taken as the fully truth as physical differences are not covered by the statistics (aleatory uncertainty), and no "new" information (epistemic uncertainty) is received by using this method. Therefore, only indications of whether or not a given model is "true" can be established. One would then never be fully certain that characteristic load criteria are being maintained using parametric bootstrapping, although the confidence intervals make sure that a conservative load is extracted.

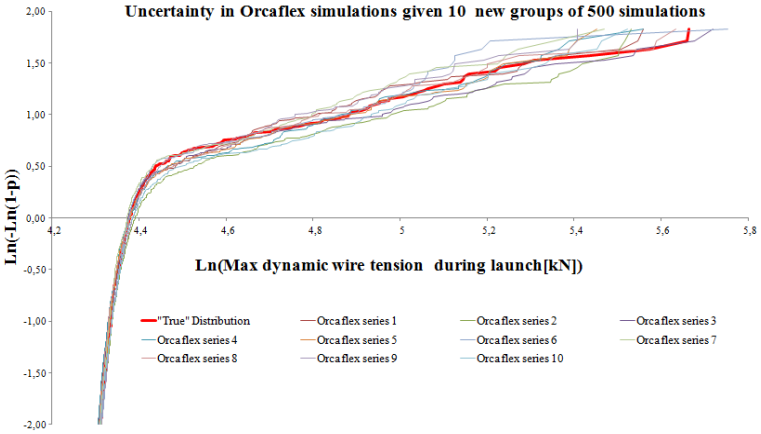

Figure 16: Illustration of the uncertainty in the assumed "true" model by generating 10 new groups of 500 simulations in Orcaflex. Comparison between Orcaflex sample generation and Monte Carlo sample generation for the tail region can be done towards the right Figure 17.

Limiting criteria #2

For the second criterion, a non-exceedance value where the design capacity is just not being exceeded may be a good starting point. For the line fitted to the 59 samples, a total probability of 98.82% non-exceedance corresponds to a 90% level for the fitted line:

$$F_{max}(x_{0.9882}) = e^{\left[\frac{\ln(-\ln(1-0.90))}{1.05}\right]} * 44.59 + 101.86 = \underline{201.46\ kN} \tag{181}$$

$$\boldsymbol{F_{max}(x_{0.9882}) < \frac{MBL}{\gamma_{sf}} \rightarrow 200.53kN < 206.66kN \rightarrow OK} \tag{182}$$

By evaluating the variation in data, one can draw Figure 17 based on the randomly generated Monte Carlo simulations, here by using the Weibull distribution relation:

$$\underbrace{\boldsymbol{x_{samples,Weibull\ form} = Ln\left[\left[e^{\left(ln\left(\frac{-ln(1-rand())}{\hat{k}}\right)\right)}\right] * \hat{\beta} + x_{min}\right]}}_{\substack{\boldsymbol{Weibull\ generated\ samples} \\ \boldsymbol{\rightarrow Generated\ to\ Weibull\ form\ (Ln(x_{samples}))}}} \tag{183}$$

Where $rand()$ gives random numbers ranging from 0 to 1. Here, $\hat{k} = 0.603$, $\hat{\beta} = 10.0$ and $x_{min} = 71.436kN$ are used.

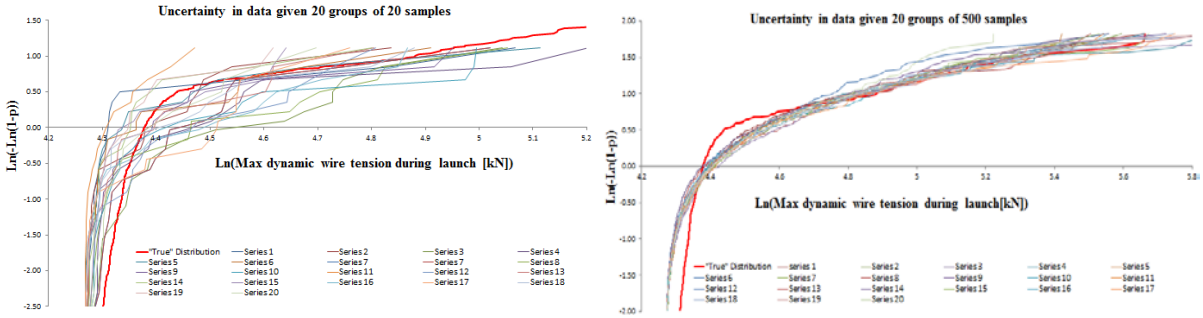

Figure 17: Visualization of the uncertainty in 20 data groups for 20 and 500 samples respectively (Weibull generated samples). Some deviation from the "true" distribution in the lower regions due the "Method of Moment" focusing on the tail region, and the fact that the samples are not following a Weibull distribution that well in other areas than in the tail region. Also, other parameters should be used for the tail region for more accuracy.

The confidence intervals for a 99% quantile (Figure 18) are extracted from the exponential distribution (Equation 177).

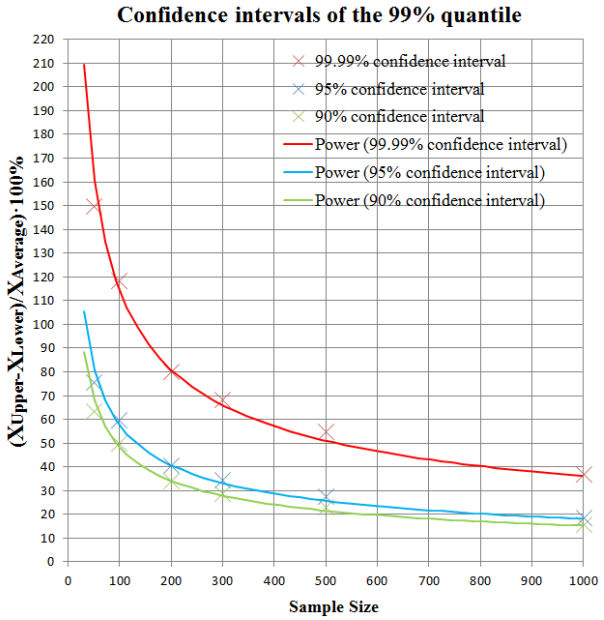

Figure 18: 99% quantile confidence intervals

From the results using 500 samples, a 99.99% confidence interval variation in the mean 99% quantile of about 50% is expected (Figure 18). Meaning that this result may emerge:

$$\boldsymbol{F_{max}(x_{0.9882}) * 1.5 < \frac{MBL}{\gamma_{sf}} \rightarrow 300.80kN < 206.66kN \rightarrow Not\ OK} \quad (184)$$

By lowering the probability of non-exceedance to 95%, the following result is generated from the tail-fitted range:

$$x_{0.95} = e^{\left[\frac{\ln(-\ln(1-0.58))}{1.05}\right]} * 44.59 + 101.86kN = \underline{140.80\ kN} \quad (185)$$

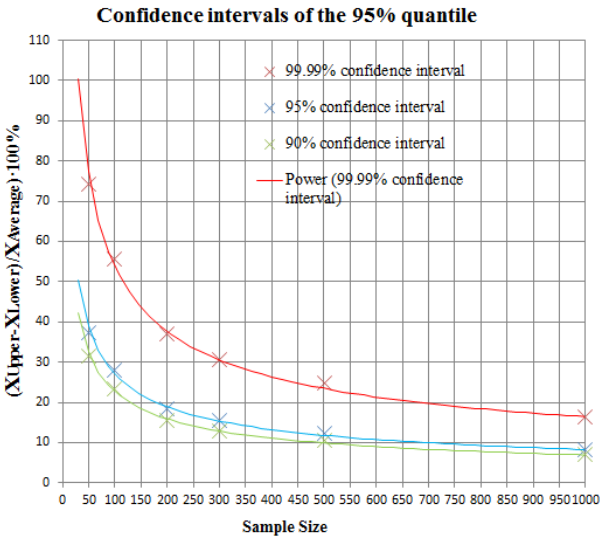

Figure 19: Confidence intervals of the 95% quantile

Given 500 samples, one can see from the figure that a variability of about 25% from the mean "true" distribution is expected using a 99.99% confidence interval (Figure 19). One thereby gets:

$$\boldsymbol{F_{max}(x_{0.95}) * 1.25 < \frac{MBL}{\gamma_{sf}} \rightarrow 176.00kN < 206.66kN \rightarrow OK} \quad (186)$$

If only 150 samples were generated and assuming the same generated trend line, about 45% uncertainty from the mean is expected given a 99.99% confidence interval:

$$\boldsymbol{F_{max}(x_{0.95}) * 1.45 < \frac{MBL}{\gamma_{sf}} \rightarrow 204.16kN < 206.66kN \rightarrow OK} \quad (187)$$

Based on results obtained, it would be advisable to keep the confidence intervals close to the same level as the level of non-exceedance. This means that the second criterion would in this case be withheld by keeping a 95% non-exceedance level and generating more than 40 samples.

8.1.2 Case 1b – Maximum forces during recovery of a Supporter Mk2

Below are two illustrations of how typical time series looks like when recovering the Supporter Mk2 ROV onboard Rem Ocean. The first one (left figure) has some occurrences of slack, resulting in snap forces/peaks at around 350kN. The second right figure is a more common case without any slack. The maximum wire force is here about 110kN.

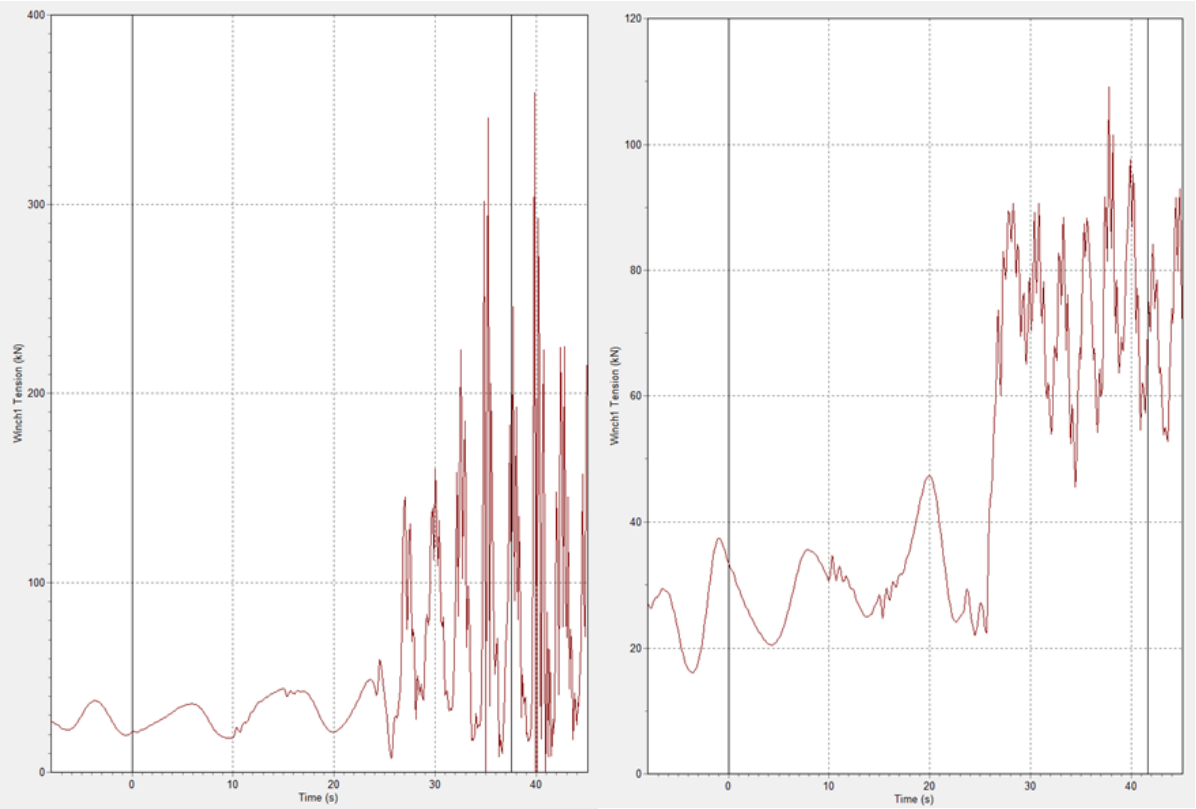

Figure 20: Two time series for the recovery of a Supporter Mk2 ROV onboard Rem Ocean

Illustration of the best suited true distribution given all 500 samples

As an illustration only, Table 11 gives the best least square errors (R^2) when considering all 500 simulations (see Appendix 5 for exact numbers), while Figure 21 gives a probability plot of the most suitable distribution. No calculations will be performed as the results will be unrealistic (ref. chapter 8.1.1).

Table 11: R^2 values for different probability papers when considering all 500 simulations

Function	R^2
Weibull	0.5115
Exponential	0.6955
Gumbel	0.5963
Normal	0.4204
Log-normal	0.6920

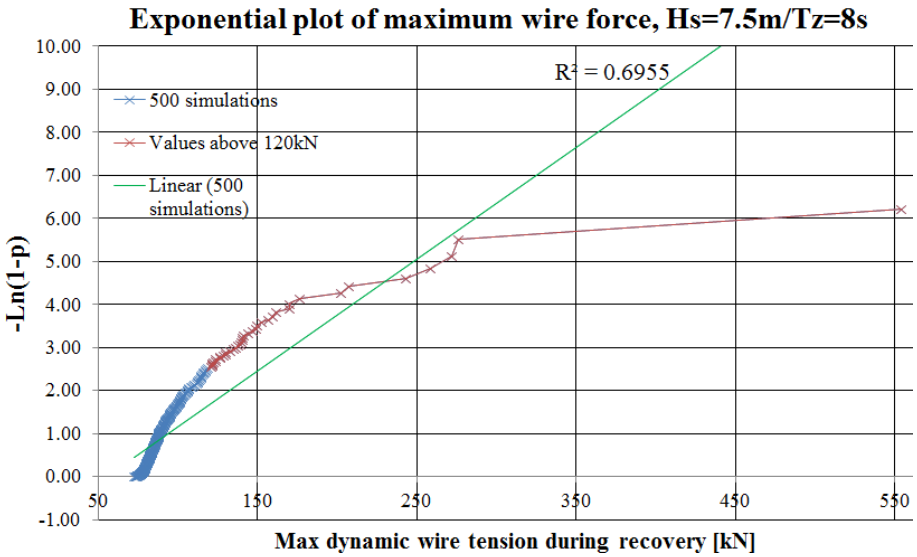

Figure 21: Least square error produced on an Exponential paper plot using all 500 samples

Results using the best suited distribution given samples above 120kN

To find a well suited distribution for the tail region, a lower threshold of 120kN is set. Table 12 below illustrates the least square errors of 5 statistical distributions, and Figure 22 and Figure 23 gives a probability plot and a CDF illustration of the most suitable distribution for use when considering the 40 samples with a value higher than 120kN.

Table 12: R^2 values for different probability papers when considering values above 120kN (the 40 upper out of 500 simulations)

Function	R^2
Weibull	0.9090
Exponential	0.7839
Gumbel	0.7806
Normal	0.7287
Log-normal	0.9114

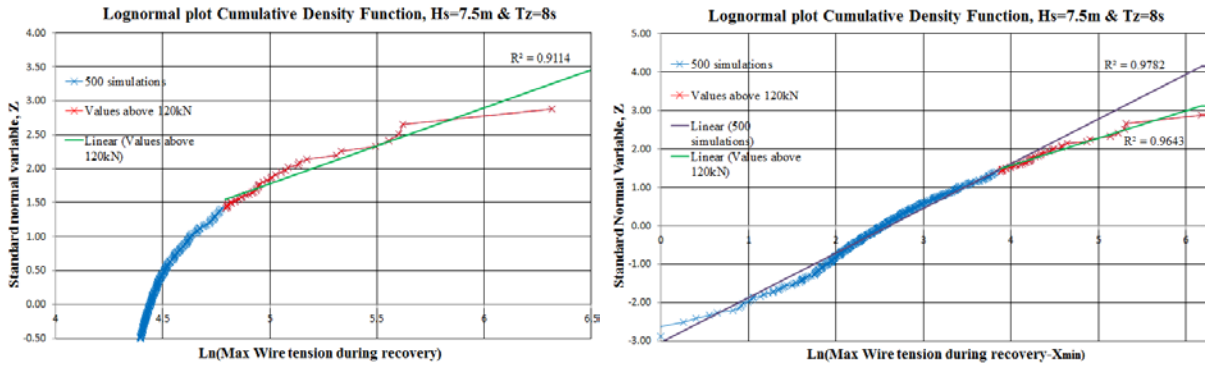

Figure 22: By considering the least square error produced for loads above 120kN, the lognormal distribution seems most suitable. The right graph is adjusted with the minimum value in the distribution, X_{min}=72.224kN.

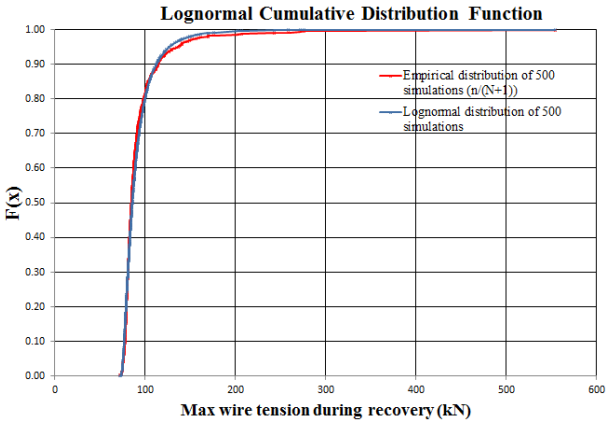

Figure 23: CDF by comparing the lognormal function with the empirical function.

From the adjusted lognormal graph (Figure 22, right), it seems like it follows a straight line quite well when using all 500 simulations as well ($R^2 = 0.9783$), although the line produced for values above 120kN follows the tail region better.

Limiting criteria #1, $p = 99.99\%$ non-exceedance

From the lognormal distribution, the following results are derived (99.87% corresponding to a 99.99% non-exceedance level for fitted line) using the 40 values above 120kN:

$$ln(x_p - x_{min}) = \mu + \sigma z_{1-\alpha/2} \quad (188)$$

$$x_p = e^{\mu+\sigma z_{1-\alpha/2}} + x_{min} \quad (189)$$

$$x_{0.9999} = e^{(4.37+0.49*3.011)} + 118.64kN = \mathbf{469.08kN < 620kN \rightarrow OK} \quad (190)$$

New data sets are then produced using a Weibull distribution for the upper 40 values, while the uncertainties are assessed by using the Lognormal distribution to find the non-exceedance level for every groups of samples. The formula used in the Monte Carlo simulation is:

$$\boldsymbol{x_{samples} = Ln\left[\left[e^{\left(ln\left(-ln(1-rand())/\hat{k}\right)\right)}\right]\right]} * \hat{\boldsymbol{\beta}} + \boldsymbol{x_{min}} \quad (191)$$

$$\underbrace{\qquad\qquad\qquad\qquad}_{\textbf{Weibull sample generation}}$$

Where $\hat{k} = 1.25$, $\hat{\beta} = 99.83$, and $x_{min} = 118.64kN$.

Looking at the confidence intervals as shown in the illustration below (Figure 24), the indication is that one should have at least 5000 samples to be within the MBL limits of a 99.99% confidence interval.

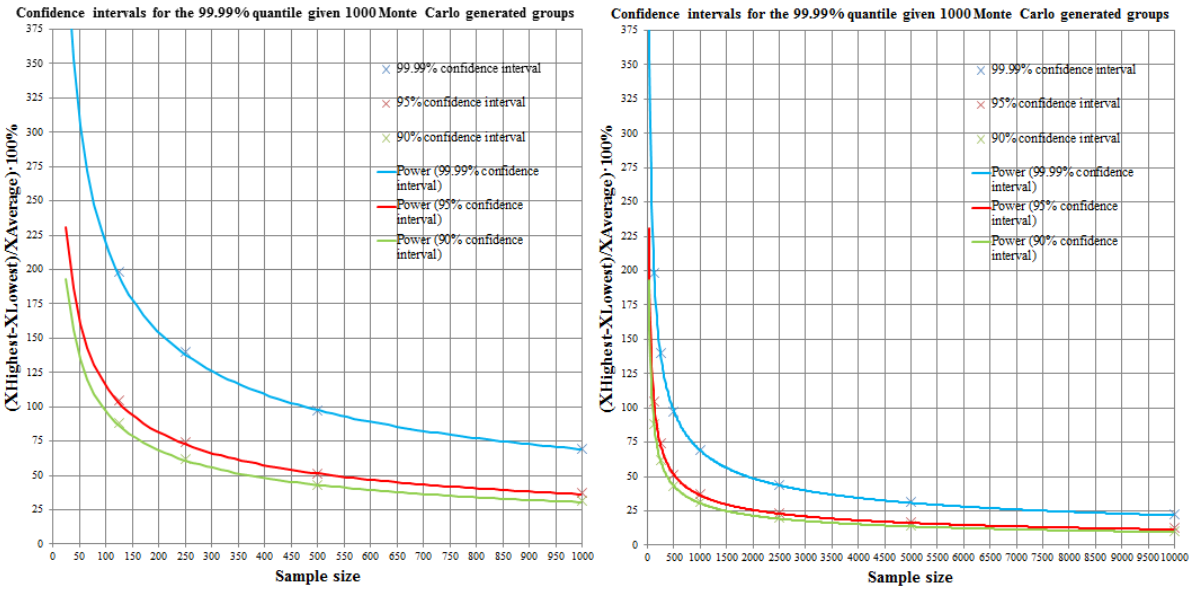

Figure 24: Confidence interval variations of the 99.99 % quantile; Left up to 1000; Right up to 10.000

Limiting criteria #2

For the second criterion, a total probability of 96.63% non-exceedance is chosen (corresponding to a 58% level for the fitted line) as the design capacity is not exceeded then:

$$x_{0.9880} = e^{(4.38+0.49*0.2)} + 118.64kN = \underline{206.16\ kN} \tag{192}$$

$$\boldsymbol{F_{max}(x_{0.9880}) < \frac{MBL}{\gamma_{sf}} \rightarrow 206.00kN < \frac{620kN}{3.0} \rightarrow OK} \tag{193}$$

By evaluating the uncertainty in the data, the following uncertainty and confidence interval graphs (Figure 25) can be made:

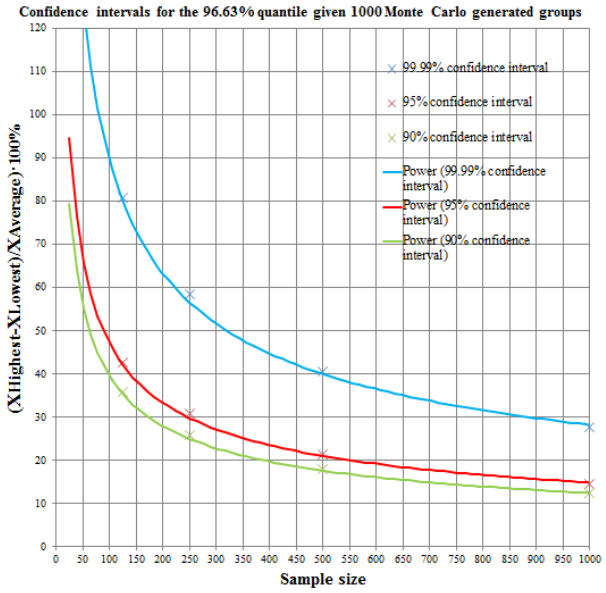

Figure 25: Confidence interval variations of the 96.63% quantile

From the power line function one may see that a 95% confidence interval variation in the 96.63% quantile of about 15% is expected for 500 samples, meaning that:

$$\boldsymbol{F_{max}(x_{0.9882}) * 1.18 < \frac{MBL}{\gamma_{sf}} \rightarrow 243.08kN < 206.66kN \rightarrow Not\ OK} \tag{194}$$

By lowering the probability of non-exceedance to 95%, the following result is generated from the tail fitted range:

$$\boldsymbol{F_{max}(x_{0.95}) = e^{(4.38+0.49*(-0.33))} + 118.64kN = 185.78kN < 206.66kN \rightarrow OK} \tag{195}$$

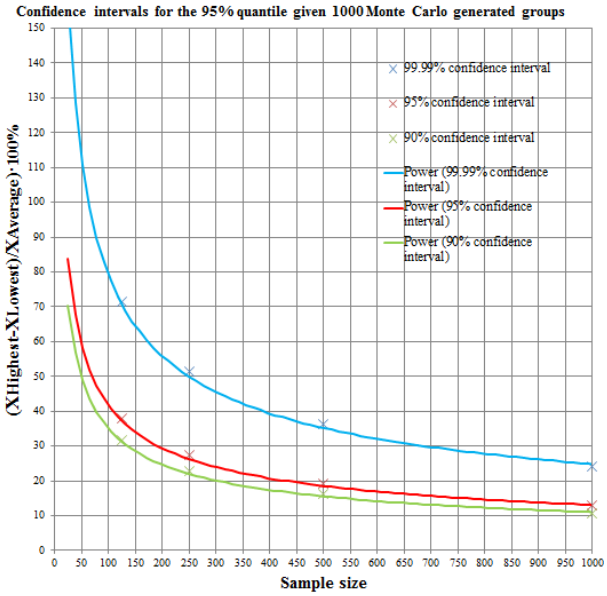

Figure 26: Confidence interval variations of the 95% quantile

From Figure 26 one can see that a variability of less than 10% in the 95% confidence interval is achieved by having more than 1000 samples. Given 1000 samples, the variability from the mean is about:

$$\boldsymbol{F_{max}(x_{0.95}) * 1.10 < \frac{MBL}{\gamma_{sf}} \rightarrow 204.35kN < 206.66kN \rightarrow OK} \tag{196}$$

The limiting H_s for the lifting wire MBL during launch and recovery based on one forecasting source and a sufficient amount of simulations performed will then be:

$$H_{s,OP} = \alpha * H_{S,Design} \tag{197}$$

$$\boldsymbol{H_{s,OP} = 0.8 * 7.5m = \underline{6meter}} \tag{198}$$

It should be noted that the limit might be higher (or lower) when considering a higher design H_s and other wave periods. Also, other limitations with regards to heave compensation, LARS frame, fundaments etc. is not evaluated.

8.2.1 Case 2 - ROV launch, Maximum forces

As an additional case, a Kystdesign Installer 4 WROV without any TMS (Figure 27) has been simulated in Orcaflex to see how the statistical distribution is acting on a neutral buoyant object alone during a launch case. It is then expected that a slack wire will occur for every simulation performed, and thereby also some responding snap forces. 500 simulations in a sea state with a significant wave height of 3 meter and zero up-crossing periods of 5 seconds are used. Appendix 6 summarizes the Orcaflex values that are obtained.

Figure 27: Installer 4 onboard Crest Bazan 2 (right picture), launched by a smaller crane. Photos are obtained from Sveen (2015).

The properties used as input for the ROV and crane are shown in the Table 13 below. The hydrodynamic properties of the Installer ROV are derived in the same manner as for the Supporter Mk2 ROV used in case 1 (Appendix 2). The vessel used is Crest Bazan 2 which is a bit smaller than Rem Ocean.

Table 13: Properties of the vessel and the Installer 4 WROV system

Structural Input	Value	Unit
Constants		
Gravity	9.81	[m/s^2]
Seawater density	1027	[kg/m^3]
Steel density	7850	[kg/m^3]
Derived added mass factors x/y/z	$A_x = 4.81$ Te and $C_{Ax} = 0.75$ $A_y = 5.65$ Te and $C_{Ay} = 0.65$ $A_z = 4.51$ Te and $C_{Az} = 0.74$	[Te and -]
Drag factors x/y/z	2.5	[-]
Water entry/exit coefficients	5.0 / 2.5	[-]
Crest Bazan 2 main characteristics		
Gross Tonnage	1944	[Te]
Deadweight	1452	[Te]
Length x Breadth	60m x 16m	[m^2]
Installer 4 WROV - Main dimensions		
Length	3.00	[m]

Width	1.50	[m]
Height	2.00 (skid included)	[m]
Displacement	4.24	[m^3]
Weight	43.50	[kN]
Weight in water	0.00 (will vary, but assumed neutral)	[kN]
Umbilical and crane - Main dimensions		
Outer diameter	19.05	[mm]
Mass/unit length	2.30	[kg/m]
Minimum Breaking Load (MBL) – Wire	308	[kN]
SWL crane at 10m arm	73.9	[kN]
Design Factor/DAF	1.3	[-]
K - Crane	10117	[kN/m]
K – Umbilical	44000	[kN/m]
K - combined	8225	[kN]

The limiting structural capacity is here the wire ($\boldsymbol{MBL = 308kN}$), while the second criterion is limited by the crane:

$$(\boldsymbol{SWL_{crane} \times DAF}) + \boldsymbol{W_{rigging}} = \boldsymbol{73.9kN * 1.3 = 96kN} \quad (199)$$

By evaluating all 500 samples (Table 14, Figure 28 and Figure 29); one can see that the exponential distribution is a good distribution model for the samples although the upper two samples seems to have a slope reduction. This makes the exponential distribution very useful also when considering the confidence interval levels.

Table 14: R^2 values for different probability papers when considering all 500 simulations

Function	$\boldsymbol{R^2}$
Weibull	0.7400
Exponential	0.9938
Gumbel	0.9581
Normal	0.8256
Log-normal	0.9086

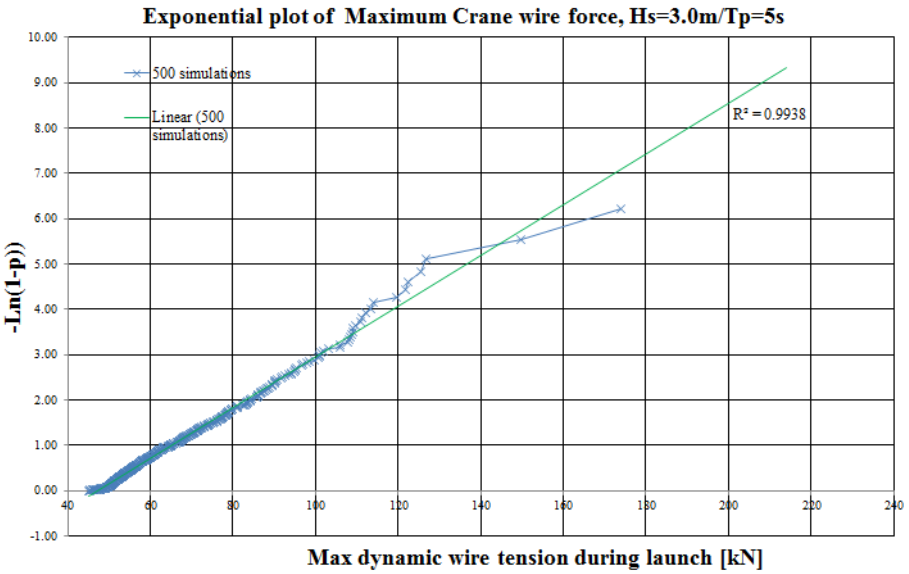

Figure 28: Probability paper plot of the Exponential distribution on probability paper

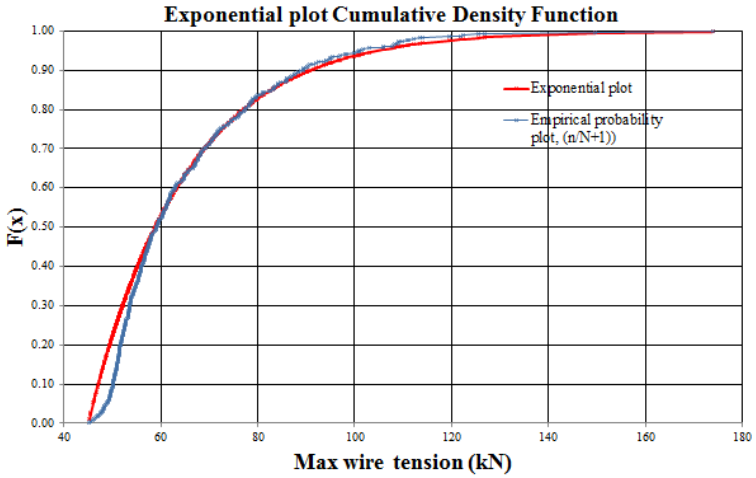

Figure 29: CDF of the Exponential distribution compared with the true distribution

Limiting criteria #1, $p = 99.99\%$ non-exceedance

From the true fitted line where all 500 samples has been taken into account, the following results are derived from the exponential linearized distribution (99.99% non-exceedance):

$$F(x) = 1 - e^{-\left(x_p - x_{min}/\hat{\beta}\right)} = p \tag{200}$$

$$-\left(x_p - x_{min}/\hat{\beta}\right) = \ln(1-p) \tag{201}$$

$$x_p = -\ln(1-p) * \hat{\beta} + x_{min} \tag{202}$$

Where x_{min} is the minimum value among the 500 samples, here 45.19kN. This value is subtracted from all the original values to have the exponential distribution starting out from 0.

$$\begin{aligned} x_{0.9999} &= -\ln(1-p) * \hat{\beta} + x_{min} \\ &= -\ln(1-0.9999) * 19.95 + 45.193kN = 228.90\ kN \end{aligned} \tag{203}$$

$$\boldsymbol{F_{max}(x_{0.9999}) < MBL \rightarrow 228.90kN < 308.00kN \rightarrow OK} \tag{204}$$

As seen from Figure 30, a 99.99% confidence interval is maintained given more than 350 samples.

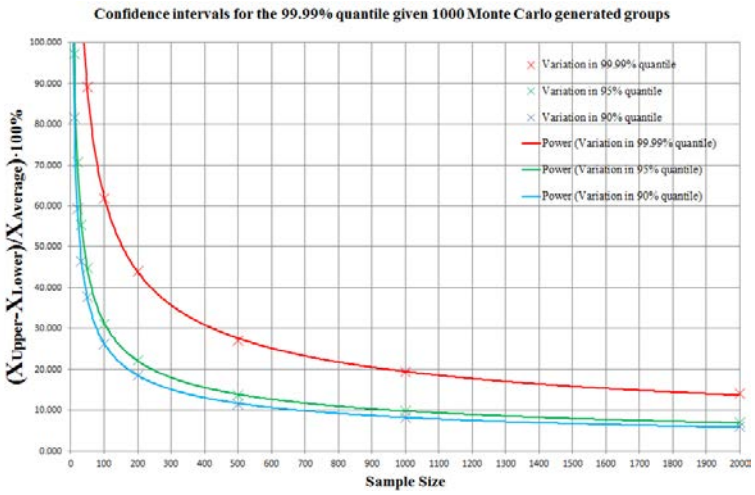

Figure 30: Confidence interval variations for the 99.99% quantile

The figures below (Figure 31 and Figure 32) are illustrating the uncertainty in the exponential distribution used given 20 and 500 Monte Carlo generated simulations.

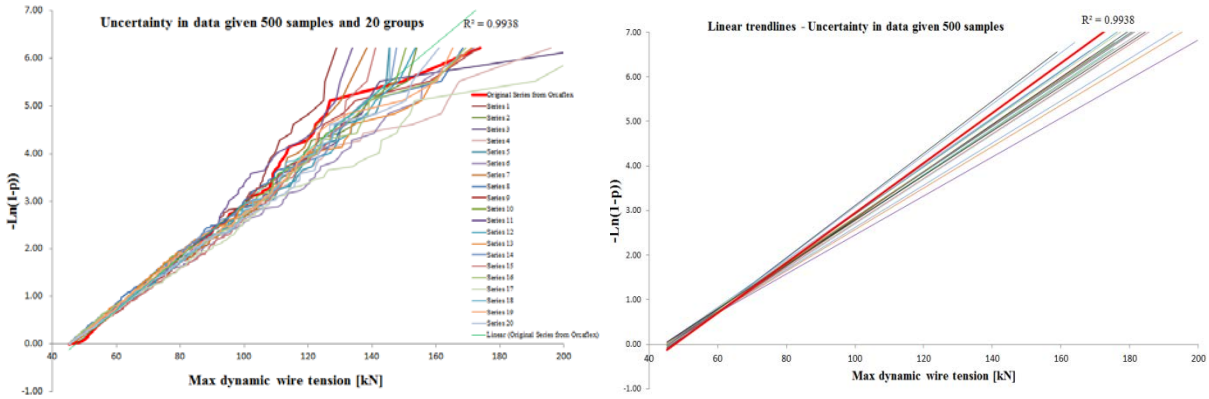

Figure 31: Illustration of the uncertainties in a sample size of 500 (20 groups generated by Monte Carlo simulations). The trend lines are shown to the right. The red line in each illustration is the original/"true" sample from Orcaflex simulations.

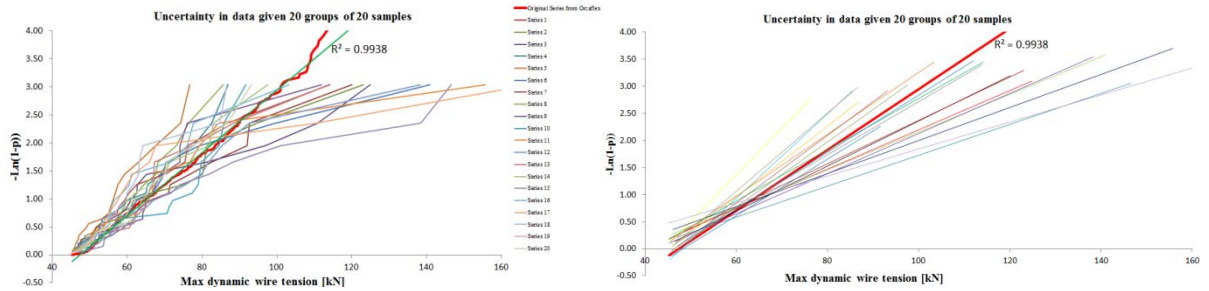

Figure 32: Illustrations of the uncertainties in a sample size of 20 (20 groups generated).

Limiting criteria #2

For the second criterion, the proposed 95% non-exceedance criterion is being generated at first:

$$x_{0.95} = -\ln(1-p) * \hat{\beta} + x_{min} = -\ln(1-0.95) * 19.95 + 45.193 \\ = 104.94\ kN \quad (205)$$

$$\boldsymbol{F_{max}(x_{0.95}) < (SWL_{crane} \times DAF) \rightarrow 104.94kN > 96kN \rightarrow NOT\ OK} \quad (206)$$

By evaluating the uncertainty in the data by use of an Exponential distribution, the following uncertainty graph (Figure 33) can be made:

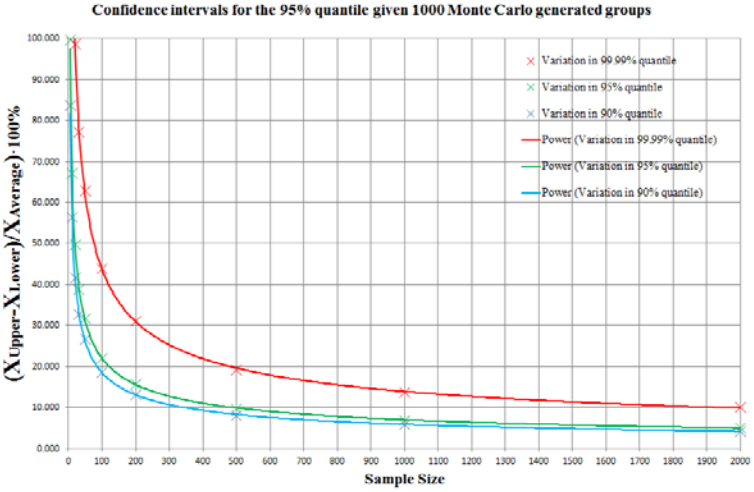

Figure 33: Confidence interval variations for the 95% quantile

A 95% confidence interval for the 95% quantile gives about 10% uncertainty from the median given 500 samples. For a sample size of 20, the uncertainty increases to 50%.

By lowering the probability to an 80% level of non-exceedance, one gets:

$$x_{0.80} = -\ln(1-p) * \hat{\beta} + x_{min} = -\ln(1-0.80) * 19.95 + 45.193 \\ = 77.29\ kN \quad (207)$$

$$\boldsymbol{F_{max}(x_{0.95}) < (SWL_{crane} \times DAF) \rightarrow 77.29kN > 96kN \rightarrow OK} \quad (208)$$

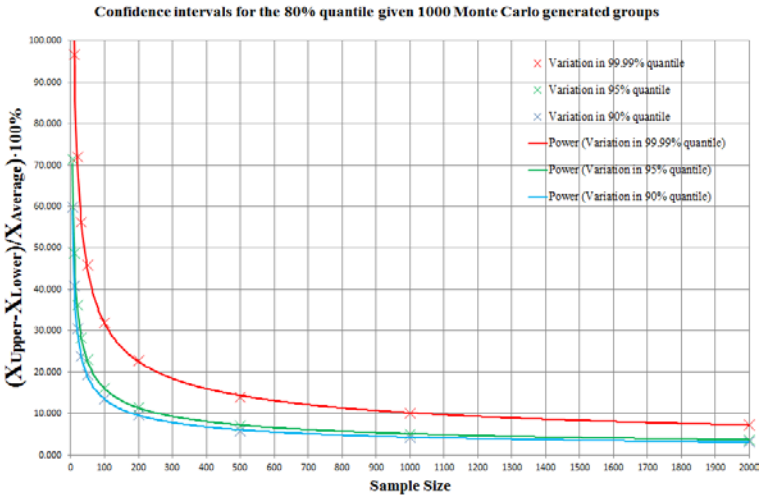

Figure 34: Confidence interval variations from the mean given an 80% quantile

Taking the uncertainty into account, one will need an uncertainty interval of less than 24.20% in order not to go beyond the crane design capacity at 10m. Based on a 95% confidence interval variation (Figure 34), this is achieved by having a sample size larger than 50.

Conclusion:

For this case, the 95% of non-exceedance may be used in order not to push the limits. Therefore, a lower maximum operational sea state will prove safer for this specific operation. Anyway, it could be argued that a lower quantile may be taken as acceptable as the consequences from a lifting wire breakdown are fairly small in this case as the ROV will still be connected by the umbilical and float/dive by its own. Also, the main criterion of a 10^{-4} probability is maintained by a 34.5% confidence interval using the "true" distribution made from the 500 Orcaflex simulations. This confidence is for a 99.99% interval here maintained by having at least 350 simulations.

Table 15 below summarizes the three cases based on the criteria stated in this thesis:

Table 15: Summarizing the amount of simulations required based on cases investigated in chapter 8

	Case 1a	Case 1b	Case 2
10^{-4} level of non-exceedance within a 99.99% interval	1000 samples	5000 samples	350 samples
95% level of non-exceedance within a 95% interval	40 samples	1000 samples	NA
80% level of non-exceedance within a 95% interval			50 samples

9. Discussion

Based on these three cases where lifts of a Supporter Mk2 WROV onboard Rem Ocean and launches of an Installer WROV onboard the Crest Bazan 2 have been investigated, it might sound reasonable to implement a 95% probability of not exceeding the safe working load times the DAF of the lifting equipment/lifting system within a confidence interval level of 95%. This is to ensure that one has a criterion that can cope with the uncertainties when evaluating the 10^{-4} probability of exceeding structural capacities given a smaller sample size. Given that the 99.99% level of non-exceedance is being maintained within a 99.99% confidence level, it would be advisable to increase the sea state to get closer to the limitations of the 99.99% quantile. As long as the 99.99% confidence interval is maintained, the second criterion might be adjusted down. But this would often mean that unfeasible many simulations have to be run.

Evaluation of accept criteria

Considering offshore lifting operations and limiting criteria, the use of a 95% percent quantile of not exceeding the design capacity means that given stationary sea state conditions, the 95%-quantile will be exceeded on average in one out of twenty runs. Anyway, by also taking into account the safety factor(s) used for the lifting device(s), a probability of structural failure in less than 1/10000 operations (10^{-4}) might be achieved although the 95%-quantile may be exceeded once every 20th run/lift.

A typical offshore IMR/survey vessel might have about 2500 launches and 2500 recoveries on the most regular used ROV in one year. Given that all lifts are done in limiting conditions (i.e. a H_s of 5 meter and a T_p of 8 seconds), a ROV lifting cable might break once every two years ($\frac{1\ exceedance}{10000\ lifts} * 5000\ \frac{lifts}{year} = \frac{1\ exceedance}{2\ years}$). If the ROV is being destroyed as well, a loss of reputation- and cash flow applies to the company. Using the scatter diagram (Table 16) for the North Sea area given by Faltinsen (1990), this limiting wave condition only applies about 0.315% of the time. As the α-factor takes into account uncertainties in the sea state, the ROV under consideration will then on average break its lifting cable once every 635 years $\left(\frac{1}{\frac{1\ failure}{10.000\ lifts} * 5000 \frac{lifts}{year} * 0.00315}\right)$ without adjusting for operational errors and other concerns that might lower this number. It should also be noted that other sea heights with different wave periods will lower this number somehow. Anyway, the risk of failure is very low, and an acceptable risk taking into the account the expenditures that will apply with regards to upgrades and/or waiting on the weather if the risk taking should be even lower.

The 95% probability of not exceeding a design capacity might be more arguable as the probability of exceeding this level is only about once every 635 lift ($\frac{1}{0.05*0.00315}$) in this case. In low risk lifting operations (i.e. ROV/baskets/light equipment/etc.) it might be argued that a

lower percentile can be used as the risk and expenditure of a possible failure is small, and timing of lifts is common among the operator(s). By using a larger sample size in the simulations, the 10^{-4} probability of exceeding the MBL might be determined with an acceptable confidence level (i.e. within a 99.99% confidence interval level). The probability of exceeding the design load might then be lowered to some degree (down 5-15% from the 95% quantile). For larger operations (i.e. module replacements, template lifts, unfamiliar lifting operations and similar) with higher risks and uncertainties, the 95% quantile should be more rigid as possible snap forces might be more inaccurate and of higher risk potential. Results from snap load calculations in Orcaflex are subject to uncertainties and should therefore be treated with caution. Loads from snaps in the wire are of short duration and the responses are highly dependent upon configuration of the system with regards to i.e. structural damping of the umbilical/wire, and stiffness of the lifting system. Therefore, some conservatism should be applied for operations with higher consequences and risk factors. Also, the third criterion of more than 10% of the object`s tension in air for any lifting appliances should normally be maintained in such cases.

Table 16: Scatter diagram for the North Sea area given by Faltinsen (1990)

$H_s \backslash T_p$	3	4	5	6	7	8	9	10	11	12	13	14	15	16	17	18	19	21	22	Sum
1	*59*	*403*	*1061*	*1569*	*1634*	*1362*	*982*	*643*	*395*	*232*	*132*	*74*	*41*	*22*	*12*	*7*	*4*	*2*	*2*	*8636*
2	*9*	*212*	*1233*	*3223*	*5106*	*5814*	*5284*	*4102*	*2846*	*1821*	*1098*	*634*	*355*	*194*	*105*	*56*	*30*	*16*	*17*	*32155*
3	*0*	*8*	*146*	*831*	*2295*	*3896*	*4707*	*4456*	*3531*	*2452*	*1543*	*901*	*497*	*263*	*135*	*67*	*33*	*16*	*15*	*25792*
4	*0*	*0*	*6*	*85*	*481*	*1371*	*2406*	*2960*	*2796*	*2163*	*1437*	*849*	*458*	*231*	*110*	*50*	*22*	*10*	*7*	*15442*
5	*0*	*0*	*0*	*4*	*57*	*315*	*898*	*1564*	*1879*	*1696*	*1228*	*748*	*398*	*191*	*84*	*35*	*13*	*5*	*3*	*9118*
6	*0*	*0*	*0*	*0*	*3*	*39*	*207*	*571*	*950*	*1069*	*885*	*575*	*309*	*142*	*58*	*21*	*7*	*2*	*1*	*4839*
7	*0*	*0*	*0*	*0*	*0*	*2*	*27*	*136*	*347*	*528*	*533*	*387*	*217*	*98*	*37*	*12*	*4*	*1*	*0*	*2329*
8	*0*	*0*	*0*	*0*	*0*	*0*	*2*	*20*	*88*	*197*	*261*	*226*	*138*	*64*	*23*	*7*	*2*	*0*	*0*	*1028*
9	*0*	*0*	*0*	*0*	*0*	*0*	*0*	*2*	*15*	*54*	*101*	*111*	*78*	*39*	*14*	*4*	*1*	*0*	*0*	*419*
10	*0*	*0*	*0*	*0*	*0*	*0*	*0*	*0*	*2*	*11*	*30*	*45*	*39*	*22*	*8*	*2*	*1*	*0*	*0*	*160*
11	*0*	*0*	*0*	*0*	*0*	*0*	*0*	*0*	*0*	*2*	*7*	*15*	*16*	*11*	*5*	*1*	*0*	*0*	*0*	*57*
12	*0*	*0*	*0*	*0*	*0*	*0*	*0*	*0*	*0*	*0*	*1*	*4*	*6*	*5*	*2*	*1*	*0*	*0*	*0*	*19*
13	*0*	*0*	*0*	*0*	*0*	*0*	*0*	*0*	*0*	*0*	*0*	*1*	*2*	*2*	*1*	*0*	*0*	*0*	*0*	*6*
14	*0*	*0*	*0*	*0*	*0*	*0*	*0*	*0*	*0*	*0*	*0*	*0*	*0*	*1*	*0*	*0*	*0*	*0*	*0*	*1*
Sum	***68***	***623***	***2446***	***5712***	***9576***	***12799***	***14513***	***14454***	***12849***	***10225***	***7256***	***4570***	***2554***	***1285***	***594***	***263***	***117***	***52***	***45***	***100000***

10. Conclusions

General conclusions

DNV says that given extreme type loads, a Gumbel distribution is suitable. The most extreme loads given from repeated dynamic simulations in a short duration have in this thesis been shown not always to follow a Gumbel distribution well, at least for splash zone lifts with a relative short timeframe (~30 seconds) through the upper water columns. It seems reasonable to believe that the load forces experienced in such short time most often are not extreme at all. Even for the tail region (upper 10-15% of the simulations) where the most extreme values are placed, other distributions than a Gumbel might prove to be the most feasible.

Further, DNV wants a maximum characteristic load to be derived from a Rayleigh distribution. This might be suitable when doing long term analysis (i.e. 3 hours) where the object is stationed in the critical wave zone, but is not feasible when doing repeated lifting simulations of shorter duration (<1 minute). For such cases, a maximum load should be extracted from each simulation, and then get a characteristic load from the distribution function used.

With regards to the required confidence interval levels given repeated lifting operations in the time domain, DNV gives the instruction to gather a large amount of simulations in order to obtain robust estimates. In this thesis, research has been performed to see how many simulations some common lifting cases needs to get a given level of confidence interval.

Procedure for finding the required level of confidence

As the confidence level is of major importance, this thesis aims to give some guidelines on how to reach a sufficient level of confidence. The following procedure is proposed based on the DNV standards and results obtained in chapter 8:

1. Run simulations for 30 minutes for every parameter (H_s and T_p/T_z) in different scenarios/object positions according to the simplified wave zone calculations proposed by DNV-RP-H103 (2014, chapter 4). A typical case would be to keep the object in the following positons; (1) When the object has just passed the waterline, (2) when the object is half immersed, and (3) when the object is 1m below the waterline (Figure 35). This is done in order to screen the allowable weather window for the operation under consideration. The most critical wave condition may then be decided.

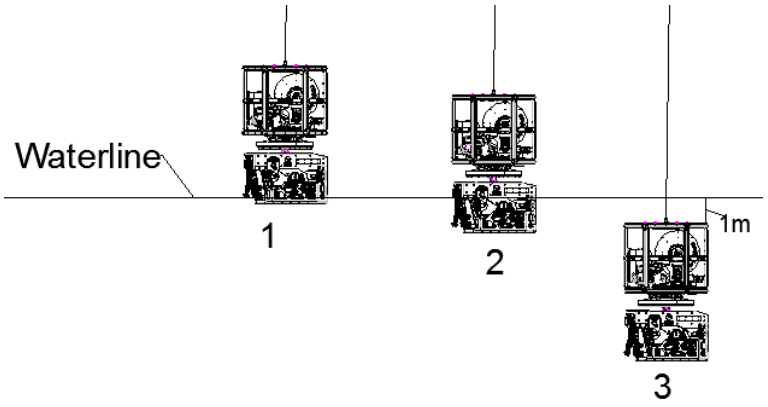

Figure 35: Load case 1-3 considering a lifting operation with a ROV cw. TMS

   It should be noted that given light objects, some unrealistic forces may be experienced if the object starts to swing in the wave zone. Therefore, a better (and more time consuming) way may be to perform a screening by doing a slowly lowering of the object through harmonic/sinusoidal waves in order to find the scenarios where the most critical load conditions occur. The most critical load conditions given harmonic waves will also give the toughest load situations in irregular waves. This would also give more accurate results given more complex structures.
2. Run analyses with 100 or more seeds for the most critical wave condition.
3. Estimate the most suitable statistical distribution by using probability paper plots (with focus on the tail region).
4. Perform Monte Carlo analysis by generating at least 100 (or optimally 1000) new groups of samples of i.e. 20, 50, 100, 250, 500 and 1000 random numbers in order to form a trend of the uncertainty/confidence interval given different amount of samples. Based on an expected normal distribution of the p-percentile (i.e. $p = 95\%$ non-exceedance) of the results obtained, the average/mean ($\bar{x}_p$) and standard deviation (σ_p) of the wire tensions during the (n) simulated groups are found.

The confidence level is then expressed as:

$$\left(x_{p_L}, x_{p_H}\right) = \left[\bar{x}_p - z_{1-\frac{\alpha}{2}} * SE\left[x_p\right], \bar{x}_p + z_{\alpha/2} * SE\left[x_p\right]\right] = 1 - \alpha \qquad (209)$$

Where the standard error for a normal distribution may be expressed as:

$$SE\left[x_p\right] = \sigma_p = \frac{\sqrt{\sum_{i=1}^{n}\left(x_i - \bar{x}_p\right)^2}}{\sqrt{n}} \qquad (210)$$

This means that the error may be reduced be either decreasing the numerator, or by increasing the denominator. The numerator may be reduced by choosing a better random number generator, or by improving/increasing the distribution of returns. The denominator will improve as the square root of the ratio of the number of additional runs.

5. Then the required amounts of seeds are run and the actual spreading errors for every combination of parameters in the simulated H_s/T_z-matrix are shown. Finally, the calculated spreading error for the most critical case is implemented in the extreme value for the maximum wire tension. An example may be that the wire tension for a given wave condition is given as 100kN for a 95% quantile with a 95% confidence interval deviation of less than 20% from the mean/"true" distribution. One may then use 100kN multiplied by 1.2 to find the conservative characteristic load of 120kN in the statistical distribution.

11. Recommendations for Further Work

To add some recommendations for further action, the following topics may be assessed:

- DNV to provide more accurate recommendations of the required level of confidence when considering offshore lifting cases. Also, it should also be noted that the simulations seems not to converge to a specific value even for very large sample sizes. Often, the uncertainty reduction in the results stalls somehow at about 1000-2000 simulations using Orcaflex software.

- As the Gumbel distribution might not be the most suitable distribution for use in every offshore lifting case performed in time domain software, it might be advisable to update the DNV standards to add some flexibility to the distribution used in different cases.

- The main criterion in the DNV standards of having less than a 10^{-4} probability of structural failure during an offshore lift is a criterion that it is hard to fully control when having smaller simulation sizes. This is related to the fact that an estimated distribution function cannot be taken as the fully truth. Even for an unlimited sample size, the model used will in some way deviate from the truth. Also, if performing new simulations with the equal amount of samples as the first sample size, deviations will appear (physical- and statistical variations).

  It is therefore advisable to add a second offshore lifting criterion to the DNV standards that can give more certain answers without guessing/hoping that a given distribution is maintained also outside the simulated range, or having to perform unjustifiable amounts of simulations that would take hours to generate and handle afterwards. A 95% non-exceedance criterion for staying below the design limits of the lifting equipment/system is proposed based on research performed in chapter 8, although a lower criterion might be accepted for in some cases (see chapter 9).

- From the probability papers obtained in chapter 8, it seems to be common in the tail region (largest 5-15% of the simulations) with a decrease in the slope of the line. This is assumed to follow from either (1) non-linear impacts as snap loads and quadratic damping, or (2) statistical spread. However, the distribution most suited for the tail region should be considered. For the future, it could be interesting to see when, how and why these larger extreme forces occur. This can be done by i.e. looking individually at each simulation and see how the minimum tension or slack duration in the wire/lifting slings corresponds with the maximum output force.

References

Aasen, A. (2015). *Supporter Mk2 WROV*. [Photograph] Norway, Bergen, Central Coast base, Onboard Rem Ocean (02.01.2015).

Blom, G.B., (1958). *Statistical Estimates and Transformed Beta Variables*. New York: John Wiley & Sons.

Cheng, P.W. (2002). *A reliability based design methodology for extreme responses of offshore wind turbines*, Dr. Thesis, The Netherlands: DUWIND Delft University.

DNV Standard for certification No.2.22 (2011). *Lifting Appliances*. DNV, Oslo, Norway.

DNV-OS-H101 (2011). *Offshore Standard DNV-OS-H101 - Marine Operations General.* DNV, Oslo, Norway.

DNV-OS-H102 (2011). *Offshore Standard DNV-OS-H102 - Marine Operations, Design and Fabrication.* DNV, Oslo, Norway.

DNV-OS-H205 (2014). *Offshore Standard DNV-OS-H205—Lifting Operations.* DNV, Oslo, Norway.

DNV-RP-C205 (2010). *Recommended practice DNV-RP-C205— Environmental Conditions and Environmental Loads*. DNV, Oslo, Norway.

DNV-RP-H103 (2014). *Recommended practice DNV-RP-H103 Modelling and Analysis of Marine Operations*. DNV, Oslo, Norway.

Edumaritime (2016). *Det Norske Veritas Germanischer Lloyd (DNV GL) - Careers in Marine Classification Industry*. [Website] Available at: http://www.edumaritime.com/marine-classification-risk-career/det-norske-veritas-dnv [Accessed 15.01.2016].

Faltinsen, O.M. (1990). *Sea Loads on ships and offshore Structures*., Cambridge University Press, Cambridge, UK.

Fisher, R.A. (1928). *Moments and product moments of sampling distributions*. Proc. London Math. Soc., 30, 199–238. Journal article, London Mathematical Society, London, UK.

Gudmestad, O.T. (2015)., *Marine Technology and Operations – Theory & Practice.*, WIT Press, Southampton, UK.

Hasselmann, K. (1973). *Measurements of wind-wave growth and swell decay during the Joint North Sea Wave Project (JONSWAP*),1-95. Deutschland, Hamburg, Deutches Hydrographisches Institut.

Haver, S. (2013). *Prediction of characteristics response for design purposes (preliminary Version)*, Statoil.

Haver, S. (2015). *Description of Metocean Characteristics for planning of marine operations*. [Lecture Notes]. University of Stavanger, TEKNAT, 2nd September.

Haver, S. (2016). Sverre.k.haver@uis.no. Attached Image. [email]. Message to A.Aasen (and.aasen@stud.uis.no). Sent 08.01.2016: 09:34.

Holsbrekken, Å. (2015). Holsbrekken@kystdesign.no. *Supporter 22 – Thrusterkraft*. [email]. Message to A.Aasen (aaasen@deepoceangroup.com). Sent 07.01.2015: 13:46. Private Communication.

Investopedia. (2015). *Probability Distribution*. Available at: http://www.investopedia.com/terms/p/probabilitydistribution.asp [02.02.2016].

Leira, B. (2014). *Stochastic Theory of Sea loads, Probabilistic Modeling and Estimation*. Norway, Trondheim, Kompendieforlaget.

Mahdi, S. & Cenac, M. (2004). *Estimating Parameters of Gumbel Distribution Using the Methods of Moments, Probability Weighted Moments and Maximum Likelihood*., Barbados, University of West Indies, Department of Computer Science., p.151-156. Available at: http://revistas.ucr.ac.cr/index.php/matematica/article/viewFile/259/239 [23.02.16].

Moan, T., Spidsøe, N., Haver, S. (1980). *Analyse av usikkerhet.* Compendium, Norway, NTH Trondheim, Marine Technology Centre.

Myrhaug, D. (2014). *Stochastic Theory of Sealoads, Statistics of Narrow Band Processes and Equivalent Linearization*. Compendium, Norway, NTNU Trondheim: Marine Technology Centre.

Naess, A. (1985). *The joint crossing frequency of stochastic processes and its application to wave theory*. Vol.7, No.1, pp. 35-50. UK, Southampton, Applied Ocean Research.

Newmark, N.M. (1959). *A method of computation for structural dynamics*. Journal of Engineering Mechanics, ASCE, 85 (EM3) 67-94. US, Illinois, University of Illinois.

Orcina (2015). *OrcaFlexManual,* Version 10.0. UK, Daltongate, Orcina Ltd.

Pierson, W.J. and Moskowitz, L. (1964). *A proposed spectral form for full-developed wind sea based on the similarity law of SA Kitaigorodoskii*, Journal of Geophysical Research, Department of Meteorology and Oceanography, NYU, US.

Sandvik, P.C, Lieng, J., and Lunde, S. (1993). *Analysis of the dynamics during installation of subsea structures*. In Offshore 93: 3rd Intl. Conference; Installation of Major Offshore Structures and Equipment, 17-18 Feb 1993; London, UK.

Sandvik, P. C., (2007). *Theory related to subsea lifting operations*. Subsea Lifting Operations, Norway, Stavanger, November 27th -28th 2007. Available at: http://www.ktf.no/fileadmin/Dokumenter/Kursdokumenter/2008/1-subsea-lifting-operations/2-theory-related-to-subsea-lifting-operations.pdf [19.02.2016].

Sandvik, P.C. and Kopsov, I.E. (1995). *Analysis of Subsea Structure Installation.* Proceedings of the Fifth International Offshore and Polar Engineering Conference, June 11-16 1995. Vol.1. The Netherlands, The Hague.

Sayer, P. (1996). *Hydrodynamic Forces on ROVs near the Air-Sea Interface*. International Journal of Offshore and Polar Engineering., Vol.6. Scotland, University of Strathclyde.

Sveen, D.A. (2015). *NO.ENG.RE.14.002-02 Dynamic analysis - ROV operation on Crest Bazan 2*. Rev.1. Norway, Haugesund.

Rao, S. (2005). *Mechanical Vibrations*. Singapore, Prentice Hall.

The Maritime Executive, (2016). Germanischer Lloyd. [Website] Available at: http://www.maritime-executive.com/maritime-directory/Germanischer-Lloyd [Accessed 15.01.2016].

Torsethaugen, K. (2004). *Simplified double peak spectral model for ocean waves, SINTEF, STF80 A048052, SINTEF Fisheries and Aquaculture*, Norway, Trondheim.

Valderhaug, H.M. 2014. *Rem Ocean*. [Photograph] Available at: http://maritimt.com/batomtaler/2014/rem-ocean.html [02.03.2016].

Vestbøstad, T. M., Haver, S., Andersen, O. J., & Albert, A. (2002). *Prediction of Extreme Roll Motions on an FPSO using Long Term Statistics*. Proceedings of the 21st International Conference on Offshore Mechanics and Arctic Engineering., June 23–28, Vol. 2, p.129-136,. Oslo, Norway.

Wheeler, J.D. (1969), *Method for calculating forces produced by irregular waves,* Offshore Technology Conference, Conference paper, 18-21 May, Houston, Texas, US.

Winterstein, S.R., Kleiven, G. and Hagen, Ø. (2001). *Comparing Extreme Wave Estimates from Hourly and Annual Data*. The Eleventh International Offshore and Polar Engineering Conference, 17-22 June, Stavanger, Norway.

Øritsland, O. and Lehn, E. (1989). *Hydrodynamic forces and resulting motion of subsea modules during lifting in the splash zone*. Monograph in the Eight International Conference on Offshore Mechanics and Arctic Engineering, International Conference on Offshore Mechanics and Arctic Engineering, volume 2., p. 161-169.

Appendix 1

Simplified double peak spectral model for ocean waves

This appendix is mainly based on notes published by Torsethaugen and Haver (2004). Parameters used here are not being refered or linked to parameters mentioned in the nomenclature. Empirical parameters are given in Table 17.

Table 17: Empirical Parameters used in the Torsethaugen simplified wave spectrum

Parameter	*Value*
a_e	2 $\mathrm{sm}^{-1/3}$
a_f	6.6 $\mathrm{sm}^{-1/3}$ for a fetch length of 370 km (Haver, 2013)
a_u	25.0 s
a_1	0.5
a_2	0.3
a_3	6.0
a_{10}	0.7
a_{20}	0.6
b_1	2.0 s
k_g	35.0 $\mathrm{m/s}^2$
ε_l	Non-dimensional scales for the spectral peak period (Wind sea)
ε_u	Non-dimensional scales for the spectral peak period (Swell sea)

Fully developed sea peak period for the location

$$T_{pf} = a_f {H_s}^{1/3}$$

Considering primary spectral peak periods less than or equal to peak periods in a fully developed sea, $T_p \leq T_{pf}$, a wind sea system generated. For $T_p > T_{pf}$, a swell system is generated.

Spectral Parameters for Wind dominated sea $T_p \leq T_{pf}$

1) Primary peak

- Significant wave height

$$H_{w1} = R_w H_s; \qquad R_w = (1 - a_{10}) e^{-\left(\frac{\varepsilon_1}{a_1}\right)^2} + a_{10}$$

$\varepsilon_l = \frac{(T_{pf}-T_p)}{(T_{pf}-T_l)}$; $\quad T_l = a_e {H_s}^{1/2}$

For values of T_p less than T_l, ε_l is set to 1.

- Spectral peak period

$T_{pw1} = T_p$;

- Peak enhancement factor

$\gamma = {k_g s_p}^{6/7}$; $\quad s_p = (\frac{2\pi}{g})(H_{w1}/T_{pw1}^2)$

2) Secondary peak

- Significant wave height

$H_{w2} = (1 - R_w^2)^{1/2} H_s$

- Spectral peak period

$T_{pw2} = T_{pf} + b_1$

- Peak enhancement factor, $\gamma = 1$

Spectral Parameters for Swell dominated sea $T_p > T_{pf}$

1) Primary peak

- Significant wave height

$H_{s1} = R_s H_s$; $\quad R_s = (1 - a_{20}) e^{-\left(\frac{\varepsilon_u}{a_2}\right)^2} + a_{20}$

$\varepsilon_u = \frac{(T_p - T_{pf})}{(T_u - T_{pf})}$; $\quad T_u = a_u$

For values of T_p above T_u, ε_u is set to 1.

- Spectral peak period

$T_{ps1} = T_p$

- Peak enhancement factor

$\gamma = k_g {s_p}^{6/7}; \qquad s_f = (\frac{2\pi}{g})(H_{w1}/T_{pw1}^2)$

$\gamma = \gamma_f(1 + a_3\varepsilon_u)$

$\gamma_f = k_g {s_f}^{6/7}$

$s_f = (\frac{2\pi}{g})(H_s/T_{pf}^2)$

2) Secondary peak

- Significant wave height

$H_{s2} = (1 - R_s^2)^{1/2} H_s;$

- Spectral peak period

$T_{ps2} = a_f H_{s2}^{1/3};$

- Peak enhancement factor, $\gamma = 1$

Resulting spectral formula:

$$S(f_n) = \sum_{i=1}^{2} E_i S_{i,n}(f_{i,n})$$

$i = 1$ - Primary sea system
$i = 2$ - Secondary sea system

$$E_1 = \frac{1}{16} H_1^2 T_{p1}$$

$$E_2 = \frac{1}{16} H_2^2 T_{p2}$$

$$S_{1,n}(f_{1,n}) = G_0 A_\gamma f_{1n}^{-4} e^{-f_{1n}^{-4}} \gamma^{e^{-\frac{1}{2\sigma^2}(f_{1n}-1)^2}}$$

$$S_{2,n}(f_{2,n}) = G_0 f_{2n}^{-4} e^{-f_{2n}^{-4}}$$

$f_{1n} = fT_{p1}, f_{2n} = fT_{p2}, G_0 = 3.26, A_\gamma = \dfrac{1 + 1.1\ln(\gamma)^{1.19}}{\gamma}$ and σ = 0.07 for $f_n < 1$ and σ = 0.09 for $f_n > 1$

For wind dominated sea cases:

$$H_1 = H_{w1} \text{ and } H_2 = H_{w2}$$
$$T_{p1} = T_{pw1} \text{ and } T_{p2} = T_{pw2}$$

For swell dominated sea cases:

$$H_1 = H_{s1} \text{ and } H_2 = H_{s2}$$
$$T_{p1} = T_{ps1} \text{ and } T_{p2} = T_{ps2}$$

Appendix 2

Estimation of mass coefficients for a ROV Supporter Mk2

This appendix is mainly based on notes published by Sandvik (2007). Parameters used here are not being refered or linked to in the nomenclature.

ROV Variables	Variable calculation and value	Reference
Seawater density:	$\rho_W := 1027 \ \frac{kg}{m^3}$	
ROV dimensions:	$l := 2.5 \ m \quad w := 1.70 \ m \quad h := 2.00 \ m$	
Perforation:	$p_x := 10\%$ $p_y := 25\%$ $p_z := 15\%$	
Projected area:	$A_x := w \cdot h \cdot (1 - p_x) = 3.06 \ m^2$ $A_y := l \cdot h \cdot (1 - p_y) = 3.75 \ m^2$ $A_z := l \cdot w \cdot (1 - p_z) = 3.613 \ m^2$	
ROV mass:	$M_{rov} := 3550 \ kg$	
ROV weight:	$F_{rov} := M_{rov} \cdot g = (3.481 \cdot 10^4) \ N$	
ROV submerged weight:	$F_s := 0 \ N$	
ROV volume:	$V_{rov} := \frac{F_{rov} - F_s}{g \cdot \rho_W} = 3.457 \ m^3$	

$$ratio_1 := \begin{bmatrix} 1.0 \\ 1.2 \\ 1.25 \\ 1.33 \\ 1.5 \\ 2.0 \\ 2.5 \\ 3.0 \\ 4.0 \\ 5.0 \\ 8.0 \\ 10.0 \end{bmatrix} \quad \alpha_1 := \begin{bmatrix} 0.579 \\ 0.630 \\ 0.642 \\ 0.660 \\ 0.691 \\ 0.757 \\ 0.801 \\ 0.830 \\ 0.871 \\ 0.897 \\ 0.934 \\ 0.947 \end{bmatrix}$$

Sandvik (2007)

$$ratio_2 := \begin{bmatrix} 0.00 \\ 0.10 \\ 0.30 \\ 0.50 \\ 0.75 \\ 1.00 \\ 1.25 \\ 1.60 \\ 2.00 \\ 2.40 \\ 2.80 \\ 3.60 \end{bmatrix} \quad \alpha_2 := \begin{bmatrix} 0 \\ 5.139 \\ 2.016 \\ 1.310 \\ 0.916 \\ 0.705 \\ 0.575 \\ 0.458 \\ 0.373 \\ 0.316 \\ 0.274 \\ 0.217 \end{bmatrix} \quad \beta_2 := \begin{bmatrix} 1.0 \\ 1.13 \\ 1.33 \\ 1.44 \\ 1.51 \\ 1.55 \\ 1.58 \\ 1.61 \\ 1.64 \\ 1.67 \\ 1.69 \\ 1.72 \end{bmatrix}$$

Perforation coefficients:

$$C_{px} := e^{\left(\frac{-p_x}{0.28}\right)} = 0.7$$

DNV-RP-H103 (2014)

$$C_{py} := e^{\left(\frac{-p_y}{0.28}\right)} = 0.409$$

$$C_{pz} := e^{\left(\frac{-p_z}{0.28}\right)} = 0.585$$

X-direction

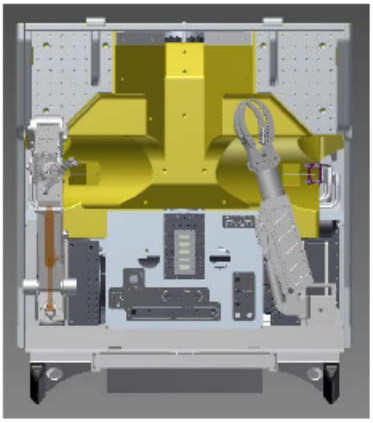

Length: $a_x := w = 1.7\ m$

Width: $b_x := h = 2\ m$

Ratio b/a: $ratio_{ba\_x} := \frac{b_x}{a_x} = 1.176$

Alfa factor: $\alpha_{ba\_x} := \text{linterp}\left(ratio_1, \alpha_1, ratio_{ba\_x}\right) = 0.624$

Beta factor: $\beta_{ba\_x} := \text{linterp}\left(ratio_2, \beta_2, ratio_{ba\_x}\right) = 1.571$

Added mass: $M_{added\_x} := \alpha_{ba\_x} \cdot \beta_{ba\_x} \cdot \rho_W \cdot \frac{\left(\pi \cdot w^2 \cdot h\right)}{4} = \left(4.571 \cdot 10^3\right)\ kg$

Mass coeffisient: $C_{Ax} := \frac{M_{added\_x}}{\rho_W \cdot V_{rov}} \cdot C_{px} = 0.901$

Y-direction

Length: $a_y := l = 2.5\ m$

Width: $b_y := h = 2\ m$

Ratio b/a: $ratio_{ba\_y} := \frac{b_y}{a_y} = 0.8$

Alfa: $\alpha_{ba\_y} := \text{linterp}\left(ratio_2, \alpha_2, ratio_{ba\_y}\right) = 0.874$

Beta: $\beta_{ba\_y} := \text{linterp}\left(ratio_2, \beta_2, ratio_{ba\_y}\right) = 1.518$

Added mass: $M_{added\_y} := \alpha_{ba\_y} \cdot \beta_{ba\_y} \cdot \rho_W \cdot \frac{\left(\pi \cdot w^2 \cdot h\right)}{4} = \left(6.184 \cdot 10^3\right)\ kg$

Mass coeffisient: $C_{Ay} := \frac{M_{added\_y}}{\rho_W \cdot V_{rov}} \cdot C_{py} \qquad C_{Ay} = 0.713$

Z-direction

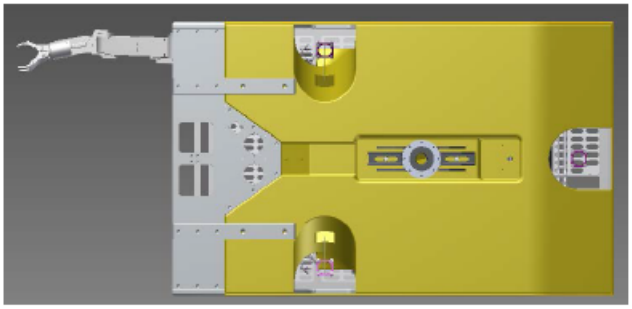

Length: $a_z := w = 1.7\ m$

Width: $b_z := l = 2.5\ m$

Ratio b/a: $ratio_{ba\_z} := \frac{b_z}{a_z} = 1.471$

Alfa: $\alpha_{ba\_z} := \text{linterp}\left(ratio_1, \alpha_1, ratio_{ba\_z}\right) = 0.686$

Beta: $\beta_{ba\_z} := \text{linterp}\left(ratio_2, \beta_2, ratio_{ba\_z}\right) = 1.599$

Added mass: $M_{added\_z} := \alpha_{ba\_z} \cdot \beta_{ba\_z} \cdot \rho_W \cdot \frac{\left(\pi \cdot w^2 \cdot h\right)}{4} = \left(5.111 \cdot 10^3\right)\ kg$

Mass coeffisient: $C_{Az} := \frac{M_{added\_z}}{\rho_W \cdot V_{rov}} \cdot C_{pz} \qquad C_{Az} = 0.843$

Appendix 3

Estimation of steady flow drag coefficients for a ROV Supporter Mk2 (Figure 36)

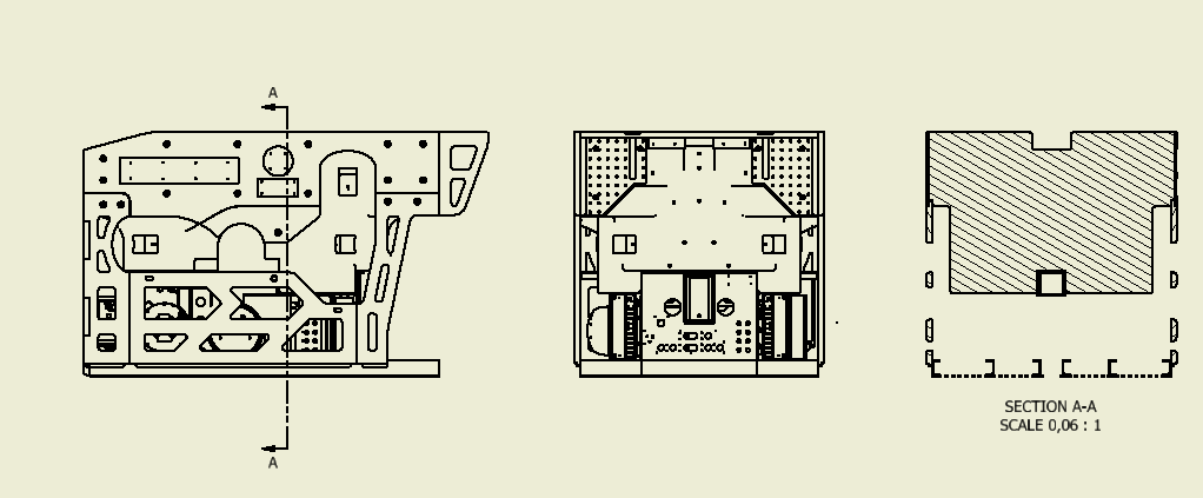

Figure 36: Illustration of the Supporter Mk2 obtained from AutoCad

First thing to do when finding estimated steady flow drag coefficients is to find an area representative for the estimated drag factor. Further, data on thruster forces are obtained from the supplier (Kystdesign, Table 18), and the maximum ROV speed in seawater close to the seabed with no currents are given based on ROV operators experiences onboard Rem Ocean. By having these three values in all X/Y/Z-directions, an estimation of the drag factors in an ideal flow can be obtained (not representative in an oscillatory flow). But, it should be noted that these values will vary dependent on for instance currents through cross sections (i.e. rotation, shadows, Reynolds number and surface roughness). Also, the thruster power values given are only representative in an ideal laminar water flow. Therefore, these numbers are likely to be reduced by about 20% due to phenomena's as for instance turbulence and currents.

Table 18: Thruster data of the Supporter Mk2 provided by the supplier (Holsbrekken, 2015)

Thrust direction	Force	Unit
Forward, x	676	kilogram
Aft, x	669	kilogram
Lateral, y	616	kilogram
Vertically up, z	633	kilogram
Vertically down, z	691	kilogram

Surge:

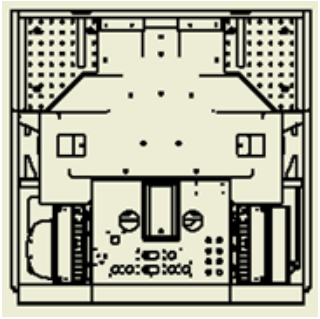

Estimated areal from Inventor data; $A_x = 1.6m^2$

$$C_{DS,x} = \frac{2F_x}{\rho * v_x^2 * A_x} = \frac{2 * 0.8 * 676kg * 9.81\frac{m}{s^2}}{1027\frac{kg}{m^3} * \left(1.8\frac{m}{s}\right)^2 * 1.6m^2} = 2$$

Sway:

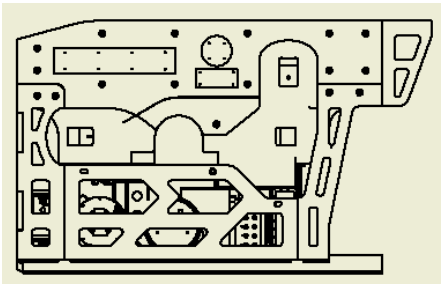

Estimated areal from Inventor data; $A_y = 2.3m^2$

$$C_{DS,y} = \frac{2F_y}{\rho * v_y^2 * A_y} = \frac{2 * 0.8 * 616kg * 9.81\frac{m}{s^2}}{1027\frac{kg}{m^3} * \left(1.3\frac{m}{s}\right)^2 * 2.3m^2} = 2.42$$

Heave:

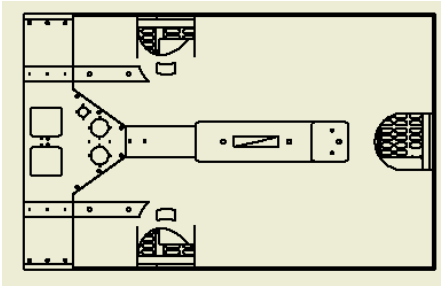

Estimated areal from Inventor data; $A_z = 3.2m^2$

$$C_{DS,z} = \frac{2F_z}{\rho * v_z^2 * A_z} = \frac{2 * 0.8 * 633kg * 9.81\frac{m}{s^2}}{1027\frac{kg}{m^3} * \left(1.1\frac{m}{s}\right)^2 * 3.2m^2} = 2.50$$

Appendix 4

Main Orcaflex dataset obtained in Case 1a

$H_s = 7.5$m and $T_z = 8$s

500 simulations performed, launch of a Supporter Mk2 at Rem Ocean

Values are in kN

288.197	106.212	84.354	80.887	79.338	78.074	76.897	76.321	75.342	74.095
286.9	106.001	84.203	80.877	79.331	78.053	76.877	76.312	75.328	74.082
263.233	105.335	84.168	80.858	79.281	78.017	76.868	76.299	75.317	74.006
229.275	104.707	84.083	80.849	79.232	78.002	76.865	76.294	75.307	73.995
201.972	104.444	83.891	80.776	79.219	77.987	76.857	76.246	75.304	73.995
197.073	103.383	83.787	80.768	79.207	77.985	76.852	76.23	75.292	73.991
186.649	102.778	83.66	80.767	79.197	77.921	76.836	76.219	75.27	73.982
184.508	101.855	83.508	80.55	79.182	77.896	76.828	76.212	75.243	73.942
173.737	101.58	83.461	80.512	79.181	77.894	76.795	76.17	75.237	73.915
171.9	98.985	83.353	80.494	79.142	77.893	76.793	76.155	75.227	73.87
171.639	98.874	83.2	80.367	79.12	77.886	76.784	76.119	75.177	73.843
170.52	98.432	83.179	80.344	79.079	77.863	76.783	76.095	75.095	73.793
164.029	98.42	83.04	80.323	78.984	77.856	76.781	76.075	75.08	73.755
161.853	97.454	82.979	80.301	78.98	77.848	76.779	76.05	75.055	73.745
158.176	97.338	82.972	80.291	78.928	77.803	76.76	76.034	75.029	73.731
156.924	96.877	82.904	80.254	78.906	77.802	76.756	75.952	75.012	73.661
154.444	96.783	82.628	80.227	78.904	77.79	76.742	75.948	74.99	73.639
152.938	96.317	82.61	80.135	78.848	77.752	76.722	75.933	74.956	73.599
151.287	94.221	82.603	80.113	78.835	77.687	76.716	75.912	74.927	73.595
149.426	92.284	82.444	80.075	78.834	77.686	76.703	75.908	74.914	73.582
144.661	92.194	82.397	80.072	78.822	77.659	76.701	75.894	74.907	73.572
144.489	92.135	82.388	80.064	78.808	77.617	76.686	75.893	74.869	73.57
141.51	91.113	82.36	80.028	78.776	77.606	76.684	75.885	74.834	73.544
141.495	90.989	82.306	80.026	78.772	77.58	76.682	75.866	74.79	73.524
140.317	90.315	82.222	79.997	78.746	77.575	76.665	75.865	74.781	73.518
138.31	90.147	82.101	79.992	78.738	77.569	76.642	75.858	74.778	73.414
138.236	89.85	82.08	79.98	78.687	77.567	76.623	75.837	74.777	73.398
137.321	89.788	82.05	79.824	78.637	77.535	76.596	75.833	74.768	73.323
136.41	89.511	82.021	79.807	78.631	77.428	76.595	75.808	74.758	73.282
135.535	89.465	82.015	79.791	78.598	77.411	76.592	75.795	74.756	73.267
132.808	88.221	81.953	79.791	78.518	77.402	76.589	75.771	74.742	73.181
132.136	87.587	81.874	79.784	78.507	77.401	76.582	75.697	74.739	73.13
131.81	87.482	81.792	79.757	78.502	77.375	76.576	75.676	74.691	73.127
131.767	87.351	81.737	79.713	78.489	77.295	76.559	75.652	74.675	73.1
129.572	87.326	81.486	79.677	78.449	77.281	76.542	75.607	74.638	72.963
129.131	87.285	81.458	79.634	78.431	77.242	76.538	75.556	74.615	72.899
127.515	87.266	81.445	79.623	78.409	77.2	76.528	75.536	74.606	72.786
124.541	87.218	81.443	79.605	78.409	77.165	76.523	75.531	74.513	72.775
124.07	86.697	81.375	79.602	78.398	77.122	76.522	75.524	74.508	72.744
123.353	86.549	81.361	79.552	78.384	77.115	76.502	75.49	74.482	72.727
120.733	86.451	81.299	79.546	78.359	77.089	76.491	75.477	74.406	72.58
119.338	85.958	81.274	79.532	78.338	77.081	76.487	75.465	74.321	72.577
118.557	85.261	81.147	79.477	78.298	77.053	76.452	75.461	74.277	72.481
117.445	85.117	81.122	79.468	78.265	77.019	76.427	75.455	74.249	72.427
115.304	84.731	81.109	79.424	78.221	77.019	76.421	75.455	74.23	72.372
115.275	84.668	81.095	79.413	78.189	77.009	76.414	75.438	74.214	72.287
111.505	84.634	81.048	79.403	78.14	77.004	76.412	75.421	74.193	71.957
111.36	84.51	80.979	79.354	78.103	76.918	76.375	75.384	74.182	71.927
110.412	84.49	80.946	79.348	78.1	76.909	76.369	75.368	74.112	71.603
110.071	84.361	80.939	79.348	78.09	76.897	76.324	75.345	74.095	71.436

Appendix 5

Orcaflex dataset obtained in Case 1b

$H_s = 7.5$m and $T_z = 8$s

500 simulations performed, recovery of a Supporter Mk2 at Rem Ocean

Values are in kN

554.294	114.369	98.107	91.161	87.469	84.831	82.753	80.964	79.446	77.992
275.974	113.889	97.942	91.006	87.466	84.83	82.723	80.926	79.434	77.822
271.583	113.415	97.709	90.922	87.419	84.79	82.548	80.891	79.383	77.67
258.831	112.877	97.655	90.851	87.403	84.778	82.526	80.873	79.344	77.576
243.194	112.562	97.437	90.84	87.386	84.764	82.469	80.846	79.34	77.571
207.133	112.103	97.295	90.767	87.22	84.509	82.404	80.785	79.337	77.471
202.586	112.081	97.255	90.566	87.105	84.474	82.372	80.762	79.335	77.402
176.304	111.777	97.209	90.44	87.05	84.364	82.361	80.735	79.322	77.307
169.965	110.446	96.722	90.438	86.919	84.359	82.327	80.732	79.282	77.268
169.717	110.419	96.479	90.434	86.891	84.261	82.27	80.718	79.27	77.241
161.739	109.553	96.338	90.405	86.878	84.203	82.262	80.685	79.26	77.239
159.769	109.024	96.026	90.288	86.787	84.202	82.242	80.684	79.256	77.232
156.625	108.535	95.682	90.158	86.651	84.193	82.216	80.674	79.215	77.216
152.596	107.109	95.619	89.909	86.598	84.188	82.157	80.625	79.21	77.192
149.556	106.888	95.291	89.893	86.55	84.165	82.109	80.623	79.19	77.091
148.91	106.744	95.277	89.62	86.428	84.112	82.108	80.615	79.108	76.938
146.72	106.324	95.274	89.512	86.406	84.112	82.091	80.486	79.05	76.912
143.923	105.978	95.117	89.498	86.384	84.097	82.056	80.451	78.986	76.798
141.204	105.905	94.891	89.453	86.338	84.089	82.044	80.433	78.954	76.728
140.745	105.844	94.89	89.396	86.307	84.059	82.033	80.415	78.937	76.686
140.736	105.399	94.874	89.367	86.152	84.001	82.022	80.389	78.9	76.455
139.948	104.982	94.849	89.363	86.014	83.896	82.014	80.31	78.879	76.325
139.073	104.754	94.825	89.221	85.907	83.842	81.978	80.281	78.795	76.301
137.485	103.955	94.666	89.118	85.903	83.83	81.963	80.233	78.792	76.234
136.482	103.179	94.537	89.019	85.873	83.82	81.946	80.135	78.739	76.11
134.81	103.029	94.49	88.8	85.87	83.657	81.92	80.103	78.599	76.071
132.902	102.508	93.884	88.743	85.79	83.651	81.896	80.092	78.587	76.057
130.144	102.42	93.874	88.636	85.786	83.623	81.846	80.088	78.576	75.864
129.649	102.27	93.81	88.506	85.774	83.557	81.787	80.068	78.566	75.828
128.622	102.131	93.391	88.484	85.667	83.519	81.755	80.067	78.536	75.816
126.71	101.947	93.298	88.481	85.653	83.518	81.733	80.055	78.518	75.621
126.354	101.945	93.232	88.194	85.639	83.44	81.698	80.037	78.501	75.475
123.998	101.793	93.067	88.174	85.609	83.439	81.636	80	78.476	75.45
123.863	101.621	92.75	88.173	85.582	83.378	81.571	79.987	78.459	75.34
122.046	101.296	92.593	88.073	85.573	83.351	81.557	79.973	78.425	75.097
121.716	101.227	92.575	88.058	85.571	83.347	81.481	79.969	78.357	75.097
121.619	101.14	92.152	87.982	85.529	83.339	81.48	79.955	78.336	75.04
121.512	100.992	92.139	87.974	85.526	83.332	81.386	79.947	78.279	74.979
120.567	100.981	92.034	87.955	85.471	83.267	81.331	79.94	78.257	74.925
118.639	100.749	92.028	87.902	85.363	83.197	81.308	79.83	78.241	74.795
117.736	100.647	91.971	87.823	85.305	83.118	81.307	79.662	78.2	74.75
117.24	100.512	91.894	87.787	85.223	83.019	81.294	79.65	78.172	74.712
117.1	100.084	91.885	87.776	85.221	83.001	81.22	79.645	78.169	74.674
116.666	99.835	91.726	87.725	85.212	82.964	81.086	79.565	78.097	74.508
116.268	99.68	91.716	87.698	85.142	82.923	81.05	79.554	78.087	74.123
115.705	99.272	91.402	87.677	85.084	82.869	81.039	79.545	78.08	73.966
114.906	99.249	91.354	87.669	85.08	82.859	81.035	79.543	78.071	73.722
114.736	99.153	91.324	87.556	85.003	82.822	80.99	79.498	78.046	73.516
114.708	98.808	91.237	87.555	84.975	82.81	80.983	79.479	78.036	73.16
114.669	98.459	91.207	87.534	84.892	82.768	80.98	79.45	78.015	72.224

Appendix 6

Orcaflex dataset obtained in Case 2

$H_s = 3m$ and $T_z = 5s$

500 simulations performed, launch of Installer at Crest Bazan 2

173.909	88.814	77.264	68.861	63.006	59.152	55.899	53.583	51.626	50.211
149.703	88.508	77.252	68.756	62.715	59.107	55.881	53.517	51.603	50.168
126.802	88.31	77.106	68.584	62.684	59.02	55.868	53.517	51.562	50.107
125.662	87.941	76.645	68.437	62.567	58.966	55.864	53.511	51.558	50.106
122.347	87.673	76.333	68.315	62.339	58.809	55.831	53.505	51.55	50.072
121.779	87.502	76.23	68.221	62.121	58.755	55.827	53.499	51.51	49.963
119.545	87.071	76.188	68.22	62.078	58.565	55.821	53.437	51.484	49.952
114.077	86.779	76.11	68.093	62.038	58.22	55.734	53.413	51.462	49.936
113.42	86.706	76.085	68.057	62.029	58.158	55.711	53.378	51.449	49.838
112.322	86.138	75.695	67.827	62.014	58.141	55.703	53.377	51.446	49.736
111.217	86.115	75.382	67.803	62.012	58.109	55.61	53.337	51.399	49.706
110.894	86.073	75.182	67.773	61.998	58.054	55.592	53.315	51.364	49.682
109.724	86.008	74.642	67.694	61.941	58.013	55.439	53.315	51.357	49.669
109.087	85.694	74.531	67.684	61.852	58.008	55.436	53.276	51.334	49.636
109.055	85.677	74.442	67.582	61.672	57.969	55.432	53.258	51.313	49.619
108.834	84.679	74.392	67.393	61.607	57.878	55.427	53.186	51.301	49.536
108.35	84.29	74.059	67.279	61.585	57.814	55.287	53.095	51.277	49.455
108.052	84.261	73.95	67.076	61.432	57.676	55.281	52.994	51.252	49.451
107.844	84.16	73.87	67.063	61.427	57.643	55.276	52.874	51.201	49.392
105.934	83.759	73.639	67.048	61.418	57.643	55.166	52.865	51.162	49.374
105.844	83.487	73.168	67.034	61.373	57.616	55.146	52.744	51.13	49.362
103.093	83.44	73.044	66.9	61.225	57.583	55.044	52.707	51.103	49.175
101.807	83.321	72.982	66.82	61.225	57.511	54.944	52.701	51.091	49.142
101.352	83.203	72.459	66.59	61.149	57.448	54.944	52.692	51.019	49.08
100.968	83.092	72.406	66.541	61.11	57.394	54.882	52.644	50.983	48.806
100.924	82.617	72.072	66.169	61.083	57.386	54.842	52.604	50.925	48.794
100.799	82.44	71.983	65.751	60.899	57.264	54.822	52.582	50.901	48.707
99.807	81.233	71.758	65.751	60.763	57.232	54.714	52.564	50.895	48.602
98.436	81.076	71.734	65.732	60.726	57.188	54.657	52.529	50.88	48.432
97.982	81.049	71.642	65.474	60.686	57.172	54.63	52.529	50.835	48.37
96.966	80.894	71.548	65.236	60.597	57.169	54.619	52.481	50.835	48.321
96.729	79.949	71.461	65.124	60.508	57.087	54.41	52.424	50.832	48.293
95.45	79.83	71.395	64.977	60.468	57.08	54.403	52.304	50.753	48.122
95.126	79.726	71.22	64.939	60.434	57.07	54.366	52.293	50.747	48.059
95.008	79.601	71.098	64.924	60.356	56.9	54.317	52.253	50.728	47.999
94.81	79.573	70.91	64.924	60.286	56.767	54.308	52.245	50.683	47.866
94.217	79.041	70.722	64.856	60.242	56.748	54.083	52.224	50.671	47.782
94.217	78.889	70.651	64.745	60.174	56.711	54.062	52.136	50.599	47.564
93.487	78.852	70.596	64.744	59.979	56.71	54.007	52.128	50.513	47.487
92.691	78.807	70.45	64.455	59.896	56.682	53.853	52.094	50.506	47.203
92.16	78.637	70.372	64.248	59.677	56.612	53.832	52.077	50.502	47.049
91.561	78.545	70.274	64.222	59.573	56.572	53.829	52.059	50.464	46.958
90.665	78.36	70.025	63.905	59.566	56.556	53.787	52.045	50.382	46.66
90.59	78.282	69.924	63.596	59.469	56.467	53.747	51.965	50.325	46.472
90.136	78.197	69.753	63.342	59.461	56.414	53.742	51.938	50.29	46.227
90.117	78.113	69.58	63.261	59.394	56.34	53.738	51.929	50.274	46.149
89.997	77.763	69.574	63.158	59.383	56.235	53.705	51.853	50.257	46.071
89.525	77.538	69.343	63.107	59.344	56.103	53.654	51.749	50.255	45.54
89.517	77.369	69.274	63.073	59.271	56.048	53.628	51.712	50.241	45.494
89.482	77.297	69.081	63.026	59.166	56.041	53.591	51.631	50.211	45.193